1983

Progress Report No. 19

Biomedical Computer Laboratory

PROGRESS REPORT

No. 19

1 July 1982 – 30 June 1983

Biomedical Computer Laboratory

Washington University School of Medicine

700 South Euclid Ave.

St. Louis, Missouri 63110

BIOMEDICAL COMPUTER LABORATORY

WASHINGTON UNIVERSITY SCHOOL OF MEDICINE

PROGRESS REPORT NO. 19

JULY 1, 1982 - JUNE 30, 1983

TABLE OF CONTENTS

I. INTRODUCTION

This progress report from the Biomedical Computer Laboratory (BCL) summarizes activities during the period from July 1, 1982 through June 30, 1983. The Biomedical Computer Laboratory collaborates with research investigators throughout the Washington University School of Medicine and its affiliated hospitals in the application of advanced computer techniques to problems in biology and medicine. This often requires work in areas stretching from basic physiology through mathematical models to equipment design. Our orientation is interdisciplinary with the recognition that effective communication for workers with differing backgrounds comes only through extended collaboration and mutual respect.

The vigorous development and evolution of specialized computer systems for use in the solution of research and clinical problems has continued to be the central focus of BCL activities. Several systems now in clinical use have seen a progression from exploratory pilot studies, to major developmental project, to local clinical trial, to clinical trials in multiple locations, to public availability through commercial manufacture. Perseverance in this sometimes tedious chain of development has found reward in the effective fielding of specialized computer systems to the medical community.

One class of computer applications requires strong coupling of the computer to its environment for digital signal processing. These applications typically involve the use of commercially available minicomputers and microprocessors in conjunction with specialized hardware designed and built locally. We have pursued many such applications by bringing signals from hospital wards and research laboratories to BCL by means of either analog or digital tape recordings or telephone lines and, more frequently, by taking the computers to the investigator's laboratory or the patient's bedside. In this context, of particular importance to current and future BCL projects is the development, in a closely related sister lab (Computer Systems Laboratory, or CSL), of a capability for the design and fabrication of custom very-large-scale integrated (VLSI) circuits. The realization of such circuits through collaboration with CSL is already opening up new opportunities for solving problems intractable with conventional computing devices.

For those classes of applications dominated by information processing requirements, provisions have matured from telephone lines linking our minicomputers to the IBM System/360-370 at the Washington University Computing Facilities, through development and support of a minicomputer based MUMPS system, to the establishment of independent groups such as the Medical Computing Facility and the Medical Computing Service Group which serve the local medical complex. Diverse needs continue to be met by these various options while collaborative work continues on more advanced information-processing developments.

Still another class of applications requires extensive use of large-scale computational services. Many investigators are assisted in their research through the use of generalized numerical, non-numerical, and statistical routines. This work is carried out in part by staff members

of BCL, but primarily by members of the Division of Biostatistics under the direction of Dr. Dabeeru C. Rao, and the University Computing Facilities whose director is Robert J. Benson.

The BCL enjoys collaboration with most departmental divisions within the medical school but also finds support and enrichment through close ties with other facilities throughout the University. These arrangements are of benefit both to the BCL and to graduate students who find projects and employment among the activities in the laboratory. The Department of Computer Science is under the direction of Dr. Jerome R. Cox, Jr., past Director of the BCL. Close collaboration with the department currently emphasizes the area of information systems. Strong ties with the Department of Electrical Engineering are sustained through the Engineering School's Biomedical Engineering Program and common interests in digital signal processing techniques. The Department of Electrical Engineering is chaired by Dr. Donald L. Snyder, past Associate Director of BCL.

A major development during the past year has been the establishment at Washington University of an interschool Institute for Biomedical Computing. The new Institute encompasses the Biomedical Computer Laboratory and the Computer Systems Laboratory in an organizational setting designed to recognize and foster the joint interests in biomedical computing of the School of Medicine and the School of Engineering and Applied Science. The purpose of the reorganization is to recognize that the development and application of advanced computing and engineering technology to problems in biomedical science is an essential component of the research and teaching activities of Washington University, and requires for its further development and continued stability an organizational structure that will 1) provide a means by which the primary academic affiliations of its faculty can be in an organizational setting with an adequately broad commitment to research and teaching in biomedical computing; 2) establish a formal administrative connection to the School of Engineering and Applied Science that will facilitate involving its students and faculty in research and instructional activities in biomedical computing; 3) establish mechanisms for administration, funding, and review of appointments, promotion, and tenure for the academic staff of this activity; 4) foster organizational and procedural coherence between the Biomedical Computer Laboratory and the Computer Systems Laboratory by placing them with a common administrative structure; 5) create a focal point for interdisciplinary teaching and student research, both in the School of Medicine and the School of Engineering and Applied Science, in areas that do not fit comfortably into existing departments; and 6) encourage a scholarly environment for the activities of the two computer laboratories that will promote and encourage teaching, research, and publication as vehicles for personal development and academic contribution.

In addition to current BCL and CSL space on the Medical School campus, space for part of the activities of the Institute will be provided on the Engineering School campus by completion of a fifth-floor addition to Lopata Hall, a new building opened in January of 1981. This new space (about 6000 square feet), called the Edward L. Bowles Laboratory, is immediately adjacent to the Departments of Computer Science and Electrical Engineering. It is expected to become available in November, 1983.

The Institute for Biomedical Computing (IBC) now replaces the former Washington University Computer Laboratories (WUCL) which was a less formal federation of BCL and CSL plus working groups within the Departments of Computer Science and Electrical Engineering. Dr. Charles E. Molnar, Director of the Computer Systems Laboratory, and Dr. Lewis J. Thomas, Jr., Director of the Biomedical Computer Laboratory, have been appointed as respective Director and Associate Director of the Institute. Both BCL and CSL continue to retain their identities and internal organizations. Accordingly, this Progress Report addresses activities centered primarily within BCL.

Planning and policy development of the Institute are overseen by a Governing Board, the membership of which is drawn from both Schools. The present composition of the Governing Board is:

J. R. Cox, Jr., Chairman, Department of Computer Science
R. G. Evens, Head, Department of Radiology
M. K. King, Dean, School of Medicine
D. M. Kipnis, Chairman, Department of Internal Medicine
E. L. MacCordy, Associate Vice-Chancellor for Research
J. M. McKelvey, Dean, School of Engineering and Applied Science
C. E. Molnar, Director, Computer Systems Laboratory
P. Needleman, Head, Department of Pharmacology
D. L. Snyder, Chairman, Department of Electrical Engineering
L. J. Thomas, Jr., Director, Biomedical Computer Laboratory

To aid in long-range planning of the health-related activities of the Institute, a National Advisory Panel is convened periodically. Particular attention is given to the confluence of important needs in biology and medicine with the technical advances capable of meeting these needs. Successful development may suggest implementation on a larger, perhaps national scale. The present composition of the National Advisory Panel is:

P. H. Abbrecht, Professor of Physiology and Internal Medicine, Uniform Services University of the Health Sciences, Bethesda, Maryland
H. L. Bleich, Associate Professor of Medicine, Harvard University
W. A. Clark, Consultant and former Director of CSL, Cambridge, Massachusetts
J. N. Gray, Tandem Computer Company, Cupertino, California
F. E. Heart, Bolt, Beranek & Newman, Cambridge, Massachusetts
D. M. Kipnis, Professor and Chairman, Department of Internal Medicine, Washington University
B. W. Matthews, Professor of Physics and Director of the Institute of Molecular Biology, University of Oregon
J. M. Smith, Computer Corporation of America, Cambridge, Massachusetts
E. A. Stead, Jr., Professor of Medicine, Duke University
C. Vallbona, Professor and Chairman, Department of Community Medicine, Baylor College of Medicine

II. SOURCES OF SUPPORT

During the period covered by this report the primary source of support for the Biomedical Computer Laboratory was from two grants from the National Institutes of Health, Division of Research Resources.

RR 00396 and RR 01380 A Resource for Biomedical Computing.

NHLBI contract NO1 HV 72941 continues to fund a Holter Monitoring Core Laboratory to support a Multicenter Investigation of Limitation of Infarct Size.

NCHSR grant HS 03792, to develop a medical information systems design methodology, continues to support the research in the Computer Science Department and this Laboratory.

The proceedings were published on a Workshop on Time-of-Flight Tomography. This workshop was supported by grant RR 01358.

Collaboration with other investigators often involved work already supported by other grants.

Public Health Services Grants.

AM 07296 Cell Biological Approaches to Diabetes Research,

AM 20579 Diabetes Research and Training Center,

EY 02044 Automated Digital Processing of the Human Visual Field,

EY 03579 Compliance with Topical (Eye Drops) Ophthalmic Therapy,

EY 03703 Chromatic Static Perimetry in the Diagnosis of Glaucoma,

GM 28232 Physical Mapping of Yeast Chromosomal DNA,

HD 09998 Clinical Correlations to Vitamin D Status in Infants,

HL 12839 Erythrocyte Deformability and Vascular Pathophysiology,

HL 13851 Cyclotron Produced Isotopes in Biology and Medicine,

HL 17646 Study of Ischemic Heart Disease,

HL 22982 Multicenter Investigation of Limitation of Infarct Size,

HL 25430 Characterization of Left Ventricular Diastolic Function,

HL 25944 Time-of-Flight Positron Tomography for Cardiac Imaging,

HL 28995 Adrenergic Factors and Arrhythmogenic Metabolites,

HL 28998 Tissue Characterization with Ultrasound,

NS 06833 An Interdisciplinary Stroke Program,

NS 14834 Mechanisms of Seizures and Anticonvulsant Drugs,

NS 15070 Regeneration and Functional Recovery in Cerebral Cortex,

RR 01379 Research in VLSI Systems for Biomedical Applications.

National Science Foundation Grants.

ECS-81-13266 Estimation and Decision for Random Point Processors,

ECS-82-15181 Study of Time-of-Flight Tomography.

Research support was also received from the following industrial collaborators.

Biosensor Corporation, Brooklyn Center, Minnesota,
Computer Services Corporation (CSK), Tokyo, Japan,
IBM Biomedical Systems, Hopewell Junction, New York,
Mead Johnson, Evansville, Indiana,
Medicomp, Melbourne, Florida,
Mennen-Medical, Clarence, New York.

III. PERSONNEL

EMPLOYEES

Personnel employed by the Biomedical Computer Laboratory during the period covered by this report were:

Director

Lewis J. Thomas, Jr., M.D., and Associate Director of Institute for Biomedical Computing, and Associate Professor of Anesthesiology, Physiology and Biophysics, Biomedical Engineering, and Electrical Engineering

Associate Director

G. James Blaine III, D.Sc., and Affiliate Associate Professor of Electrical Engineering and Computer Science, and Senior Research Associate, Computer Systems Laboratory

Senior Research Associates

Jerome R. Cox, Jr., Sc.D., and Chairman and Professor of Computer Science, and Professor of Electrical Engineering, and Senior Research Associate, Computer Systems Laboratory
Harold W. Shipton, C.Eng., and Chairman and Professor of Biomedical Engineering
Donald L. Snyder, Ph.D., and Chairman and Professor of Electrical Engineering, and Senior Research Associate, Computer Systems Laboratory

Business Manager

Virginia M. Bixon, B.S.

Research Associates

Robert J. Arnzen, Ph.D., and Computer Systems Laboratory
R. Martin Arthur, Ph.D., and Associate Professor of Electrical Engineering
Kenneth W. Clark, M.S.
James G. Dunham, Ph.D., and Associate Professor of Electrical Engineering
Robert O. Gregory, D.Sc., and Professor of Electrical Engineering
Ronald W. Hagen, M.S.
Richard E. Hitchens, B.S., and Lecturer in Computer Science
Kenneth B. Larson, Ph.D.
James G. Miller, Ph.D., and Professor of Physics, and Associate Director for Biomedical Physics, Laboratory for Ultrasonics, and Research Associate Professor of Medicine
Frederick U. Rosenberger, D.Sc., and Associate Director, Computer Systems Laboratory, and Assistant Professor of Electrical Engineering

Research Assistants

H. Dieter Ambos, and Research Assistant Professor in Medicine (Cardiology)
David E. Beecher, M.S.
Michael W. Browder, M.S.
John C. Chabut, B.S.
John D. Gorman, B.S.
Alexander J. Gray, M.S.
Russell E. Hermes, M.S.
Timothy J. Holmes, M.S.
Patrick H. Johnston, M.A.
Joanne Markham, M.S.
Charles N. Mead, M.D.
J. Philip Miller, A.B., and Associate Professor of Biostatistics in Preventive Medicine
Patricia Moore, Ph.D.
Stephen M. Moore, B.S.
Jack G. Mottley, M.A.
David G. Politte, B.S.
Heino R. Pull, M.S.
Kenneth B. Schechtman, Ph.D., Instructor in Biostatistics in Preventive Medicine, and Research Instructor in Medicine
Chung-Dak Shum, B.S.

Visiting Research Assistants

Ren Kang Yu
Tian-Ge Zhuang

Engineering Assistant

Stanley R. Phillips, A.A.S.

Technical Assistants

John D. Baker
Melissa A. Marlo, A.B.
Patrick W. McLear, A.B.
Donald W. Stein, Jr.

Electronic Technicians

Joseph H. Flacke, B.S.
Michael J. Rainey
Deborah A. Schwab

Librarian

Monica W. Shieh, M.L.S.

Secretaries

Rebecca J. Bozesky
Shirley A. Gonzalez-Rubio
Polly E. Raith

The following members from other departments and divisions have joint appointments with the Biomedical Computer Laboratory to facilitate collaboration and enhance interdisciplinary research:

A. Maynard Engebretson, D.Sc., Assistant Director of Research in Engineering, Central Institute for the Deaf, and Affiliate Associate Professor of Computer Science
Rexford L. Hill, III, M.S., Associate Professor of Computer Applications in Radiology
Burton E. Sobel, M.D., Professor of Medicine and Director, Cardiovascular Division
J. Stevadson Massey, M.S., Research Assistant in Neurological Surgery

RESEARCH COLLABORATORS

During the period covered by this report the following investigators from other laboratories, departments, or institutions, collaborated with BCL staff members on problems of joint interest.

J. Achtenberg, A.B., Medical Computing Service
F. Arias, M.D., Ph.D., Obstetrics and Gynecology
G. G. Ahumada, M.D., Medicine
H. D. Ambos, Medicine
T. R. Baird, Medicine
W. E. Ball, D.Sc., Computer Science
C. D. Barry, Ph.D., Computer Systems Laboratory
B. Barzilai, M.D., Medicine
B. Becker, M.D., Ophthalmology
R. J. Benson, J.D., Computing Facilities
S. R. Bergmann, Ph.D., Medicine
D. R. Biello, M.D., Radiology
S. B. Boxerman, D.Sc., Health Care Administration and Planning Program
T. L. Buettner, Medicine
M. E. Cain, M.D., Medicine
T. J. Chaney, M.S., Computer Systems Laboratory
K. C. Chang, Ph.D., Pathology
B. K. Clark, B.S., Cardiothoracic Surgery
R. E. Clark, M.D., Cardiothoracic Surgery
P. B. Corr, Ph.D., Medicine and Pharmacology
M. R. Courtois, M.A., Medicine
J. O. Eichling, Ph.D., Radiology
B. Emami, M.D., Radiology
R. G. Evens, M.D., Radiology

D. C. Ficke, B.S., Radiology
K. A. A. Fox, M.B., Ch.B., Medicine
P. T. Fox, M.D., Neurology
M. H. Gado, M.D., Radiology,
E. D. Galie, R.N., Medicine
R. A. Gardner, Ph.D., Mechanical Engineering
E. M. Geltman, M.D., Medicine
W. D. Gillette, Ph.D., Computer Science
R. M. Glueck, M.D., Medicine
S. Goldring, M.D., Neurological Surgery
M. E. Gordon, Ph.D., Ophthalmology
E. M. Gregorie, M.D., Neurological Surgery
R. G. Gross, M.D., Ph.D., Medicine
R. L. Grubb, Jr., M.D., Neurological Surgery
W. M. Hart, Jr., M.D., Ph.D., Ophthalmology
K. H. Haserodt, M.S., Computer Science
P. Herscovitch, M.D., Neurology and Radiology
L. S. Hillman, M.D., Pediatrics
G. R. Hoffman, B.A., Radiology
J. T. Hood, B.S., Radiology
B. Hughes, Ph.D., Medicine
S. Igielnik, Ph.D., Medical Computing Facilities
A. S. Jaffe, M.D., Medicine
G. C. Johns, B.S., Computer Systems Laboratory
E. G. Jones, M.D., Ph.D., Anatomy
R. G. Jost, M.D., Radiology
M. A. Kass, M.D., Ophthalmology
J. E. Knobbe, Obstetrics and Gynecology
P. B. Kurnik, M.D., Medicine
J. L. Lauter, Ph.D., Central Institute for the Deaf
S. P. Leara, Obstetrics and Gynecology
F. Lifshits, Medicine
P. Lombardo, B.A., Neurological Surgery
P. A. Ludbrook, M.D., Medicine
R. E. Marshall, M.D., Pediatrics
J. S. Marvel, B.S., Pathology
J. W. Matthews, D.Sc., Computer Systems Laboratory
M. M. Maurer, Jr., M.D., St. Louis Children's Hospital
J. M. McAninch, Medicine
D. W. Meltzer, M.D., Ph.D., Ophthalmology
M. A. Mintun, M.D., Neurology
C. E. Molnar, Sc.D., Computer Systems Laboratory
R. A. Moses, M.D., Ophthalmology
S. R. Mumm, Medicine
H. Nomura, M.D., Medicine
R. E. Olson, A.A.S., Computer Systems Laboratory
M. V. Olson, Ph.D., Genetics
D. S. Payne, Medicine
B. A. Pearson, B.S., Neurological Surgery
C. A. Pérez, M.D., Radiology

J. E. Pérez, M.D., Medicine
M. L. Peterson, M.S., Electrical Engineering
W. J. Powers, M.D., Neurology and Radiology
J. L. Price, Ph.D., Anatomy
J. A. Purdy, Ph.D., Radiology
M. E. Raichle, M.D., Neurology and Radiology
D. C. Rao, Ph.D., Biostatistics
A. D. Richardson, Computer Systems Laboratory
C. S. Ritter, Medicine
A. Roos, M.D., Physiology and Biophysics
A. M. Rosenblum, M.D., Medicine
J. E. Saffitz, M.D., Pathology and Medicine
S. J. Salmons, C.P.N.P., Pediatrics
S. P. Sedlis, M.D., Medicine
M. L. Seiger, B.S., Electrical Engineering
K. E. Shafer, M.D., Medicine
B. A. Siegel, M.D., Radiology
B. E. Sobel, M.D., Medicine
K. Socha, Neurological Surgery
J. J. Spadero, Jr., M.D., Medicine
A. W. Strauss, M.D., Pediatrics and Biochemistry
S. P. Sutera, Ph.D., Mechanical Engineering
A. G. Swift, B.A., Radiology
M. M. Ter-Pogossian, Ph.D., Radiology
L. J. Thomas, III, M.S., Physics
A. J. Tiefenbrunn, M.D., Medicine
R. G. Tilton, Ph.D., Pathology
K.-H. Tzou, M.S., Electrical Engineering
J. R. Udell, B.S., Pathology
D. F. Wann, D.Sc., Electrical Engineering
M. J. Welch, Ph.D., Radiology
C. S. Weldon, M.D., Cardiothoracic Surgery
R. A. Wettach, Medicine
J. R. Williamson, M.D., Pathology
F. X. Witkowski, M.D., Medicine
K. F. Wong, M.S., Computer Science
J. W. Wong, Ph.D., Radiology
T. A. Woolsey, M.D., Anatomy
M. Yamamoto, M.S., Radiology
A. L. Ysaguirre, Medicine

Columbia University, New York, New York

J. T. Bigger, Jr., M.D.

Creighton University, Omaha, Nebraska

F. M. Nolle, D.Sc.
Z. Zencka, M.D.

Indiana University School of Medicine, Indianapolis, Indiana

C. Fisch, M.D.
S. B. Knoebel, M.D.

Jewish Hospital, St. Louis, Missouri

B. R. Hieb, M.D.
J. R. Humphrey, R.N.
R. E. Kleiger, M.D.
R. J. Krone, M.D.
R. Ruffy, M.D.

Massachusetts General Hospital, Boston, Massachusetts

H. K. Gold, M.D.
H. W. Strauss, M.D.

Pennsylvania State University, University Park, Pennsylvania

D. B. Geselowitz, Ph.D.

Peter Bent Brigham Hospital, Boston, Massachusetts

E. Braunwald, M.D.

Research Triangle Institute, Research Triangle Park, North Carolina

W. K. Poole, Ph.D.

Roosevelt Hospital, New York, New York

H. M. Greenberg, M.D.

University of Illinois at Chicago Circle, Chicago, Illinois

R. Langendorf, M.D.

University of Iowa, Iowa City, Iowa

R. C. Arzbaecher, Ph.D.

University of Kentucky College of Medicine, Lexington, Kentucky

B. Surawicz, M.D.

University of Louisville School of Medicine, Louisville, Kentucky

N. C. Flowers, M.D.

University of Rochester School of Medicine, Rochester, New York

A. J. Moss, M.D.

University of Texas Health Science Center, Dallas, Texas

J. T. Willerson, M.D.

University of Vermont College of Medicine, Burlington, Vermont

D. S. Raabe, M.D.

As in the past, collaborative efforts with various commercial firms continue (see Section VI). This year projects of joint interest have involved:

Biosensor Corporation, Brooklyn Center, Minnesota,
Computer Services Corporation (CSK), Tokyo, Japan,
International Business Machines (IBM) Biomedical Systems,
Hopewell Junction, New York,
Mead Johnson, Pharmaceutical Division, Evansville, Indiana,
Medicomp, Inc., Melbourne, Florida,
Mennen-Medical, Inc., Clarence, New York.

IV. PHYSICAL RESOURCES

The Biomedical Computer Laboratory (BCL) was formed on April 15, 1964 and the original staff moved into 3,800 square feet (net) of laboratory space at 700 South Euclid Avenue in Saint Louis. While remaining at this location, adjacent to the Washington University School of Medicine's main building complex, the floor space has been increased to the present 12,000 square feet (net). In addition to this space, BCL staff members and systems frequently occupy other areas within the Washington University Medical Center at the sites of collaborative project activities. Facilities for staff offices, laboratory areas and computational applications are located within BCL at the Euclid Avenue address. A machine shop and reference room are also located on the premises and shared with a sister laboratory, the Computer Systems Laboratory. Other physical resources include a well-stocked electronics shop, a large inventory of electronic and computer test equipment, a variety of digital system modules and both analog and digital recording instruments. Systems for use in developing eight-bit, sixteen-bit and bit-slice microprocessor applications are available.

The Laboratory has gradually increased its computing resources since the time when a single Laboratory Instrument Computer (LINC) provided the original staff with an opportunity to apply digital computing to a few interesting problems in medicine and biology. The small stored-program LINC computer was designed specifically for use in biological and medical laboratories where there was a requirement for strong coupling between the computer, the investigator and the experiment. That first LINC is still used for a few service functions. During the past eighteen years BCL has addressed diverse biomedical problems for which digital computing techniques seemed promising and appropriate. Today BCL has interest and involvement in over one hundred minicomputer systems (representing twenty different makes and models) within the Washington University Medical Center. BCL has primary responsibility for a complement of computing hardware and software from a variety of system manufacturers. These resources include: PDP-11's and LSI-11's from Digital Equipment Corporation, TI-980's from Texas Instruments Incorporated, PC-12's from Artronix, Inc., 135's from California Data Processors and Versamodule M68000's from Motorola, Inc. An MMS-X stroke graphics display system developed by the Computer Systems Laboratory and a Lexidata raster graphic display system are available for biomedical imaging studies.

A local computer network, TERRANET, provides remote terminal-to-computer and inter-computer data communications at rates up to 9600 bps among twenty-three stations located throughout WUCL. At present, TERRANET resources include twelve video terminals, ten host processor ports, and a 300/1200 baud modem. Access to an IBM 360/370 system at the Washington University Computing Facility and to a MUMPS system at the Medical Computing Facility is available through several data terminals at the BCL. Personal-class microcomputer systems have been incorporated into the design of biomedical research systems and numerous special-purpose devices have been developed using microprocessor chip-sets and microcomputer board-level assemblies.

V. RESEARCH PROJECTS

Introductory Summary

The goal of the Biomedical Computer Laboratory (BCL) is the application of digital computing techniques to problems in medicine and biology. This often requires work in areas stretching from basic physiology through mathematical modeling and frequently to the design of specialized equipment. The Laboratory's capability to respond to a broad range of research needs is the direct result of long-standing BRP support. BCL's research program is organized into several major project areas with the staff grouped into teams whose interests are focused correspondingly. Because of the growth of the Laboratory's activities in the category of quantitative imaging, this year that category has been divided into three sections, each dealing with a different imaging modality (ultrasound, radiation-treatment planning, and positron-emission tomography). A total of 68 distinct project activities are grouped into the six project areas briefly summarized below. More complete summaries are given at the beginning of each of the subsequent project-report subsections.

In the area of ischemic heart disease and ECG analysis, algorithm developments for high-speed ECG processing have continued progress toward a major revision of Argus, with emphasis on frequency-domain analysis. Very promising evaluation results have stimulated implementation of the new algorithms in the Argus environment as well as exportation via industrial collaborations. Two ECG processing systems have full Argus/2H capability and have seen heavy use for local, national, and international collaborative studies ranging from fundamental electrophysiology to large-scale clinical trials. During the past year, the Laboratory's work on the MPIP study was completed and MILIS activities have reduced to follow-up analyses of patient recordings. The American Heart Association database for the evaluation of dysrhythmia detectors is still not quite complete, but early distribution to users has stimulated enthusiasm. Collaborative studies include several antidysrhythmic drug evaluations. Other work is being carried out in collaboration with investigators at Barnes and Jewish Hospitals to study the effects of ischemic injury on myocardial vascular integrity, infarct size modification, electrophysiological and biochemical factors underlying dysrhythmias, autonomic modulation of cardiac potentials, ventricular mechanics and regional myocardial perfusion and metabolism.

Work in quantitative imaging: ultrasonic tissue characterization has been supported separately as a BRP Resource Technology Development Project since July of 1982. Earlier work had demonstrated the ability to identify abnormal tissue (e.g. infarcted myocardium) using tomographic reconstructions of data from transmitted ultrasound. Current work focuses on tissue characterization employing reflected ultrasound, which is more clinically practical. A highlight of recent studies is the demonstration that tissue attenuation estimated from backscatter varies as a function of isometric contractile state for both myocardial and skeletal muscle. Other work includes the evaluation of spatial moments of the received field

as useful parameters, the development of improved methods for estimating attenuation from backscatter, the study of dispersive tissue models, and the examination of several aspects of the transduction process.

Longstanding activities in quantitative imaging: radiation treatment planning continue progress toward the development of improved methods for precise estimation of three-dimensional dose distributions within inhomogeneous tissues for radiation fields of arbitrary shape and size. This project has benefitted, during the past year, from Dr. John Wong's joining the Physics Section of the Oncology Division, with which the Laboratory collaborates. The previously reported algorithm has now been extended to include compensation for multiple-scattering effects. Also, the work on customized VLSI circuits to render practical the formidable computational requirements has seen rapid progress as the result of cooperation from CSL, from which Dr. Frederick U. Rosenberger has joined the project on a part-time basis.

Quantitative imaging: positron-emission tomography continues to be a major project which spans algorithm development, system design and fabrication, and biomedical applications. Through collaborative work with the Cardiovascular Division of the Department of Medicine, the Department of Neurology, and the Department of Radiology, applications have emphasized the unique capabilities of emission tomography to study, in vivo, the biochemistry and pathophysiology of heart and brain. Following construction, in 1982, of the first emission-tomography system to utilize time-of-flight (TOF) information, subsequent work has focused on new data-acquisition strategies, new image-reconstruction algorithms, algorithms for three-dimensional display of the data, and the early consideration of enhancements based on custom VLSI designs. During the past year, the proceedings of a locally hosted International Workshop on Time-of-Flight Tomography were edited and published.

Grouped under the title, Systems for Specialized Biomedical Studies, are diverse efforts focused on specific applications of computing to biomedical problems. Our previously developed system for autoradiographic analysis has been extended from its original application in neuroanatomical studies to the analysis of retinal images, the examination of cells in division, and the study of image compression. The automated electrophoretic-gel system reported last year has been moved to the genetics laboratory for trial application to DNA restriction-mapping studies. Also, our data-acquisition system for chromatic perimetry is now in use in ophthalmology for the study of early glaucomatous visual defects. The Laboratory continues to support work in the Department of Neurosurgery to develop an automated system for localizing seizure foci by monitoring via epidural electrodes. Other projects address radiotracer kinetics (both modeling and data acquisition support), the recording of multi-channel analog data, and compliance with ophthalmic therapy.

Resource development activities span exploratory biomedical applications, system development aids, and digital hardware and software

designs of general utility to other Laboratory activities. Installation and augmentation of a UNIX-based cross-compiler system developed at MIT provides support for M68000 systems. We continue to collaborate with the Department of Computer Science and CSL in Information Systems Group work in the areas of modeling, design studies, system implementation, and applications. Previous MUMPS-based information-system applications supported in BCL have been moved to other facilities during the past year. Following our development and installation of a local-area-network, "TERRANET," it has been successfully exported to the commercial sector in Japan. In the area of "electronic radiology," design studies have been carried out for a distributed picture archiving and communication system for the Mallinckrodt Institute of Radiology, where a broadband cable distribution system has been installed, and for which data-compression studies have been initiated. Other work has addressed the Laboratory's increasing needs for generalized programming and image processing through upgrading and enhancement of RSX11M on twin PDP 11/34s.

Individual Projects

A. Ischemic Heart Disease and ECG Analysis

The projects reported in this section continue longstanding work in real time and high-speed ECG analysis. Many of the clinical studies reported here are natural outgrowths of the ECG analysis work, as are the strong interests in the evaluation of automated arrhythmia detectors. Modeling and signal-processing endeavors in the field of cardiology have supported collaborations which address other aspects of ischemic heart disease, such as myocardial metabolism and blood flow, the electrophysiologic characterization of abnormal myocardial depolarization, various antidysrhythmic drug studies, infarct-size modification, and the study of ventricular diastolic mechanics.

A real-time computer-based arrhythmia monitoring system, called Argus, in operation in the Barnes Hospital Coronary Care Unit from 1969-1975, was replaced in 1975 by "Argus/Sentinel," a commercially available version developed through collaboration with the Mennen-Greatbatch Company. The experience garnered with Argus led directly to the development of a system, called Argus/H, for the high-speed (60 times real time) processing of long-term ECG recordings. Argus/H has since processed several thousand recordings for a study of ventricular arrhythmias in survivors of myocardial infarction and several hundred recordings for a host of other studies. Extensive evaluations have verified the integrity of the analysis algorithms, proven the value of the quantified results as compared to conventional manual-scanning techniques, and confirmed the consistency of results on reprocessing. The importance of such issues stimulated the more recent development of a stochastic model for the performance evaluation of event detectors.

By the mid-1970's, it was apparent that Argus/H could not support rigorous algorithm development, could not efficiently process the now more-popular dual-channel recordings, and could not meet the demand for the system from the growing volume of recordings resulting from interests in therapeutic trials of antiarrhythmic agents and interventions designed to protect the ischemic myocardium. A newer system, called Argus/2H, emerged in 1977 and was duplicated in 1978. The two Argus/2H systems have processed long-term ECGs for national multicenter clinical studies of interventions to limit infarct size and of post-infarction risk stratification. The systems also provide the power and flexibility necessary for work on algorithm revision and on new signal-processing strategies and they have further served the analysis and documentation needs of other work to generate an annotated digital ECG database for the evaluation of automated arrhythmia detectors. Newer signal-processing strategies employing frequency-domain analysis of the ECG are now bearing fruit, and have led, during the past year to a new industrial collaboration to implement the algorithms in a CMOS processor for real-time dysrhythmia analysis in the ambulatory setting.

A-1. Argus Algorithm Development

Personnel: K. W. Clark, BCL
C. N. Mead, BCL
H. R. Pull, BCL
L. J. Thomas, Jr., BCL

Support: RR 01380
Washington University

Efforts to develop algorithms for efficient analysis of the ECG have spanned more than a decade and a half at BCL. Initial efforts focused on real-time ECG analysis in the Barnes Hospital Coronary Care Unit. In the last ten years, emphasis has been placed on high-speed analysis (approximately 60 times real-time) of long-term, tape recorded ECGs from ambulatory patients. During our 15-year involvement in ECG processing, considerable outside interest in the algorithms in both real-time and high-speed environments has led to close collaborations with other university-based investigators, both in this country and abroad, and more recently, to the algorithms finding their way into the commercial sector (see VI, Industrial Collaboration). During the past year, major efforts have been devoted to sharing our ECG-analysis experience with industrial personnel, evaluating their implementations of our algorithms, and gaining from them, in turn, some education about the issues and problems involved in transferring a technology from the research environment to the commercial sector.

Historically, our ECG analysis algorithms have concentrated on time-domain analysis of a single-channel ECG signal. Research efforts in recent years have combined a more sophisticated, noise-resistant QRS detector/delineator with a hybrid QRS classification strategy utilizing single-channel time-domain and intermittent dual-channel frequency-domain analysis. An initial evaluation of this updated approach (A-2) produced extremely gratifying results and, as a result, much effort has been spent in the past year in realizing a computationally workable, cost-effective implementation of the new algorithms into both the Argus real-time and Argus high-speed environments (A-2, VI). In particular, the QRS detector/delineator, originally developed and evaluated in 1978-79, has been recoded for higher efficiency, re-evaluated, and thoroughly documented. The hybrid classification strategy is currently undergoing a similar process. These efforts are being performed in anticipation of adaptation of the algorithms by both Mennen Medical, Inc. and Biosensor, Inc. (VI).

The intermittent 2-channel classification approach offers considerable computational advantages over a more straightforward "brute force" approach in which each channel is analyzed separately "in total" with a comparison algorithm resolving inter-channel disagreements. Although there is an arguable theoretical advantage to the "brute force" approach over the intermittent strategy, our initial evaluation results suggest that this advantage may be clinically insignificant. Additionally, practical issues have hindered implementation of the continuous dual-channel process. Specifically, if

the same hardware is to be used to analyze both channels, sequential analysis would by definition double the processing time. Alternatively, simultaneous analysis of the two channels would require the costs of parallel hardware and interwoven, updated software. General interest in the M68000 prompted efforts to translate a portion of the Argus algorithms into M68000 code, however that work has been deferred due to the demands of commercial exportation of the existing intermittent 2-channel algorithm.

A-2. Frequency-Domain-Based Analysis of the ECG

Personnel: C. N. Mead, BCL
K. W. Clark, BCL
H. R. Pull, BCL
L. J. Thomas, Jr., BCL

Support: RR 00396
RR 01380

As described in a previous Progress Report (PR 18, A-2) and in a recent publication,[1] we have concentrated our efforts in ECG algorithm development during the past several years in the area of frequency-domain (FD) analysis of the ECG. Specifically, we have developed a hybrid QRS classification strategy which utilizes traditional Argus time-domain (TD) QRS features (QRS duration, height, percent of complex below baseline, and area) in combination with a set of FD features calculated on a candidate waveform's frequency and amplitude-normalized power spectra (frequency-domain correlation coefficient 2-30 Hz, power spectral moment 2-30 Hz, power spectral dispersion 2-30 Hz, power spectral correlation coefficients 2-12 Hz and 10-30 Hz). All correlation coefficients are calculated relative to a suitably chosen "local" Normal QRS complex. Because the strategy involves comparison and classification of waveforms using features extracted from the amplitude-normalized power spectrum, portions of the algorithm are relatively fiducial-point (position) independent. This attribute allows the application of the strategy to the second channel of a dual-channel ECG without the necessity of QRS detection in the second channel since the algorithm tolerates inter-channel waveform onset skew. An initial evaluation of the algorithm using a subset of the AHA database produced extremely gratifying results: specificity .999 and sensitivity .992. During the past year, work has been done to refine and recode the algorithm in order to implement it in the routine Argus-processing environment. A final evaluation of the algorithm on the entire AHA and MIT databases is in progress.

Central to the process of moving the new algorithm from the "off-line" research environment to the "on line" processing environment is the issue of the increased processor load caused by intermittent processing of the second ECG channel in the frequency domain. Final hardware/software configuration

decisions have not been made as of yet, with the options of traditional machine language code, off-the-shelf special-purpose chips, distributed processing, and VSLI technology still under active consideration. A major reason for hesitation in this area has been that the central implementation effort during the past year has been directed toward a real-time, commercially available, microprocessor-based, ambulatory "Event Recorder," the algorithmic core of which would be the complete set of revised Argus algorithms (see VI). Progress toward complete documentation and transfer of the algorithms to a C-MOS microprocessor is nearing completion. To date, no specialized hardware has been necessary. Lessons learned in this implementation promise to contribute heavily to the specifics of a high-speed implementation of the FD algorithms.

1. C. N. Mead, H. R. Pull, K. W. Clark, and L. J. Thomas, Jr., "Expanded Frequency Domain ECG Waveform Processing: Integration into a New Version of Argus/H," Proceedings of the IEEE Conference on Computers in Cardiology, IEEE Catalog No. 82CH1814-3, Seattle, Washington, pp. 205-208, October 12-15, 1982.

A-3. Processing of Long-term ECG Recordings

Personnel: K. W. Clark, BCL
M. A. Marlo, BCL

Support: RR 01380
HV 72941
Jewish Hospital

After many years of analyzing long-term ECG recordings for a variety of local studies and multicenter trials, these activities have been reduced over the course of the past year. A few recordings are still analyzed for Jewish Hospital patients who are being studied with a variety of antiarrhythmic agents. Processing of recordings for the Multicenter Investigation of the Limitation of Infarct Size (MILIS) has concluded (A-12). Throughout the 5-year MILIS study, analysis quality-control procedures were applied by both supervisory personnel within BCL and by the MILIS Data Coordinating Center at Research Triangle Institute, North Carolina. These procedures involved blinded reprocessing of a subset of all recordings. Reproducibility figures proved to be: correlation coefficient = 0.96 (log-PVC rate) and percent agreement = 87% (PVC couplets and runs).[1] Our broader experiences with quality-control methods for the MILIS and other studies have also been reported.[2]

1. K. W. Clark, E. M. Geltman, J. P. Miller, P. Moore, K. A. Madden, L. J. Thomas, Jr., T. D. Hartwell, A. S. Jaffe, D. S. Raabe, P. H. Stone, H. K. Gold, R. E. Rude, and the MILIS Study Group, "Reproducibility of Dysrhythmia Findings by a Centralized Laboratory Within a Major Multicenter Trial," Proceedings of the IEEE Conference on Computers in Cardiology, IEEE Catalog No. 82CH1814-3, Seattle, Washington, pp. 55-60, October 12-15, 1982.

2. L. J. Thomas, Jr. K. W. Clark, and J. P. Miller, "Perspectives on Quality Control for Long-Term ECG Analysis in Multicenter Clinical Trials," presented at the Fourth Annual Meeting of the Society for Clinical Trials, St. Louis, Missouri, May 1983 (abstract).

A-4. American Heart Association Database

Personnel: R. E. Hermes, BCL
J. R. Cox, Jr., BCL

Support: RR 00396
RR 01380

Development of the American Heart Association Database has been described in previous reports (PR 17, A-5; PR 18, A-4), however work still continues in an effort to complete the ventricular tachycardia and R-on-T classes. Although all database tapes are not yet available to users, those that are have been in great demand.

Database tape distribution is being handled by ECRI of Plymouth Meeting, PA. Tapes are distributed in many forms including: 9-track digital tape, Holter-like recordings, and analog FM-style recordings. There are now over 35 users of the database from industry and research institutions located not only in the United States but also in Europe, Japan, Israel, and Canada.

As a result of the development of this database, studies are now being conducted to find better methods for reporting performance results obtained from use of the database (PR 19, A-5). In addition, the American Heart Association has formed a subcommittee to recommend new standards for devices related to ambulatory electrocardiography. The database will be an integral part of these new standards as will new methods for reporting device performance.

To help users of this database and other databases share information and their experiences, a database users group is being organized. Interest in the users group seems strong and participation is expected from domestic as well as foreign users.

A-5. Performance Evaluation of Ventricular-Arrhythmia Detectors

Personnel: R. E. Hermes, BCL
J. R. Cox, Jr., BCL

Support: RR 00396
RR 01380

We last reported the development of a performance parameter for reporting the correct detection performance of automated ventricular-arrhythmia detectors (PR 18, A-5). Recent work has involved the development of a bound on the estimation error for this performance parameter.

The correct-detection parameter $\hat{\alpha}$ is a function of the number of tapes, number of PVC annotations, and the number of PVC detections in an ECG test database. This parameter is related to a performance estimator $\hat{p}$ by $\hat{p} = \hat{\alpha}/\hat{\alpha} + 1$, where $\hat{\alpha}$ is the maximum likelihood estimation parameter. The development of this parameter is significant in itself, however to gain confidence in the accuracy of this parameter, a bound on the estimator error has also been derived.

The derived bound is a mean-squared-error bound on the variance of the estimator, and is a function of the correct-detection parameter, the number and length of recordings, and the annotation rate. This bound can be used to determine the number and length of recordings necessary for testing a detection system. Applying this bound calculation to the data contained in the American Heart Association Database has shown that this model estimator can produce an estimate of performance with less than 3% rms error when evaluating systems which have a performance estimate of 90% or better.

Since the introduction of this new method for reporting performance, several companies and research institutions have expressed interest in using the method for reporting results. They have found it to be a stable and reliable method for performance reporting.

At present, only the estimator for the correct-detection parameter has been developed. A similar parameter for reporting the false-detection rate is a possibility for future study. Although this method has been applied only to automated ventricular-arrhythmia detectors, it would be a natural extension of this work to develop parameters for other types of automated event detectors.

A-6. Fast-Fourier Transform Analysis of Signal-Averaged Electrocardiograms

Personnel: H. D. Ambos, BCL
M. E. Cain, M.D., Medicine
R. E. Hitchens, BCL
J. Markham, BCL
H. R. Pull, BCL
F. X. Witkowski, M.D., Medicine

Support: RR 00396
RR 01380
RR 05389

Standard ECGs in arrhythmia-free intervals do not identify patients who manifest sustained ventricular tachycardia (VT). To determine if frequency-domain analysis facilitates detection of latent depolarization abnormalities and ultimately identifies patients at high risk for VT, procedures for fast-Fourier-transform analysis (FFTA) were developed (PR 18, A-6) and rigorously tested using a computer-based mathematical model designed to simulate an oscillatory waveform superimposed on a trailing edge of a QRS complex. After demonstrating that FFTA facilitated detection of low amplitude oscillatory waveforms in a signal-averaged ECG and that certain waveforms not visible in the time domain were readily detected in the frequency domain, FFTA of signal averaged X, Y, and Z ECG leads were performed in three groups of patients: 1) prior myocardial infarction and sustained VT; 2) prior myocardial infarction without sustained VT; and 3) controls. Results of FFTA showed significant differences in the attenuation at 40 Hz and in the area under the curve from the fundamental frequency to the frequency at which a 60 dB attenuation is seen. These analyses were performed for the terminal 40 msec of the QRS and the ST segment in all three groups of patients. There were no significant differences between Groups 2 and 3, but highly significant differences ($p < 0.0001$) between Groups 1 and 2 and Groups 1 and 3 were shown. Results were independent of QRS width, left ventricular ejection fraction, or the complexity of spontaneous ventricular ectopic activity. Patients with sustained VT have greater high-frequency content in the terminal portion of the QRS and ST segment than do patients without sustained VT. Accordingly, FFTA offers promise for noninvasive detection of patients at risk for developing sustained VT.

A-7. Assessment of Vascular Integrity of the Myocardium Following Ischemic Injury Using Mathematical Models to Interpret Kinetic Radiotracer Data

Personnel: R. G. Tilton, Ph.D., Pathology
K. C. Chang, Ph.D., Pathology
R. A. Gardner, Ph.D., Mechanical Engineering
K. B. Larson, BCL
J. S. Marvel, B.S., Pathology
B. E. Sobel, M.D., Medicine
S. P. Sutera, Ph.D., Mechanical Engineering
J. R. Udell, B.S., Pathology
J. R. Williamson, M.D., Pathology

Support: RR 00396
RR 01380
AM 07296
HL 12839
HL 17646
The Kilo Diabetes and Vascular Research Foundation

We have continued our previously reported studies (PR 15, A-10; PR 16, A-10; PR 17, A-7; PR 18, A-7) of the pathophysiology of ischemic injury to the heart. In these studies, we employed bolus-injection, external-detection radiotracer techniques to quantify albumin transport across the coronary vasculature under physiological conditions, and during reperfusion after selected intervals of global, no-flow ischemia in isolated-perfused rabbit hearts. The resulting residue-detection data, analyzed on the basis of a two-compartment model of tracer transport, were used to estimate parameters indicative of microvascular integrity such as permeability and ultrafiltration conductance of the endothelium. We have demonstrated that 30 minutes of no-flow ischemia produced compromised functional integrity of vascular endothelium as evidenced by marked increases in albumin permeation and in perfusion pressure, and have concluded that compromised vascular functional integrity is an early manifestation of ischemia.[1] We have suggested that the increased perfusion pressure is due, at least in part, to coronary vasospasm and our research efforts during the past year have been directed toward the elucidation of pathogenetic mechanisms involved in coronary vasoconstriction following ischemia. The following is a summary of this work.

We have studied the effects of vasodilating drugs to assess the efficacy of pharmacologic interventions on ischemia-induced changes in the coronary vasculature and musculature. We have shown that diltiazem (a calcium-channel blocking drug) prevented both perfusion pressure and albumin permeability increases. On the other hand, phentolamine (an α-adrenergic blocker) was without effect on the coronary vasculature. We are currently assessing effects of additional pharmacologic agents on vascular contractility and permeability, including verapamil, prazosin and PGI_2.

During the past year, we have demonstrated the feasibility of using injurious agents confined to the vascular lumen to selectively damage vascular

endothelium. Proteolytic and lipolytic enzymes have been covalently linked to 0.2-μm surface-modified polystyrene latex spheres using a carbodiimide method. We have shown that phospholipase A_2 and trypsin retain enzymatic activity when covalently bound to "carboxylate-modified" 0.2-μm latex particles at the amino-terminal end, and we are using these enzyme-bound microspheres to characterize effects of specific endothelial cell damage on vascular tone and reactivity, vascular permeability, and left ventricle contractility.

Finally, we have conducted experiments to assess vascular permeability changes and ventricular function following ischemia in hearts treated with hyaluronidase. Increases in albumin permeability during reflow tended to plateau at lower levels in the hyaluronidase-treated hearts. In view of unexplained differences in baseline values for albumin permeability in control experiments versus hyaluronidase-treated hearts, these experiments have been repeated during the past year under rigorously controlled conditions. However, the finding that hyaluronidase completely blocked water uptake but reduced perfusion-pressure elevations by only 50% in isolated hearts during reperfusion indicates that increases in perfusion pressure during reflow were not due entirely to fluid accumulation.

1. R. G. Tilton, K. B. Larson, J. R. Udell, B. E. Sobel, and J. R. Williamson, "External Detection of Early Microvascular Dysfunction after No-Flow Ischemia Followed by Reperfusion in Isolated Rabbit Hearts," Circulation Research, vol. 52, pp. 210-225, 1983.

A-8. Modification of Infarct Size

Personnel: A. S. Jaffe, M.D., Medicine
H. D. Ambos, BCL
B. Barzilai, M.D., Medicine
E. M. Geltman, M.D., Medicine
P. B. Kurnik, M.D., Medicine
P. A. Ludbrook, M.D., Medicine
J. Markham, BCL
A. M. Rosenblum, M.D., Medicine
S. P. Sedlis, M.D., Medicine
K. E. Shafer, M.D., Medicine
B. E. Sobel, M.D., Medicine
J. J. Spadaro, Jr., M.D., Medicine
A. J. Tiefenbrunn, M.D., Medicine

Support: RR 00396
RR 01380
HL 17646

Studies were performed in the Cardiac Care Unit at Barnes Hospital to assess the effects of selected pharmacological agents on infarct size. Infarct size was estimated from serial plasma creatine kinase changes during a 72-hour interval and/or a serial positron-emission transaxial tomograph. Results in controls were compared to those observed in the treated groups.

Recently, we completed a study to evaluate whether or not subjects with diabetes are prone to larger infarctions than patients without diabetes. One hundred patients with diabetes had infarct size calculated as part of the SCOR database. This group was compared to 426 control patients similarly evaluated. In addition, infarct size was analyzed in relation to the severity of congestive heart failure and to subsequent mortality. Infarct size was estimated from serial determinations of MB CK, the presence or absence of congestive heart failure by physical examination and mortality from follow up studies conducted as part of the SCOR follow up clinic. Demographic characteristics were similar in patients with and without diabetes with the exception that diabetic patients tended to be younger and a larger percentage were female. Otherwise there were no differences in the distribution of infarction (transmural versus non-transmural) or the location of transmural infarction when it occurred. There was a roughly equal incidence of hypertension (49% in the diabetic group compared to 42% in the non-diabetic group), and a comparable incidence of previous myocardial infarction (32% in the diabetic group and 25% in the patients without diabetes). Despite these similarities, infarct size was statistically less in the diabetic population compared to non-diabetic patients ($P < .02$). Infarct size averaged 16.2 $\pm$ 2.2 (SE) CK/gm eq/m^2 in diabetic patients, 17% less than the value of 19 $\pm$ 9 in non-diabetic patients. This was in large part due to the effect on diabetic subjects with transmural infarction where the difference, 16.9 $\pm$ 2.5 compared to 21.4 $\pm$ 1.2 CK/qm eg/m^2 was most prominent. This difference was due to smaller infarcts in diabetic subjects with inferior myocardial

infarction (14.5 $\pm$ 2.2 compared to 19.6 $\pm$ 1.2 [$P < .03$]), although a similar but non-significant trend was observed in patients with anterior myocardial infarction. In addition, this effect was only observed in patients without previous myocardial infarction. Despite comparable or less extensive infarctions, pulmonary congestion was significantly more frequent in patients with diabetes ($P = .003$) and diabetic subjects had significantly more severe infarction by MIRU class ($P = .006$). This was most prominent in patients with previous myocardial infarction but also occurred in patients without previous infarction (26 compared to 16%). The trend was particularly clear in patients with moderate sized infarctions (15 to 30 CK/gm eq/m^2) where 40% of diabetic subjects exhibited pulmonary congestion compared to only 10% of non-diabetic patients ($P < .006$). The incidence of pulmonary congestion in patients with extensive infarction (>30 CK/gm eq/m^2) was 43% for diabetic patients and 32% for non-diabetic subjects. The increase in congestive heart failure presaged a reduction in survival (Figure 1). Survival patterns were significantly different ($P < .04$) for the diabetic and non-diabetic patients. Within the first 6 months, actuarial survival was 68% for diabetic compared to 78% for non-diabetic patients. When diabetic and non-diabetic patients were stratified by pulmonary congestion, actuarial survival was similar ($P = .59$ when congestion was present and $P = .39$ when congestion was absent). Thus, our findings document that diabetics have more congestive heart failure despite less extensive infarction. Our data provide a probability of .98 that diabetics do not suffer larger infarctions than non-diabetic subjects but congestive heart failure is more frequent. Thus, other factors must contribute to the development of ventricular dysfunction in these individuals. The importance of these other factors is underscored by the fact that survival was significantly worse in patient groups with congestive heart failure and that this effect accounted for the mortality differences between the groups. We can not definitively exclude silent non-Q-wave infarctions which could differentially impact on one group versus the other.

Other investigations on the effects of pharmacologic therapy on infarct size have utilized serial evaluations of positron tomography. Positron-emission tomography allows for the assessment of an initial area of biochemical abnormality with subsequent delineation of change in such an area after therapy. Prior to the evaluation of pharmacologic interventions, data on the natural history of PET defects during infarction was developed. Twenty-seven patients, 18 with anterior and 9 with inferior infarction were evaluated to assess changes in the metabolic deficits over time. Nine patients were studied within 24 hours of the onset of chest pain, 4 in the first 6 to 8 hours. Other patients included in this study were studied somewhat later. PET infarct size did not change significantly either in the group enrolled in less than 24 hours or in the group studied from 24 to 72 hours or beyond. Thus it appears that metabolic deficits are fairly stable between the early and late hours of acute infarction.

These data allowed us to use infarct size determined by positron-emission tomography to pursue studies both with thrombolysis and with nifedipine. Seventeen patients with initial myocardial infarction were evaluated in the streptokinase arm of the evaluation. Studies were performed immediately after admission, again after intracoronary streptokinase, and 7 to 10 days

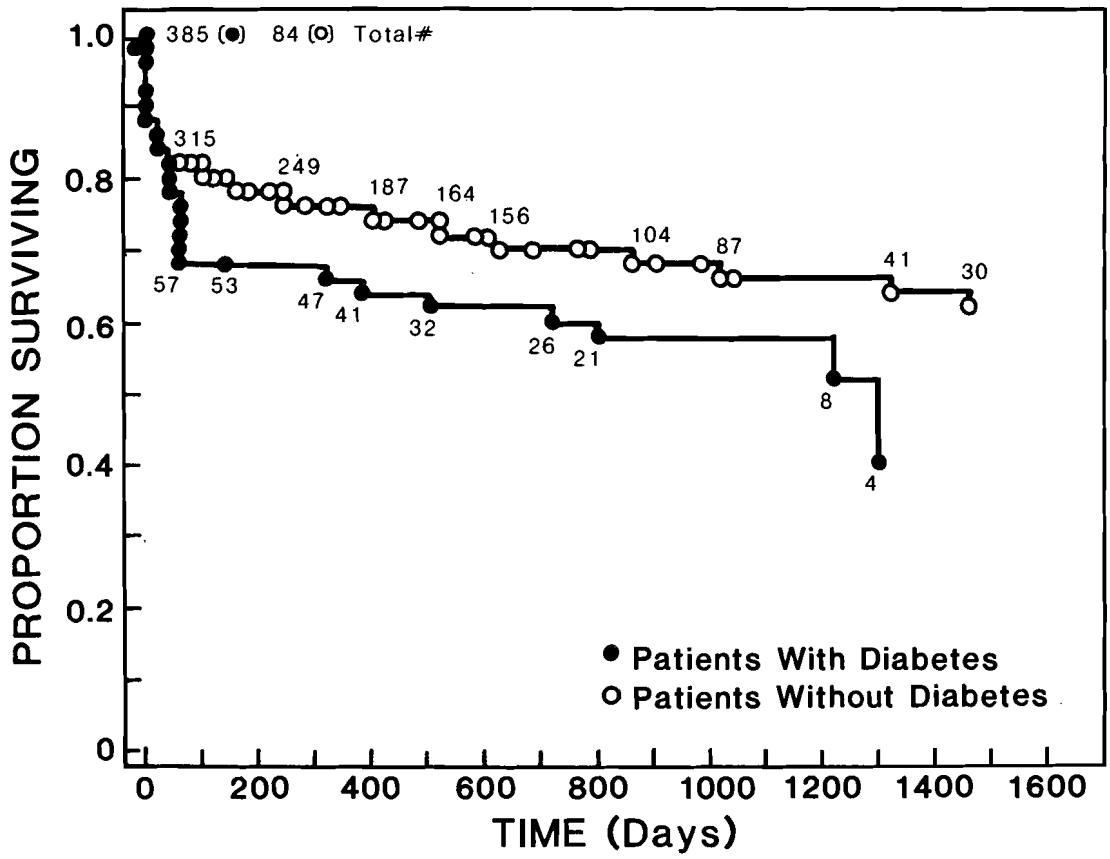

Figure 1. Post-infarction survival of patients with and without diabetes.

later. Clots persisted in 9 patients despite a mean dose of 336,000 units and marked fibrinogen depletion. Only 2 of these patients exhibited improved regional metabolism (> 20% change in late compared with early tomographs). Without lysis, mean metabolic impairment increased by 4 $\pm$ 18 (SD). In contrast all of the patients who manifested lysis (mean time to lysis = 5.5 hours after the onset of pain) exhibited improved metabolism with 75% exhibiting a 20% improvement later compared with early studies. The mean improvement for the entire group was 28 $\pm$ 2% ($P < .01$). Results were comparable in patients with anterior and inferior infarction. There were no bleeding complications due to thrombolytic therapy. These results document improvement in regional myocardial metabolism as evaluated by PET and thus begin to define the benefit of such therapy in more objective terms.

The investigations utilizing nifedipine in patients with acute myocardial infarction have enrolled 42 patients to date. Fourteen have undergone PET evaluation, 10 in the treated group and 4 in the placebo group. Nifedipine was well tolerated and hypotension has not occurred. Seven of the 10 patients receiving nifedipine manifested improvement from the initial metabolic deficit. Improvement was > 20% in 6 of 7. In 3 patients, improvement was not seen, 2 did not change substantially (2 and 9% differences) and in only 1 patient did PET infarct size become larger. The mean percentage change was an improvement in metabolic deficit of 19 $\pm$ 8% (SE). Only 4 patients have been evaluated with positron-emission tomography in the placebo group, 3 had improvement in metabolic deficits of > 20% and one had an exacerbation in the extent of metabolic deficits by 12%. The randomization sequence has resulted in relatively small infarcts in the placebo group; thus, small changes have been associated with marked percentage increments. Therefore a definitive statement cannot be made concerning treated versus control patients, however the results are promising. Nifedipine did not affect the amount of morphine required during the first 24 hours for control of pain (12 $\pm$ 3.6 compared to 13 $\pm$ 3.6 mg) but did markedly reduce the incidence of chest discomfort during the subsequent hospital course. Half of the patients receiving placebo complained of recurrent chest discomfort whereas that was true for only 1 patient receiving nifedipine. Thus, preliminary data suggest a salutary effect of this well tolerated agent in patients with acute myocardial infarction.

A-9. Electrophysiological and Biochemical Factors Underlying the Genesis of Dysrhythmias Due to Myocardial Ischemia and Infarction

Personnel: P. B. Corr, Ph.D., Medicine and Pharmacology
S. R. Phillips, BCL
J. E. Saffitz, M.D., Medicine
B. E. Sobel, M.D., Medicine
F. X. Witkowski, M.D., Medicine

Support: RR 00396
AHA 81-108
HL 17646
HL 28995

The overall purpose of these studies is the correlation of electrophysiological derangements with biochemical and adrenergic neural factors underlying malignant dysrhythmia due to ischemia. The overall concept of the research is that potential arrhythmogenic metabolites accumulate in ischemic tissue and exert deleterious effects on membranes and that their effects may be exacerbated by the concomitant influences of the adrenergic nervous system. During the last several years, we have demonstrated that disparate electrophysiological alterations underlie those dysrhythmias induced by ischemia alone compared to those dysrhythmias induced by reperfusion of the coronary artery. Since both types of dysrhythmias may be collectively important in sudden death in man, each may require different therapeutic interventions. Studies have been completed demonstrating a major electrophysiological role of α-adrenergic stimulation during both coronary occlusion and reperfusion.[1] More recently, we have demonstrated, using radioligand binding, a two-fold reversible increase in α-adrenergic receptors in ischemic myocardium.[2] Thus, it appears that during both coronary occlusion alone, as well as during subsequent reperfusion, enhanced electrophysiological responsivity occurs to α-adrenergic input and is associated with the induction and the persistence of malignant ventricular dysrhythmias.

Lysophosphatides, including lysophosphatidylcholine (LPC) and ethanolamine (LPE) accumulate in ischemic myocardium in situ and have been implicated in arrhythmogenesis.[3,4] However, the time course of their accumulation and its relation to the severity of dysrhythmia are unclear. In a recently completed series of studies, phospholipids in fast-frozen biopsies obtained from the normal and ischemic region of cats anesthetized with chloralose were extracted with $CHCl_3$:CH_3OH (2:1), separated by HPLC and quantified by phosphate assay. Although the sum of LPC + LPE did not increase at 2 min of ischemia in animals without dysrhythmia (n = 6) (4.6 $\pm$ .7 nmol/mg protein compared with 4.7 $\pm$ 0.3 in controls), it did increase in animals that developed spontaneous ventricular fibrillation (VF) (n = 9) between 90 and 135 sec of ischemia to 6.6 $\pm$ .26 ($p < .002$). Electrical induction of VF at 2 min of ischemia failed to increase LPC + LPE (4.1 $\pm$ .4). In other animals (n = 9) with ventricular dysrhythmias but without VF, the increase in LPC + LPE was intermediate (5.2 $\pm$ 1.4) though significantly increased ($p < .0005$) compared with values in control regions 3 min after

ischemia (4.3). Thus, increases in lysophosphatides appear within 90 sec of ischemia and in close relation to the severity of dysrhythmia.

Ischemia increases myocardial α_1-adrenergic receptors in association with augmented α-adrenergic responsivity. To determine whether lysophosphatides, which also accumulate in the ischemic heart, may mediate the increase in α-receptor number, the binding of ^{3}H-prazosin in intact myocytes was evaluated. Binding was saturable, reversible, stereospecific, with an affinity (K_d = 0.88 nM) typical of α_1-receptors. Incubation of myocytes for 2 min at 37° with Krebs buffer containing 100 μM lysophosphatidyl choline (LPC) increased receptor (R) number from 20,057 ± 242 to 36,271 ± 683 R/cell ($p < .005$) without significantly altering affinity. Incubation with 50 μM LPC for 5 min or 10 μM for 20 min also increased receptor number to 28,969 and 37,885 R/cell, respectively. Pretreatment of cells with phenoxybenzamine (10^{-7}M) blocked all specific binding. Nevertheless, subsequent treatment with LPC resulted in exposure of 13,070 R/cell. Triton X-100 (300 μM) was without effect. ^{3}H-QNB binding to muscarinic receptors was not altered by LPC. Thus, LPC produces a reversible, specific increase in α_1-adrenergic receptors, implicating this membrane active metabolite as a moiety potentially responsible for the increase in α_1-receptors during ischemia.

Previously, we found that α_1-adrenergic blockade with prazosin markedly attenuates arrhythmias associated with reperfusion of ischemic tissue in the cat, at a dose (0.5 mg/kg), three times the dose ratio 10 (DR_{10}) (i.e. that required to shift the agonist response by 1 log unit) of 0.175 mg/kg defined by the pressor response to phenylephrine. Other investigators recently reported no antiarrhythmic influence in the dog with a similar dose (1 mg/kg). The present study was performed to define the appropriate DR_{10} for prazosin in the dog compared with the cat and to assess the antiarrhythmic effect of an appropriate dose of prazosin during LAD occlusion for 25 min followed by reperfusion in 51 chloralose anesthetized dogs. The DR_{10} of prazosin in the dog (.006 mg/kg) was 29-fold lower than in the cat (0.175 mg/kg). Pretreatment with a dose of 0.020 mg/kg (3 times the DR_{10}) reduced the incidence of reperfusion-induced ventricular tachycardia (VT) and fibrillation (VF) from 69% to 37%, ($p < .05$). In treated animals who developed VT and VF, heart rate was significantly ($p < .05$) elevated (160 ± 18). Thus, prazosin is antiarrhythmic with reperfusion in the dog at appropriate doses selected based on pharmacological criteria under conditions which avoid reflex tachycardia.

Previously, isochronic and isovoltaic mapping with simultaneous transmural recording from multiple sites has been limited by the need for analysis of stable repetitive rhythms. In a new system developed at Washington University, electrograms from epicardial and transmural electrodes (500μ inter-electrode distance) are separately processed by a guarded signal conditioner that isolates, amplifies, filters, analog-to-digitally converts synchronously and stores the digital sample with 12 bits of resolutions at a 2-KHz sampling rate. Signals from up to 1920 separate sites can be obtained simultaneously with digital storage on a Sangamo Sabre IV high-density digital tape recorder (HDR). With 240 channels, continuous storage capability is 60 min with rapid interactive computer graphics that permit viewing of all electrogram data with computer-selected activation points via displays of the activation sequences at a time resolution of 0.5 msec. Data obtained from patients

in the operating room are transmitted by fiber optics to the HDR and PDP 11/34A computer and processed graphic information is transmitted back to the operating room. The system permits rapid 3-dimensional acquisition of the sequence of depolarization from a single beat, thus obviating the need for multiple repetitive beats. Currently, both experimental animal and clinical studies in the operating room are underway utilizing this unique system.

1. D. J. Sheridan, P. A. Penkoske, B. E. Sobel, and P. B. Corr, "α-adrenergic Contributions to Dysrhythmia During Myocardial Ischemia and Reperfusion in Cats," Journal of Clinical Investigation, vol. 65, p. 161, 1980.

2. P. B. Corr, J. A. Shayman, J. B. Kramer, and R. J. Kipnis, "Increased α-adrenergic Receptors in Ischemic Cat Myocardium: A Potential Mediator of Electrophysiological Derangements," Journal of Clinical Investigation, vol. 67, p. 1232, 1981.

3. P. B. Corr, D. W. Snyder, B. I. Lee, R. W. Gross, C. R. Keim, and B. E. Sobel, "Pathophysiological Concentrations of Lysophosphatides and the Slow Response," American Journal of Physiology, vol. 243 (Heart and Circ. 12), p. H187, 1982.

4. P. B. Corr, R. W. Gross, and B. E. Sobel, "Arrhythmogenic Amphiphilic Lipids and the Myocardial Cell Membrane," Invited Editorial for Journal of Molecular and Cellular Cardiology, vol. 14, p. 619, 1982.

A-10. Research Projects Utilizing the Isolated-Probe Data-Acquisition System

Personnel: H. D. Ambos, BCL
D. E. Beecher, BCL
S. R. Bergmann, Ph.D., Medicine
K. A. A. Fox, M.B., Ch.B., Medicine
B. Hughes, Ph.D., Medicine
H. Nomura, M.D., Medicine
B. E. Sobel, M.D., Medicine

Support: RR 01380
AM 20579
HL 13851
HL 17646

The research in this project is designed to define the kinetics of positron-emitting tracers that are potentially useful for the noninvasive characterization of myocardial perfusion, metabolism and adrenergic-receptor occupancy. Studies are conducted in isolated rabbit hearts perfused with washed sheep erythrocytes suspended in a modified Krebs-Henseleit buffer.

The methodology permits control of factors that can modify myocardial perfusion and metabolism. Studies are also conducted in anesthetized, open-chest dogs prior to the implementation of approaches of proven value in studies using positron-emission tomography.

The development of accurate, quantitative, noninvasive measurements of myocardial metabolism and perfusion is dependent on the thorough characterization of the factors that can influence tracer kinetics. Since fatty acid is the major fuel for the myocardium under normal circumstances, we currently utilize ^{11}C-palmitate to estimate myocardial metabolism. In addition to the external detection of myocardial time-activity curves via coincidence detection of emitted gamma photons in isolated hearts and via a β probe in open-chest dogs (with data fed to the Isolated-Probe Data Acquisition System) we measure a number of myocardial and metabolic functions such as left-ventricular pressure and arteriovenous differences of substrate simultaneously. Washout curves of ^{11}C-palmitate are analyzed and correlated with myocardial work and substrate utilization.

During the past year, we completed a study in 35 isolated hearts to determine whether myocardial fatty acid extraction can be quantified externally. We characterized myocardial time-activity curves after bolus injections of 50 μCi of ^{68}Ga-transferin into the aorta of retrogradely perfused isolated rabbit hearts. The use of transferin enabled us to define vascular transit time. Subsequently, myocardial time-activity curves were obtained after a bolus injection of ^{11}C-palmitate, which were then corrected for the vascular component. The resultant curve was biphasic, with an early rapid phase and a later slow phase. Effluent was analyzed for the proportion of injected ^{11}C-palmitate metabolized to $^{11}CO_2$.

In two groups of hearts, one made to perform low myocardial work (by adjustment of the left ventricular end-diastolic pressure and heart rate) and the second designed to perform a high level of myocardial work, myocardial extraction of ^{11}C-palmitate measured externally was 9.6 $\pm$ 3% and 17.7 $\pm$ 4.4% respectively. These values correlated closely with chemical extraction fraction measured directly from arteriovenous differences (8.7 $\pm$ 3.2% and 15.0 $\pm$ 4.6% respectively).[1]

When flow was decreased by 50% while cardiac work was held constant, net palmitate utilization remained constant while the externally measured extraction fraction increased from 10.9 $\pm$ 1.5% to 19.3 $\pm$ 4.4% (N = 5). Comparable changes were observed with direct chemical measurements (9.3 $\pm$ 2.0% to 17.8 $\pm$ 3.4%).

The results of these studies indicate that myocardial fatty-acid extraction can be quantified externally if the proportion of fatty acid being oxidized to CO_2 during the period of measurement is known.

We have extended these observations in the open-chest intact dog. We previously demonstrated that myocardial washout of extracted ^{11}C-palmitate is diminished with ischemia or hypoxia. These studies were performed using an extracorporeally perfused LAD coronary artery preparation in which flow

to the cannulated LAD can be adjusted. To define the quantitative influence of back diffusion of non-metabolized ^{11}C-palmitate, we used intracoronary tracer injection in open-chest dogs. Under baseline conditions 60 ± 13% of extracted ^{11}C-palmitate was oxidized to $^{11}CO_2$ and 10 ± 6% was liberated unaltered as ^{11}C-palmitate from the period of 1-20 minutes after tracer injection (n = 15). With ischemia created by reducing arterial flow to less than 20% of control (n = 6), or hypoxia (venous-blood perfusion at normal flow, n = 6), less than 25% of extracted ^{11}C-palmitate was liberated as $^{11}CO_2$, but greater than 17% appeared as unchanged ^{11}C-palmitate. With ischemia or hypoxia, back diffusion of tracer comprised 50 ± 24% of total efflux. The results of these studies showed that with hypoxia or ischemia, assessments of oxidation of fatty acid based on residue time-activity curves must be corrected for back-diffusion of initially extracted but non-metabolized fatty acid.[2]

Since alterations in myocardial perfusion play an important role in the etiology of cardiac disease, we are currently pursuing methods to quantify myocardial perfusion noninvasively. To determine whether radiolabeled water ($H_2{}^{15}O$) can be employed to quantify myocardial perfusion, we assessed myocardial blood flow with a 2-compartment model and compared results to those obtained with microspheres. To create flow inhomogeneity, a branch of the LAD coronary was ligated in 5 open-chest dogs. Radioactive microspheres were injected into the left atrium and $H_2{}^{15}O$ was then infused intravenously at a constant rate for 60 seconds and sequential arterial blood samples were drawn to define the arterial input curve. After 1 minute of infusion the heart was rapidly excised for direct determination of radioactivity in normal and ischemic zones. Flow determined with labeled water correlated closely with flow measured with microspheres (r = .81 over the flow range of .3-1.2 ml/gm/min, n = 56 determinations). It thus appears that myocardial blood flow can be estimated quantitatively with $H_2{}^{15}O$.[3]

Since the myocardium can use a number of substrates depending on relative states of perfusion and substrate availability, we are interested in evaluating whether the direct myocardial extraction of oxygen can be determined noninvasively. During the past year, we performed an initial study in open-chest, anesthetized dogs and monitored the myocardial time-activity curves, characterized with a β-probe after injection of ^{15}O-oxygenated blood as a bolus into the circumflex coronary artery. Myocardial blood flow and oxygen utilization were altered by infusion of dipyridamole (1 mg/kg, n = 5) and subsequently by ligation of a marginal coronary artery (n = 3). Myocardial blood flow and oxygen utilization were analyzed after equilibration under each set of conditions. Extraction fraction of ^{15}O was determined by back extrapolation of the monoexponential portion of the myocardial time-activity curve. Epicardial veins were cannulated for direct determination of oxygen utilization. Myocardial blood flow, calculated by analysis of the time-activity curve by a bolus injection of ^{15}O-labeled water varied between .1 and 3.4 ml/gm/min. Directly measured oxygen utilization varied from 0.01 to .213 ml O_2/gm/min. Correlation between oxygen utilization measured directly and utilization assessed externally was close (r = .83, n = 39 determinations). Thus, it appears that assessment of myocardial oxygen utilization can be accomplished with ^{15}O-oxygenated blood, a method potentially applicable to patients with the use of positron-emission tomography.[4,5]

It has been established that adrenoreceptor number and binding affinities may change in a number of cardiac disease states such as ischemia and congestive heart failure. To assess the feasibility of characterizing cardiac β-receptors noninvasively, an initial study was performed in the past year in 27 isolated, isovolumically beating rabbit hearts. ^{125}I-hydroxybenzylpindolol was added to the recirculating perfusate for 40 minutes. Uptake and release were monitored externally with a single gamma probe and the Isolated-Probe Data-Acquisition System. Specificity of binding was assessed by measuring the clearance of the ligand from the heart during perfusion with D- or L-isomers of adrenoreceptor agonists and antagonists. The L-isomers of epinephrine, norepinephrine and isoproterenol cause significant dissociation of the ligand from its binding sites, while no effect was seen with D-isomers or perfusate. Thus specific binding of ^{125}I-hydroxybenzylpindolol to cardiac β-receptors can be detected externally.[6] Hearts were then studied from rats, rabbits, and cats that had been treated with thyroid hormone, an intervention known to increase β-adrenoreceptor number. Hearts from animals treated with hormone exhibited increased uptake of the ligand detectable externally, and a 50% increase in receptor number by Scatchard analysis of ventricular membrane preparations. Specificity of binding was assessed by measuring the turnover rate during perfusion of the hearts with specific agonists and antagonists and these studies showed that a significant portion of the binding was displacable, and therefore specific. Thus increases in β-receptor number can be detected externally in an isolated perfused heart preparation.[7] Further development of this technique should enable in vivo detection of alterations in β-adrenoreceptor number in intact animals and ultimately in patients.

The studies performed in the past year with ^{11}C-palmitate have permitted a better understanding of factors that influence the uptake and efflux of this tracer in intact animals. Studies planned for the next year include characterization of the influence of diabetes on the kinetics of ^{11}C-palmitate and ^{11}C-glucose in isolated perfused hearts. In open-chest dogs we plan to evaluate the influence of reperfusion on the utilization of ^{11}C-palmitate. The studies with $H_2{}^{15}O$ and ^{15}O-oxygenated blood have been encouraging, and we are currently working on mathematical models so that we may extend their use to intact animals and positron-emission tomography. Finally, the results with β-adrenoceptor ligands have encouraged us to begin development of a positron-emitting ligand, and evaluation of this ligand in intact animals with positron-emission tomography.

1. H. Nomura, S. R. Bergmann, K. A. A. Fox, K. D. McElvany, M. J. Welch, and B. E. Sobel, "Myocardial Fatty Acid Metabolism Quantified Externally with ^{11}C-palmitate," Circulation, vol. 66, p. II-14, 1982 (abstract).

2. K. A. A. Fox, H. D. Ambox, H. Nomura, S. R. Bergmann, and B. E. Sobel, "The Importance of Back-Diffusion on Myocardial Kinetics of ^{11}C-palmitate," submitted to Circulation (abstract).

3. S. R. Bergmann, K. A. A. Fox, A. L. Rand, J. Markham, and B. E. Sobel, "Quantitation of Myocardial Perfusion with Radiolabeled Water," Journal of the American College of Cardiology, vol. 1, p. 577, 1983 (abstract).

4. K. A. A. Fox, S. R. Bergmann, A. L. Rand, H. D. Ambos, and B. E. Sobel, "External Measurement of Myocardial Oxygen Extraction with ^{15}O-labeled Oxygen," Journal of the American College of Cardiology, vol. 1, p. 577, 1983 (abstract).

5. K. A. A. Fox, S. R. Bergmann, A. L. Rand, H. D. Ambos, and B. E. Sobel, "External Measurement of Myocardial Oxygen Extraction with O-15-labeled Oxygen," Journal of Nuclear Medicine, vol. 24, p. 20, 1983 (abstract).

6. B. Hughes, S. R. Bergmann, and B. E. Sobel, "External Detection of β-adrenoreceptor Occupancy in Isolated Perfused Hearts," Circulation, vol. 66, p. II-206, 1982.

7. B. Hughes, S. R. Bergmann, P. B. Corr, and B. E. Sobel, "External Detection of Increases in β-adrenoreceptor Density in Isolated Perfused Hearts with I-125 Hydroxybenzylpindolol," Journal of Nuclear Medicine, vol. 24, p. 19, 1983 (abstract).

A-11. Analysis of Plasma CK Isoforms

Personnel: B. E. Sobel, M.D., Medicine
R. G. Gross, M.D., Ph.D., Medicine
J. Markham, BCL
A. W. Strauss, M.D., Pediatrics and Biochemistry

Support: HL 17646

Multiple MM CK subforms of individual isoenzymes (isoforms) appear in plasma after acute myocardial infarction. Early recurrent infarction is common (occurring in more than 20% of patients hospitalized in cardiac care units). This phenomenon is detectable with conventional criteria including re-elevation of MB CK after a decline from peak values. However, conventional methods of detection are limited by the relatively long half-lives in the circulation of the enzymatic markers used. Furthermore, the long half-lives make accurate dating of episodes of initial or recurrent infarction difficult.

Recently we have sought to characterize the kinetics of CK isoform conversion in vitro and in vivo by separating individual subforms by chromatofocusing and delineating the fractional contributions of each to total isoenzyme activity as a function of time after incubation in vitro or release into the circulation in vivo. Computer simulations have been developed to elucidate mechanisms of conversion with the use of kinetic models employing rate constants determined experimentally. Initial results demonstrate that kinetics are most closely simulated by a model which involves the sequential and irreversible alteration of one of the subunits to form a heterodimer

followed by conversion of the other subunit to form the homodimer. This kinetic model is being utilized to characterize results in intact dogs in whom purified isoforms are injected intravenously and to define the utility of CK-isoform analysis for dating of infarction and documenting early recurrence in animals subjected to coronary occlusion.

Additional studies are designed to characterize factors relevant to accurate dating of myocardial infarction in patients based on CK-isoform profiles as a function of time. Computer analysis will be utilized to determine the time of onset of infarction from sequential analysis of ratios of individual isoforms to total activity. The approach is designed to ultimately improve selection of patients suitable for early aggressive interventions such as surgical revascularization or coronary thrombolysis under conditions in which myocardial injury is sufficiently recent so that substantial salvage of jeopardized tissue can be anticipated.

A-12. Multicenter Investigation of Limitation of Infarct Size (MILIS)

Personnel:
A. S. Jaffe, M.D., Medicine
G. G. Ahumada, M.D., Medicine
H. D. Ambos, BCL
D. R. Biello, M.D., Radiology
T. L. Buettner, Medicine
K. W. Clark, BCL
E. D. Galie, R.N., Medicine
E. M. Geltman, M.D., Medicine
F. Lifshits, Medicine
J. M. McAninch, Medicine
J. P. Miller, BCL
S. R. Mumm, Medicine
D. S. Payne, Medicine
J. E. Pérez, M.D., Medicine
C. S. Ritter, Medicine
B. A. Siegel, M.D., Radiology
B. E. Sobel, M.D., Medicine
L. J. Thomas, Jr., BCL
A. J. Tiefenbrunn, M.D., Medicine
R. A. Wettach, Medicine
A. L. Ysaguirre, Medicine

Support:
RR 01380
HV 72941
Washington University

For the MILIS study, patients have been enrolled at Washington University since August 1, 1978. The goals of the study are to evaluate the efficacy of the administration of hyaluronidase and of propranolol in limiting the

extent of infarction. Data are being collected from five clinical centers including Washington University, Massachusetts General Hospital, The Medical Center Hospital of Vermont, Parkland Hospital in Dallas, and the Peter Bent Brigham Hospital of Boston. All data have been analyzed in core laboratory facilities in a blinded fashion. These facilities include a CK Reference Laboratory (at Washington University), a Holter Recording Analysis Reference Laboratory (at Washington University), an Electrocardiographic Reference Laboratory (at the Peter Bent Brigham Hospital), a Myocardial Infarct Scintigraphy Laboratory (at Parkland Memorial Hospital), a Radionuclide Ventricular Function Laboratory (at Massachusetts General Hospital), and a Pathology Reference Laboratory (at Duke University). Data from the clinical units and core laboratories are forwarded to the Data Coordinating Center (Research Triangle Institute; North Carolina) so that objectivity in data management and statistical analyses is assured.

The Washington University components of this project include the Clinical Unit, directed by the Clinical Unit Director, Dr. Allan S. Jaffe, the Creatine Kinase (CK) Core Laboratory, directed by Dr. Burton E. Sobel, and the Holter Core Reference Laboratory, directed by Dr. Lewis Thomas, Jr. The Principal Investigator for this study at Washington University is Dr. Jaffe.

The protocol for this trial, in brief, includes early identification of patients with acute myocardial infarction (<18 hours) and if electrocardiographic criteria for infarction are present, randomization of those patients who are <76 years of age and without significant illnesses that might affect their response to therapy. Patients are randomized to either a propranolol-acceptable or propranolol-contraindicated arm, and within those arms, therapy with either propranolol, hyaluronidase or placebo. Management of patients is standardized by a plan agreed to by all of the investigators prior to the study to provide maximum safety and yet to avoid potentially conflicting effects of unnecessary medications. Nonetheless, medical management of the patient remains the responsibility of his or her own private physician.

The endpoints of the study were defined prospectively and the primary endpoint chosen was infarct size index, as determined enzymatically, and the incidence of myocardial infarction between groups receiving hyaluronidase versus placebo (both Group A and Group B patients combined) and those receiving propranolol versus placebo, Group A patients only. Secondary endpoints included infarct size measured by ^{99m}Tc-pyrophosphate myocardial scintigraphy, electrocardiographic measures of infarction, changes in quantitative regional wall motion by radionuclide angiocardiography, mortality, ventricular ectopic activity and exercise performance. Other areas of scientific inquiry utilizing MILIS data include definition of the natural history of infarction, comparison of the techniques utilized in the study, the occurrence of recurrent infarction, the relationship of infarct size to peak total CK and MB CK activity, the incidence of persistently positive ^{99m}Tc-pyrophosphate myocardial scintigrams, changes in global ejection fraction with infarction and changes in R-wave over time.

The protocol has included radionuclide ventriculography and electrocardiographic mapping prior to therapy, treatment and then subsequent evaluation by CK infarct size estimated by serial values obtained over time and sequential

ST maps at 90 minutes, 72 hours, 10 days and 6 months. Radionuclide imaging initially was repeated at 90 minutes and at 10 days and 3 months, and pyrophosphate images were obtained on Day 2 through Day 3 and Day 5 through Day 7. Holter monitors were obtained in patients with infarction at Day 10 and 3 and 6 months and at 72 hours in patients where infarction was excluded. An exercise stress test was done at 6 months and follow-up mortality data collected by periodic calls every 6 months to assess mortal status.

Over the past 18 months, several components of the study have been discontinued. On January 26, 1982 the 90-minute radionuclide ventriculogram, 90-minute ECG recordings and the ambulatory Holter monitors obtained at 3 and 6 months were discontinued. On December 16, 1982, the pyrophosphate image obtained at 6 months was deleted. Effective May 1, 1983, all Holter monitor studies were discontinued along with the 12-lead electrocardiogram and radionuclide ventriculograms at 3 months, all pyrophosphate scintigraphy and the follow-up visit at 3 months is made by telephone contact. In addition, on February 1, 1983, the Policy Board mandated that propranolol administration be discontinued. The Principal Investigators were notified and reviewed the data which confirmed that propranolol had neither beneficial nor detrimental effects within the limitations of the study. Accordingly, although stratification into Group A and Group B was to continue, no further patients would receive propranolol. Further elucidation of the data upon which these decisions were made was restricted until appropriate manuscripts can be prepared.

Since the MILIS clinical unit began operations in August of 1978 to the last Progress Report deadline, 6,242 patients have been admitted to the Barnes Hospital Coronary Care Unit and 43% were screened for the MILIS protocol. Two-hundred and five patients have been enrolled and the contracted level of 50 patients per year has been maintained after initial difficulties in 1978. During the interval from March 1, 1982 through February 29, 1983, 53 patients (more than the promised enrollment) were randomized. More than half of these were randomized within 8 hours of symptoms and a smaller percent (13%) compared to previous years were found not to have suffered acute myocardial infarction on the basis of local analysis of MB CK determinations.

Our studies continued to be of high quality with greater than 90% of all studies accomplished despite frequent malfunctions of the QRS map acquisition cart (ICR cart) and the need for frequent use of the back-up system. Some studies were missed due to the underlying illness of the patient or the need for an emergent medical management. Follow-up evaluations, supervised by Dr. Edward Geltman and Ms. Liz Galie, were attempted in 98% of the patients and 66% of the tests were accomplished. Two percent of the tests could not be accomplished because of medical complications and in 32% of instances, patients refused. Overall, 82% of the studies mandated were accomplished.

The Creatine Kinase Core Laboratory has been equally active and as of March 1, 1983, had analyzed blood samples from 929 patients from the study. Eighty-six percent had suffered acute myocardial infarction. In patients with acute myocardial infarction, infarct size could be estimated

in 84%, in part due to the recently completed study documenting the ability to estimate infarct size from incomplete creatine kinase curves. These activities necessitated 32,918 assays in addition to purifications of specific isoenzymes to provide antigens to be used in radioimmunoassays and for quality-control determinations. The creatine kinase core laboratory has invariably had the lowest delinquency rate and the highest performance of any of the core facilities.

The Holter Core Laboratory which was discontinued in May of 1983 had processed 1,721 recordings over the course of the study. The reproducibility of their data was excellent with a correlation coefficient for duplicate analysis of 0.96 for the log PVC rate and 87% agreement for PVCs and runs. The study has agreed to continue some support of the Holter Core Laboratory for follow-up analysis until the study is terminated in July of 1984.

A-13. Multicenter Post Infarction Program

Personnel: R. J. Krone, M.D., Jewish Hospital
J. R. Humphrey, R.N., Jewish Hospital
R. E. Kleiger, M.D., Jewish Hospital
J. P. Miller, BCL
L. J. Thomas, Jr., BCL

Support: RR 00396
RR 01380
HL 22982

The purpose of the Multicenter Post Infarction Program (MPIP) has been described in previous reports (PR 15, A-19, PR 16, A-19, PR 17, A-15, and PR 18, A-15). The analysis of the Holter recordings was completed in 1982, thus discharging BCL's active responsibilities. The data clean-up for the first year follow-up has been completed and a report of the prognostic indicators for myocardial infarctions has been prepared. Continued follow-up through patient questionnaires (PR 18, A-15) continues. Further analysis of the collaborative database continues with incorporation of the longer follow-up using non-BCL personnel.

A-14. Noninvasive Localization of Electrical Activity in the Heart

Personnel: R. M. Arthur, BCL
H. D. Ambos, BCL
M. E. Cain, M.D., Medicine

Support: RR 00396
RR 07054
Washington University

This project was undertaken to validate the electrical-center method (PR 18, A-11) for finding the origin of cardiac electrical activity from measurements made solely on the body surface. In recent years new techniques for understanding and controlling arrhythmias have been introduced which employ catheter electrodes to pace the heart. We intend for these invasive studies, which we will perform, to serve as the basis for assessing the accuracy of the electrical-center method for noninvasively finding origins of cardiac activity.

The first phase of this project has been completed. We wrote FORTRAN programs which determine the electric center of the heart from measurements of torso geometry and from maps of electrocardiographic surface potentials at any instant during the cardiac cycle. Torso geometry and surface electrocardiograms, however, have not been measured as yet.

Instead, we have begun to study the significance of the electrical center before repeating procedures to calculate it.[1] The electric-center method is not likely to replace invasive studies before surgery or during life threatening situations. Rather its most important benefit probably will be in its ability to follow the progress of recovery from a myocardial infarction noninvasively. The question then is how sensitive is the electrical-center method to changes in small regions of the heart. To approach this question we calculated the electric center for the 20-dipole heart model developed by Cuffin and Geselowitz[2] and have begun to study the effect of modifications to the Cuffin model on the electric center.

1. R. M. Arthur, D. B. Geselowitz, S. A. Briller, and R. F. Trost, "The Path of the Electrical Center of the Human Heart Determined from Surface Electrocardiograms," Journal of Electrocardiography, vol. 4, pp. 29-33, 1971.

2. B. N. Cuffin and D. B. Geselowitz, "Studies of the Electrocardiogram Using Realistic Cardiac and Torso Models," IEEE Transactions on Biomedical Engineering, vol. BME-24, pp. 242-252, 1977.

A-15. Model Development for Cardiac Diastolic Mechanics

Personnel: J. Markham, BCL
M. R. Courtois, M.A., Medicine
P. B. Kurnik, M.D., Medicine
P. A. Ludbrook, M.D., Medicine

Support: RR 01380
HL 17646
HL 25430
Barnes Hospital
Washington University

During the past year, our studies of cardiac diastolic mechanics (PR 18, A-14), i.e., the passive mechanical properties of the left ventricular (LV) muscle and chamber, have continued with emphasis on defining the relationship between stress on the wall and the radius of the cavity. Stress can be derived as a function of strain and strain as a function of radius yielding a stress-radius relationship which can be used to estimate elastic stiffness of the LV muscle.

Values for stress are computed from several variables including intra- and extra-cavitary pressures, measured in the cardiac catheterization lab using catheter-tip micromanometers, and the cavity radii calculated from the area and the longest chord of the ventricle as measured from single-plane angiographic silouettes. To reduce the errors associated with the angiographic measurements, the area and the major chord were smoothed by fitting to a fourth-order polynomial. Using this procedure, the resultant stress-radius curves computed for a set of four patients had several points of inflection rather than the convex, monotonically increasing shape usually seen in this type of stress data. The same curvature was seen in stress-radius curves calculated without the smoothing step, suggesting that the curvature was inherent in the measured data or the calculation procedure rather than an artifact of the smoothing process.

The algorithms for calculating stress, including the smoothing procedure, were implemented on the Hewlett-Packard 5600M Catheterization Data Analysis computer system to facilitate processing of large numbers of patient data. Data for a set of 32 patients for whom multiple studies had been performed were analyzed and the stress-radius curves plotted. For these 32 patients, 12 untreated and 20 treated with nifedipine, all tracings of the LV chamber and measurements of LV wall thickness were performed by the same person. The resultant stress-radius curves did not generally have more than one point of inflection, suggesting that the variations in curvature seen in the first set of data may be related to insufficient accuracy in the measurement of the dimensions of the ventricle.

Efforts to fit the stress-radius relationship with a function derived from known properties of stress and strain will continue during the next year. At present, our model assumes an average stress and strain can be used to represent the true stress and strain of the ventricle. More realistically,

the ventricle does not contract and expand uniformly in all directions, and stress and strain may vary accordingly. A model which includes these regional variations may be required in order to obtain a meaningful estimate for elastic stiffness of the ventricle.

A-16. SCOR Patient Information Database

Personnel: K. B. Schechtman, BCL
H. D. Ambos, BCL
E. D. Galie, R.N., Medicine
E. M. Geltman, M.D., Medicine
A. S. Jaffe, M.D., Medicine
J. Markham, BCL
B. E. Sobel, M.D., Medicine

Support: RR 00396
RR 01380
HL 17646

The Specialized Center for Research (SCOR) database (PR 17, D-5) currently contains information pertinent to 874 patients who suffered acute myocardial infarction (AMI). The variables contained in the AMI database describe the patient's cardiovascular history, in-hospital course, and long-term progress via follow-up examinations. Each patient is followed every three months for a year following the index episode and then yearly thereafter. The data records are entered into the Interdata 7/16 computer system in the coronary care unit (CCU) and then transferred via magnetic tape to the IBM System/370 at the University's Computing Facilities. There, a permanent SAS database is maintained in order to address a variety of clinical questions. Future plans include a reconsideration of all aspects of the data entry process. This review will determine whether more efficient data entry procedures can be instituted.

In order to assess the effect of platelet factor 4 (PF4) on the pathogenesis of AMI, 52 patients from the SCOR database with AMI and 69 controls were considered. Initial mean PF4 was 6.2 ± 3.2 ng/ml (SD) in the AMI group compared with 5.1 ± 2.4 in the non-MI group. Serial values were consistently normal without regard to the presence of chest pain (N = 34), mild heart failure (n = 20) or pericarditis (n = 9). No evidence was found which suggests that PF4 increases in association with transmural infarction or that elevations presage complications potentially attributable to platelet aggregation. This is contrary to several other reports.

Other studies (A-8) which involve the SCOR database include a consideration of factors which contribute to the low survival of diabetics with AMI; a study of the effect of streptokinase on clot lysis in AMI patients; and a consideration of the effect of nifedipine on infarct size as determined by positron-emission transaxial tomography.

B. Quantitative Imaging: Ultrasonic Tissue Characterization

Although ultrasound has proven to be a useful source of diagnostic information, results of examinations based on current ultrasonic methods are primarily qualitative and pictorial. In a collaborative effort with Cardiology and the Department of Physics work has continued on methods of tissue characterization via ultrasound. Our overall goal is to use ultrasound for the non-invasive identification of tissue pathologies within two-dimensional images of tissue properties. Specific objectives of this effort are 1) to investigate the magnitude and character of anisotropy in tissue, 2) to systematize the representation of the ultrasonic field and to reduce the data needed to describe that field by determining the moments of the spatial distribution of energy over the receiver aperture, 3) to seek improvement in measurement capability of imaging systems via interactive, adaptive beamforming for both linear and variable-aperture transducer arrays, 4) to test the hypothesis that quantitative images based on intrinsic tissue properties can be produced with reflected ultrasound, and 5) to construct a digital multiprocessor system to perform post-echo estimation of ultrasonic attenuation, phase velocity and backscatter in two dimensions.

Quantitative images based on ultrasonic tissue properties have been made at the BCL for several years using transmitted ultrasound with a multiple-frequency tomographic reconstruction system. In the past year considerable effort has been put forth to expand our processing capability for addressing problems in ultrasonic tissue characterization with reflected ultrasound. We have established a processing environment with a computer interfaced to the tomographic scanner, an existing digital echocardiograph, and a newly acquired array processor (B-7). This environment supports both experimental studies of tissue samples and simulations of tissue and transducer models.

Three experimental studies were conducted last year. A cyclic variation in backscatter from canine myocardium has been found in which the maximum backscatter occurs near the end of diastole, and the minimum occurs near the end of systole (B-1). Spectral filtering and generalized substitution techniques were applied to backscattered ultrasound to improve estimates of attenuation and to assess the computational burden in generating two-dimensional images of tissue properties (B-2). An excised, intact dog heart was scanned with a two-dimensional receiving array (B-3). The first three spatial moments of the acoustic field at the receiver, which represent the incident intensity, lateral deviation, and mean beamwidth of the field, respectively, were calculated to find how much they changed with a change in density of elements in the transducer array.

Three simulations were also performed. We demonstrated that the transfer function, impulse response, and equivalent circuit for a dispersive model of soft tissue can be computed from measurements of the magnitude of the frequency response alone (B-4). The diffraction-limited performance of linear phased arrays in pulse-echo mode was simulated to provide estimates of the size of tissue regions which could be characterized at locations throughout the field of view of the array (B-5). We are also developing a phenomenological model for the acousto-electric transfer function of transducer elements (B-6).

B-1. Variation of Ultrasonic Parameters of Muscle with State of Contraction and Its Influence on Quantitative Imaging

Personnel: J. G. Mottley, BCL
R. M. Glueck, M.D., Medicine
J. G. Miller, BCL
J. E. Perez, M.D., Medicine
B. E. Sobel, M.D., Medicine

Support: RR 01362
HL 17646
HL 28998

Recent experience in our laboratory indicates that the backscatter from canine myocardium changes during the cardiac cycle in a way which correlates well with the electrocardiogram[1,2] and with the left ventricular pressure. Averaged over the entire left ventricle, the backscatter varies by approximately 4 dB during the cardiac cycle, with the maximum occurring near end diastole, and the minimum occurring near end systole. These cyclic variations exhibit marked differences in magnitude from one region of the heart to another (see Figure 1.1), and are modified by the induction of ischemia (see Figure 1.2).[3] Also, our preliminary experiments have shown that the attenuation of skeletal muscle (frog gastrocnemius) changes during contraction, with attenuation increasing with contraction and decreasing during relaxation. These findings have possible clinical significance as future tissue signatures, while imposing complications on quantitative measurements of the attenuation anisotropy of muscle, and on any attempts to quantitatively image the beating heart. As a necessary prelude to the continuation of our studies on the anisotropy of soft tissues, (PR-18, B-4, B-5, B-6), we have undertaken a study to investigate the relation of ultrasonic parameters of skeletal and cardiac muscle to the state of contraction of that muscle.

The current study consists of several stages. First, the variation of attenuation coefficient with contraction of skeletal muscle is being studied in an isolated frog gastrocnemius muscle preparation which allows electrical stimulation of the sciatic nerve to induce either twitch or tetany of the muscle. As stated above, preliminary results of this study indicate that the attenuation coefficient of muscle increases with contraction, an effect which could simulate the observed variation of backscatter in which the apparent backscatter decreases with contraction. Research to elucidate the relationship between the force of the contraction and the magnitude of the change in attenuation is continuing.

The protocol for the study includes the measurement of ultrasonic backscatter, from the same muscle preparation, as a function of the state of contraction, including compensation of the apparent backscatter for the attenuation of intervening muscle tissue. Following these studies, techniques for measuring the attenuation from backscattered signals will be used

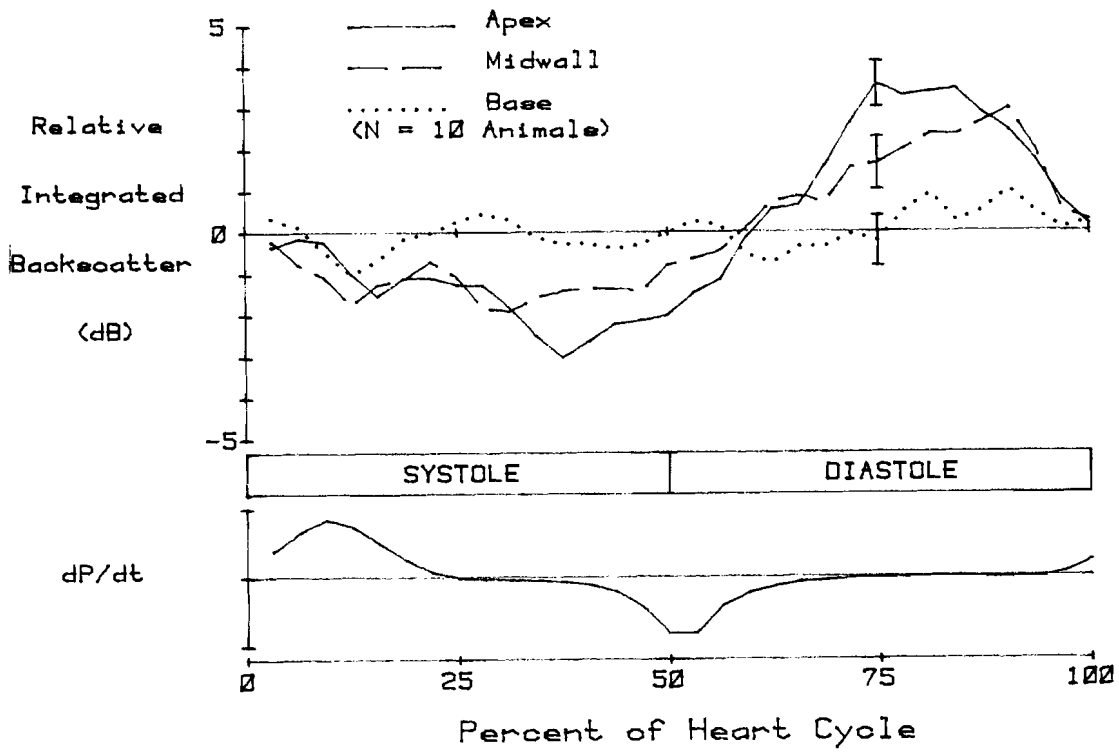

Figure 1.1. The cyclic variation of backscatter from canine heart over the cardiac cycle. The upper panel shows integrated backscatter as a function of time from three regions of the heart; apex, midwall, and base. The lower panel shows the time derivative of the left ventricular pressure, recorded simultaneously with the backscatter. The peak-to-trough variations are largest near the apex (magnitude of variation approximately 5.5 dB.), intermediate in the midwall (magnitude approximately 4 dB.), and the smallest near the base (magnitude 1 dB.)

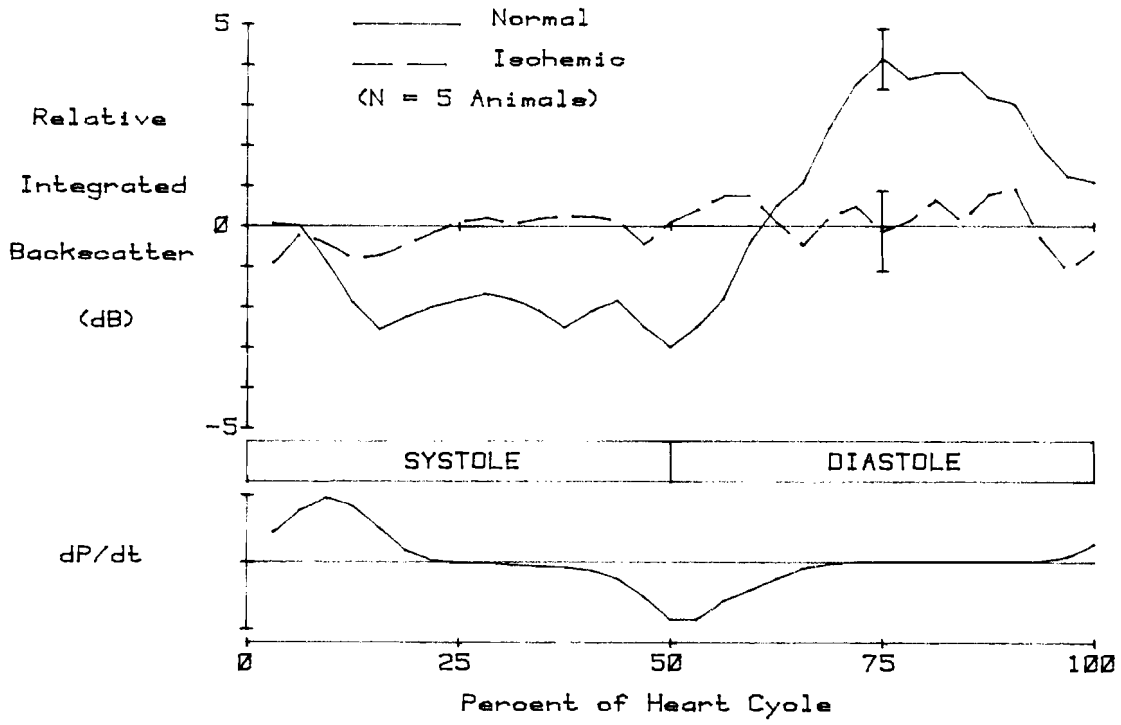

Figure 1.2. The cyclic variation of backscatter from normal and ischemic canine heart over the cardiac cycle. The upper panel shows integrated backscatter as a function of time from the apical region of five canine hearts prior to and during ischemia. The lower panel shows the time derivative of the left ventricular pressure, recorded simultaneously with the backscatter. The cyclic variations present in the normal heart are strongly diminished by the induction of ischemia.

to measure the attenuation throughout the cardiac cycle in normal and ischemic canine hearts. These measurements will permit determination of the variation of the ultrasonic backscatter of myocardium over the cardiac cycle.

1. E. I. Madaras, B. Barzilai, J. E. Perez, B. E. Sobel, and J. G. Miller, "Systematic Variations of Myocardial Ultrasonic Backscatter During the Cardiac Cycle in Dogs," Ultrasonic Imaging, vol. 4, p. 185, 1982 (abstract).

2. B. Barzilai, J. E. Perez, E. I. Madaras, J. G., Miller and B. E. Sobel, "The Influence of Contraction on Ultrasonic Backscatter of Normal and Ischemic Myocardium," Circulation, vol. 66, p. II-30, 1982 (abstract).

3. J. G. Mottley, R. M. Glueck, J. E. Perez, B. E. Sobel, and J. G. Miller, "Regional Differences in the Cyclic Variation of Myocardial Backscatter and Modification by Ischemia," Ultrasonic Imaging, vol. 5, p. 183, 1983 (abstract).

B-2. Spectral Filtering and Generalized Substitution for Estimating the Slope of Attenuation from Backscattered Ultrasound

Personnel: P. H. Johnston, BCL
R. M. Glueck, M.D., Medicine
J. G. Miller, BCL
J. E. Perez, M.D., Medicine
B. E. Sobel, M.D., Medicine
L. J. Thomas, III, M.S., Physics

Support: RR 01362
HL 17646
HL 28998

In recent years some progress has been reported by other laboratories in estimating the slope of attenuation in tissue from backscattered ultrasound. Two major frequency-domain techniques are a generalized substitution technique, where the power spectra from signals emanating from tissue closer to the transducer are logarithmically compared with power spectra from deeper tissues,[1,2,3,4] and a method based on the effective shift in center frequency of a Gaussian-shaped pulse upon suffering attenuation.[5-10] These methods have produced promising results in applications where it is possible to average over long path lengths and/or many independent views of the organ under interrogation, such as the abdominal organs (liver, spleen). For quantitative imaging, extensive spatial averaging is not desirable, so techniques must be sought to derive more localized estimates of the slope of attenuation than these. We have begun[11] by investigating the feasibility of applying to small tissue volumes the generalized substitution method used by Kuc to characterize liver.[1]

The basic process of generalized substitution is shown graphically in Figure 2.1. In panel (a) is shown a digitized rf backscattered A-scan from an excised dog left ventricular wall. The ultrasonic beam was incident upon the epicardium. Panel (b) displays two gated and windowed segments of this trace, and the thickness of tissue between the two scattering volumes is indicated. The log power spectra of these segments are shown in panel (c). Note the considerable structure in the spectra, quite different from the smooth broadband spectrum of the transmitted pulse. This structure occurs because the signals arise from a volume distribution of scatterers rather than a single smooth interface. The difference between these spectra is the jagged curve in panel (d). This curve should represent the total loss of signal due to the attenuation coefficient, and thus should be a straight line. A linear least squares fit line is shown, the slope of which is used to estimate the slope of attenuation. The maximum likelihood estimate of the slope along the entire A-line is calculated to be the mean of estimates made using all possible independent pairs of segments separated by $d = (x_2 - x_1)$.

Based on a one-dimensional random reflector model, Kuc has derived a statistical description for the errors expected in maximum likelihood estimates of slope along a single A-scan line.[12] In this formulation the variance of slope estimates derived from entire A-scan lines has the form

$$\text{var } [\beta] = \frac{\sigma^2}{4Nd^2 \sum_{i=1}^{m} F_i^2} \qquad (1)$$

where d is the distance between the scattering volumes in each pair, N is the number of pairs of tissue echoes averaged to form the slope estimate and is a function of d, F_i are the m harmonic frequencies lying within the bandwidth of the transducer, and σ^2 is the mean squared deviation of log spectral differences about a straight line (see panel (d) of Figure 2.1). The mean squared deviation is a constant depending only on the assumed randomness of the scattering distribution. It was calculated by Kuc to be equal to 62.1 dB^2. The variance in equation (1) is minimized with respect to separation d at $d = 2L/3$, where L is the total thickness of tissue. At this value of d the variance becomes

$$\text{var } [\beta] = \frac{Cs\sigma^2}{L^3 \sum_{i=1}^{m} F_i^2} \qquad (2)$$

where C is a constant, and s is the distance between adjacent segments. The quantity s has a lower limit set by considerations of sampling and independence of segments. The L^{-3} dependence in equation (2) presents a strong hindrance to applying this method to pixels of small size.

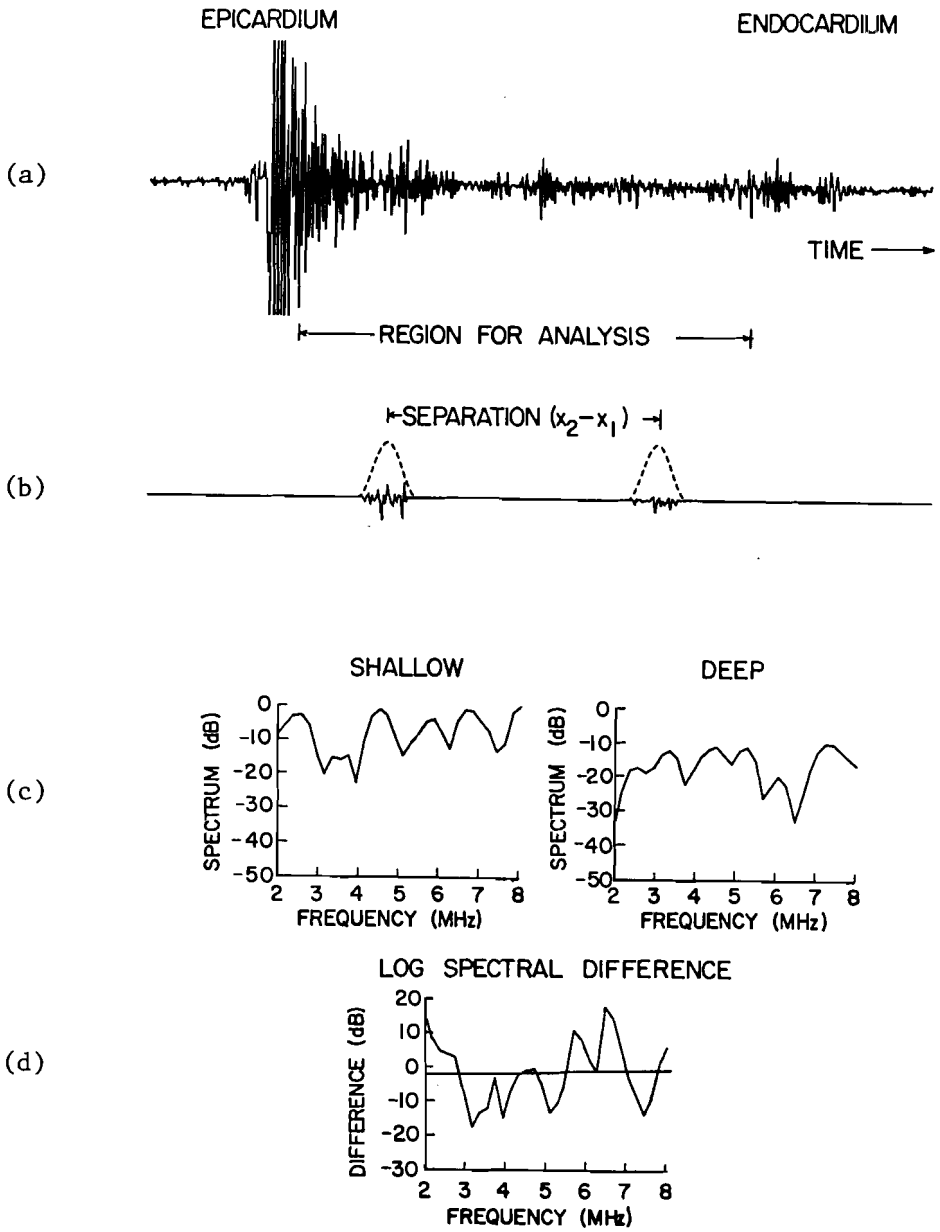

Figure 2.1. A typical rf A-line from our data set is shown in panel (a). The backscattered signals from a representative shallow tissue volume and a deeper volume are shown in panel (b). The roundtrip separation between the tissue volumes is shown where x_i is the depth of the i^{th} tissue volume. The log power spectra of these two signals are shown in panel (c), and their difference in panel (d). This log spectral difference represents the loss of signal due to attenuation by the tissue between the scattering volumes. Also present are sizable fluctuations due to interference effects and phase cancellation. The least squares line fit to this curve is shown, the slope of which is an estimate of the slope of attenuation of the tissue. The slope estimates made in this fashion from all independent pairs of signals gated from the region for analysis are averaged to form the maximum likelihood estimate of slope for the tissue along this A-line.

The variance in equation (2) can also be reduced by means of the frequency summation in the denominator. The use of higher frequencies will increase the value of each F_i, and the use of higher bandwidths will increase the number m of frequencies used to calculate the sum. This tendency to higher frequencies and bandwidths is limited by Nyquist sampling theory, and perhaps even more strongly by the increasing attenuation of tissue with frequency, which effectively reduces the maximum range of the image.

A final approach to minimizing the variance of slope estimates is to attack the factor σ^2. As mentioned earlier, this deviation is caused by interference effects and phase cancellation due to the presence of many randomly located scatterers within the volume of tissue delineated by the length of the segments and the lateral extent of the ultrasonic beam. As an approach toward reducing this contribution to the variance in slope estimates, we investigated the effects of smoothing the power spectra prior to estimating slope. The methods used were lag windowing (i.e. windowing the autocorrelation function, which is the Fourier transform of the power spectrum)[13] and power cepstral windowing (i.e. windowing the power cepstrum, which is the Fourier transform of the log power spectrum).[14] Figure 2.2 shows graphically the application of cepstal windowing to the segment spectra in Figure 2.1. Panel (a) reproduces the spectra. The Fourier transforms of the logged spectra are shown in panel (b). Panel (c) displays the cepstra after application of a tapered window around the center. Such a window removes all rapid fluctuations in the power spectrum, leaving only the smoothly varying spectra shown in panel (d). The difference spectrum formed from these smoothed spectra is shown as the solid curve in panel (e) with the unfiltered result from Figure 2.1 shown for comparison as the dashed curve. Considerable improvement is seen in σ^2, the mean squared deviation about a line fit, due to the cepstral windowing. The results of lag windowing are qualitatively similar to those shown here.

Figure 2.3 displays the standard deviation of maximum likelihood estimates of slope made over 328 rf A-lines (12 mm each) from the hearts of 5 dogs, using cepstral windowing. One independent variable is the roundtrip separation (2d) between segments. The other variable is the effective width of the cepstral window applied to each spectrum, defined as the inverse of the 3dB width of a smoothing filter. As predicted by Kuc, the minimum standard deviation is seen to occur for separation equal to about two thirds the total tissue thickness. As a function of cepstral window width, we see that for larger windows (i.e. little filtering) there is only slow reduction in standard deviation. There is a point where application of narrower windows causes the deviation to plummet to zero. Unfortunately, the mean value of slope estimates plummets along with the standard deviation, because the spectrum is being filtered too strongly. The results for lag windowing agree with the cepstral results to within a few percent.

Figure 2.4 summarizes the mean and standard deviation of slope estimates made without filtering (direct), and using cepstral and lag windowing. For comparison the mean and standard deviation of the slope measured in transmission using a phase insensitive acoustoelectric receiver is shown for the same 328 tissue sites. For the three backscatter-based methods,

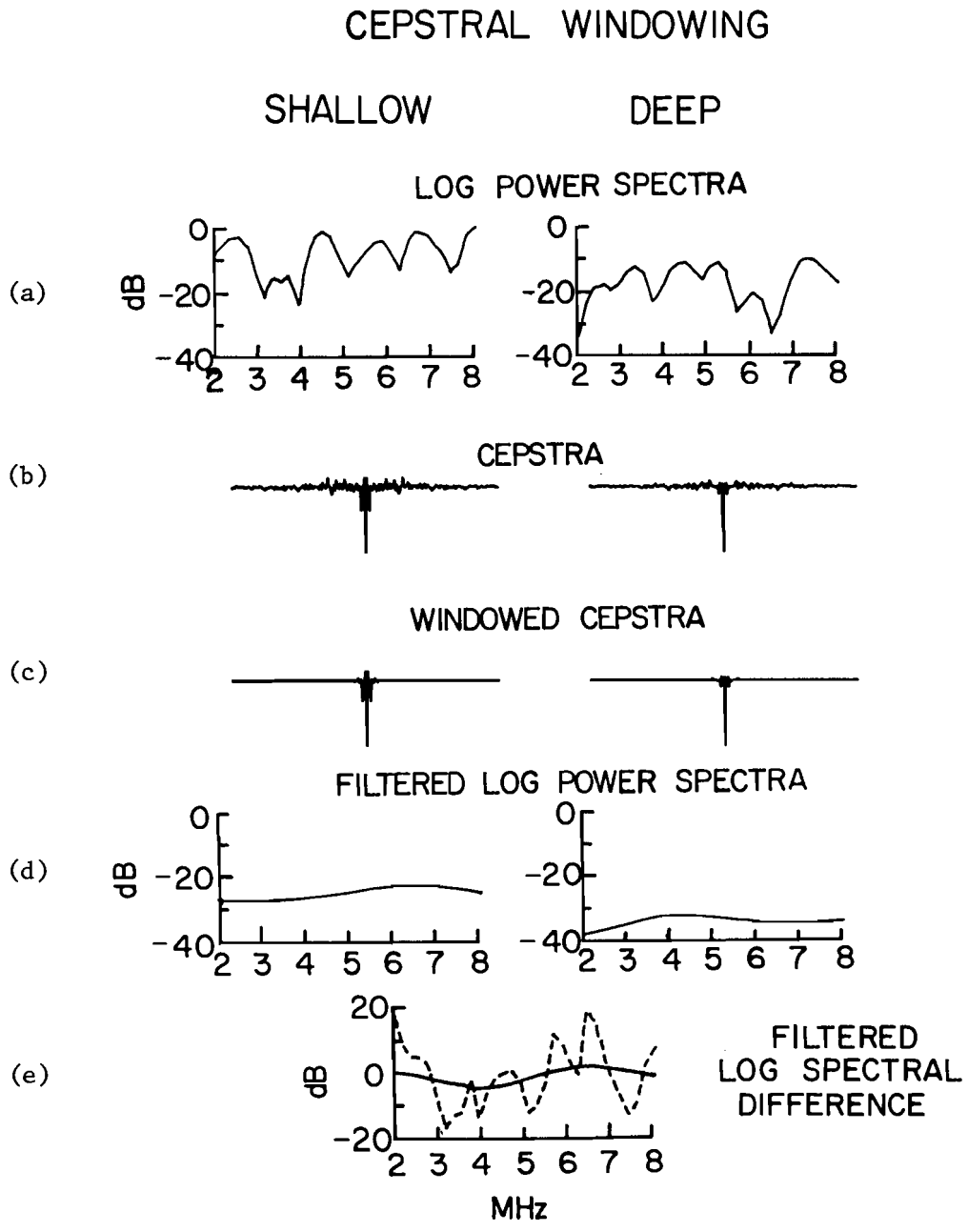

Figure 2.2. A graphical demonstration of cepstral windowing is presented here. Panel (a) reproduces the log power spectra from Figure 2.1(c). The Fourier transforms of these spectra are the power cepstra shown in panel (b). These are seen to be symmetrical about zero, in the center of each trace. A window is applied to these cepstra which zeros cepstral components outside a certain cutoff (panel (c)) and the results are Fourier transformed to produce smoothed log power spectra as seen in panel (d). The log spectral difference formed from these spectra is the solid curve in panel (e), compared with the dashed curve which is the unfiltered spectral difference. The smoother log spectral difference may represent an improved estimate of the attenuation due to the tissue.

DOGS N4-N8, CEPSTRAL WINDOWING

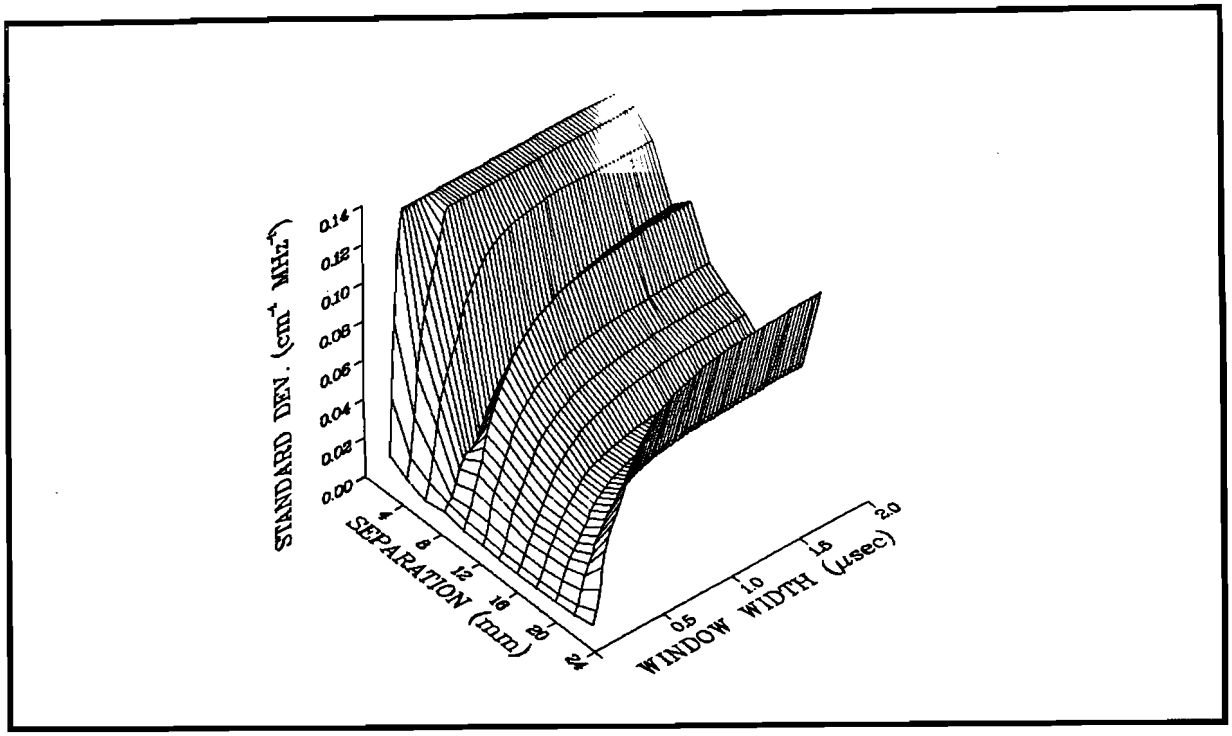

Figure 2.3 Here is shown the standard deviation of experimental maximum likelihood estimates of slope as a function of roundtrip separation and cepstral window width. The standard deviation is seen to be minimum with respect to separation near two thirds the maximum separation, as predicted by the model of Kuc. As a function of window width, we see that larger window widths (milder filtering) have small effect while beyond a certain point, smaller widths (stronger filtering) cause the deviation to plummet to zero. This same shoulder occurs in a plot of mean value of slope, and indicates that the filtering is too severe and that entire spectra are being averaged, producing zero slope. An "optimum" window width was chosen in this shoulder region for purposes of comparison. The results for lag windowing were quantitatively similar to these.

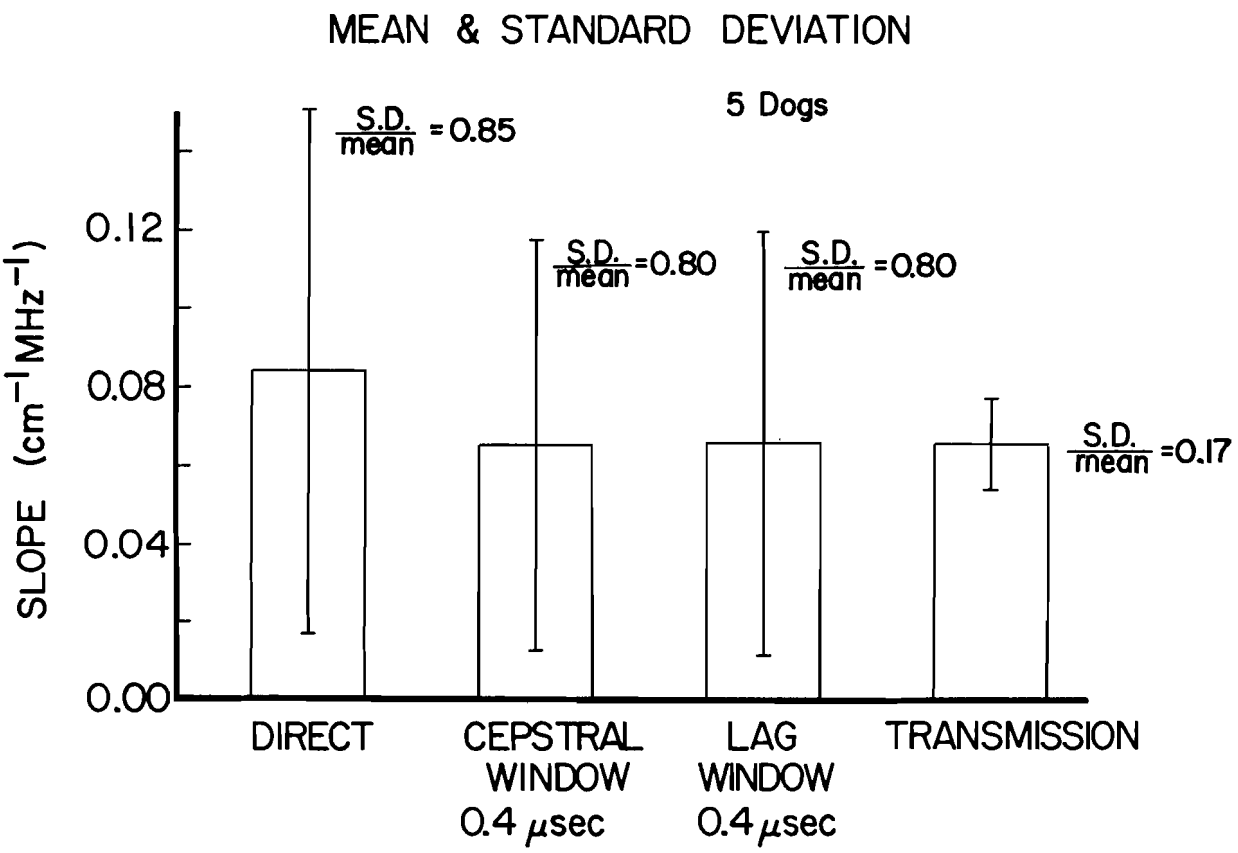

Figure 2.4. Here we show the results for "optimum" conditions for direct generalized substitution, cepstral windowing, and lag windowing, compared with the results of the transmission measurements of slope made at the same tissue sites. The separation chosen for the backscatter-based estimates was 16 mm. or two thirds the maximum 24 mm. and the lag and cepstral window widths were chosen on the shoulder of the curve seen in Figure 2.3. We note that the spectral smoothing produced little improvement in the ratio of standard deviation to mean (i.e. the coefficient of variation) over the estimates made without smoothing. For the backscatter based methods the S.D./mean was over 4 times that for the more reliable transmission measurements.

the separation between segments is 2/3 the total tissue thickness, and lag and cepstral windows were chosen on the shoulder of the curve in Figure 2.3. As can be seen from the figure, the maximum likelihood estimates of slope all exhibit fractional errors greater than 4 times that of the transmission measurements. Thus we see that the windowing methods applied here begin to filter too strongly before they produce much improvement in slope estimation. With the large error bars displayed here, one might wonder if generalized substitution could be useful in practice. What follows is a thought experiment using these results and some published values for slope in heart.

In a previous study using a transmission technique, we found values of slope of attenuation of 0.075 $cm^{-1}MHz^{-1}$ for normal dog myocardium and in the same hearts 0.2 $cm^{-1}MHz^{-1}$ for scar due to infarct. Assuming that the 328 sites represented in our data adequately define the distribution of errors for backscatter-based estimates of slope and that the ratio of standard deviation to mean is 0.85 as shown in Figure 2.4, the number of measurements necessary to distinguish between these tissues can be estimated using the method of Kuc. Assigning a standard error according to $\sigma/\sqrt{N}$, to achieve a statistical confidence of 95%, i.e. $p < 0.05$, a minimum of 25 measurements each of normal and infarcted tissue would have to be averaged for 12 mm of tissue.

Consider now the application of this technique to a two-dimensional scan of 120 A-lines with a range of 24 cm. Table (1) summarizes the following discussion. The above thought experiment was conducted using the statistics found for tissue elements 12 mm in length, and thus correspond to image pixels 12 mm long. The L^{-3} dependence in the variance then implies the need for $8 \times 25 = 200$ measurements per pixel for pixels 6 mm long, and $64 \times 25 = 1600$ measurements per pixel for 3 mm pixels. Using a two-dimensional imaging system operating at 30 frames/sec such data could be acquired by digitizing every A-line for 0.8 sec to achieve 12 mm pixels, 6.7 sec for 6 mm pixels, or 53.3 sec for 3 mm pixels. Assuming 8-bit digitization at 20 MHz rate, these acquisition schemes would require 19.2, 154, and 1229 MBytes storage, respectively, unless some processing were done in parallel. Dividing each pixel into segments as done in our experiment, and using the FPS-100 array processor to perform 64-point FFT's at 0.3 msec each, the time to form a complete image of slope would be greater than 3 minutes for 12 mm pixels, more than 30 minutes for 6 mm pixels, and over 5 hours for 3 mm pixels. Clearly, while the acquisition times seem modest, the requirements for memory and processing time are prohibitive.

Table 1

Pixel Size (mm)	12	6	3
#Measurements	25	200	1600
Acquire Time (sec)	0.8	6.7	53.3
# Lines Recorded	3000	24000	192000
MBytes Stored	19.2	154	1229
#FFT's/Pixel	10	6	4
#Pixels/Line	20	40	80
Imaging Time	>3 min	>30 min	>5 hr

However, we see tissue characterization as a complementary process to conventional imaging, not necessarily a replacement. Therefore we propose that regions of interest may be delineated based on conventional two-dimensional images, and these regions may then be scrutinized using tissue characterization techniques such as generalized substitution slope estimation. Let's consider the application of this technique to a region consisting of 20 A-lines wide by the pixel length. This situation is outlined in Table 2. The reduced number of lines drastically reduces acquisition times. Storing only the amount of digitized rf necessary for the analysis cuts down the mass storage requirements to achieveable levels. As seen in the table, the time to characterize a half-centimeter resolution cell is about 10 seconds. One might expect to be able to characterize 50 to 75 such regions during a 30-minute clinical session. Such quantitative information in conjunction with the information available in conventional images should lead to much improved characterization of the state of the myocardium.

Table 2

Pixel Size (mm)	12	6	3
#Measurements	25	200	1600
Acquire Time (sec)	0.14	1.1	8.9
# Lines Recorded	500	4000	32000
MBytes Stored	0.18	0.7	2.8
# FFT's/Region	10	6	4
Imaging Time (sec)	>1.5	>7.2	>38

1. R. Kuc, "Clinical Application of an Ultrasound Attenuation Coefficient Estimation Technique for Liver Pathology Characterization," IEEE Transactions on Biomedical Engineering, vol. BME-27, no. 6, pp. 312-319, June 1980.

2. J. P. Jones and M. Behrens, "In Vivo Measurement of Frequency Dependent Attenuation in Normal Liver, Pancreas, and Spleen," Ultrasonic Imaging, vol. 3, p. 205, 1981 (abstract).

3. F. L. Lizzi and M. E. Elbaum, "Clinical Spectrum Analysis Techniques for Tissue Characterization," National Bureau of Standards Special Publication 525, Washington, D.C., pp. 111-119, 1979.

4. J. Ophir, N. F. Maklad, and R. H. Bigelow, "Ultrasonic Attenuation Measurements of In Vivo Human Muscle," Ultrasonic Imaging, vol. 4, pp. 290-295, 1982.

5. R. Kuc, M. Schwartz, and L. V. Micsky, "Parametric Estimation of the Acoustic Attenuation Coefficient Slope for Soft Tissue," 1976 Ultrasonic Symposium Proceedings, pp. 44-47, 1976.

6. A. C. Kak and K. A. Dines, "Signal Processing of Broadband Pulsed Ultrasound: Measurement of Attenuation of Soft Biological Tissues," IEEE Transactions on Biomedical Engineering, vol. BME-25, no. 4, pp. 321-344, July 1978.

7. L. Ferrari, J. Jones, V. Gonzalez, and M. Behrens, "In Vivo Measurement of Attenuation Based on the Theory of Gaussian Pulse Propagation," Ultrasonic Imaging, vol. 4, p. 172, 1982 (abstract).

8. M. Fink and F. Hottier, "Short Time Fourier Analysis and Diffraction Effect in Biological Tissue Characterization," Acoustical Imaging, vol. 12, pp. 493-503, 1983.

9. M. O'Donnell, "Effects of Diffraction on Measurements of the Frequency-Dependent Ultrasonic Attenuation," 82CRD217, General Electric Technical Information Series (D).

10. J. Ophir and P. Jaeger, "Spectral Shifts of Ultrasonic Propagation Through Media with Nonlinear Dispersive Attenuation," Ultrasonic Imaging, vol. 4, pp. 282-289, 1982.

11. P. H. Johnston, L. J. Thomas, III, and J. G. Miller, "A Comparison of Methods for Estimating Attenuation Using Backscattered Ultrasound," Ultrasonic Imaging, vol. 4, p. 177, 1982 (abstract).

12. R. Kuc, M. Schwartz, N. Finby, and F. Dain, "Statistical Estimation of the Acoustic Attenuation Coefficient Slope for Liver Tissue from Reflected Ultrasonic Signals," National Bureau of Standards Special Publication 525, Washington D.C., pp. 125-132, 1979.

13. D. E. Robinson, "Computer Spectral Analysis of Ultrasonic A-Mode Signals," National Bureau of Standards Special Publication 525, Washington D.C., pp. 281-286, 1979.

14. J. Fraser, G. S. Kino, and J. Birnholz, "Cepstral Signal Processing for Tissue Signature Analysis," National Bureau of Standards Special Publication 525, Washington, D.C., pp. 287-295, 1979.

B-3. Determination of the Spatial Moments of Acoustic Fields

Personnel: P. H. Johnston, BCL
J. G. Miller, BCL
L. J. Thomas, III, M.S., Physics

Support: RR 01362
HL 17646
HL 28998

We have proposed that the first few spatial moments of an acoustic field represent a limited variable set which contains most of the information that is meaningful for quantitative imaging. Specifically, the first three moments, M_0 through M_2, allow one to calculate the incident intensity (PR-18, B-4), lateral deviation, and mean beamwidth of the acoustic field. Random and systematic variations in the ultrasonic properties of tissue degrade the effective resolution element for imaging, therefore accurate determination of the low order spatial moments of an ultrasonic beam transmitted through tissue does not require the high information density that sampling theory suggests (i.e. samples spaced by less than one-half wavelength). Thus, the spatial moments are a limited set of parameters which may be used for quantitative imaging, and may be measured with a sparse array.[1,2]

To experimentally test the hypothesis that the spatial moments of the field due to an inhomogeneous source may be accurately determined using a sparsely sampled array, an excised, intact dog heart was scanned. A two-dimensional receiving array was simulated by mechanically scanning a $\sim$ 1 mm diameter CdS acoustoelectric transducer over a 2 cm square region with 1 mm spacing. Data were taken using 3-μsec gated 2-MHz tone bursts. Spatial moments calculated using all elements represented the dense array results. We were able to calculate the results that would have been obtained with wider spacing by dropping appropriate elements from the moments calculations. A comparison of measurements of attenuation based on M_0 for element spacings of 1, 3, and 5 mm is shown in Figure 3.1, panel b). Panel a) shows schematically the region covered by the scan line, that is, from a water-only path to a path approximately normal to the heart walls and centered on the left ventricle. Note that the 1 and 3 mm results are in quantitative agreement, while there is degradation in the accuracy for the 5 mm measurement. In

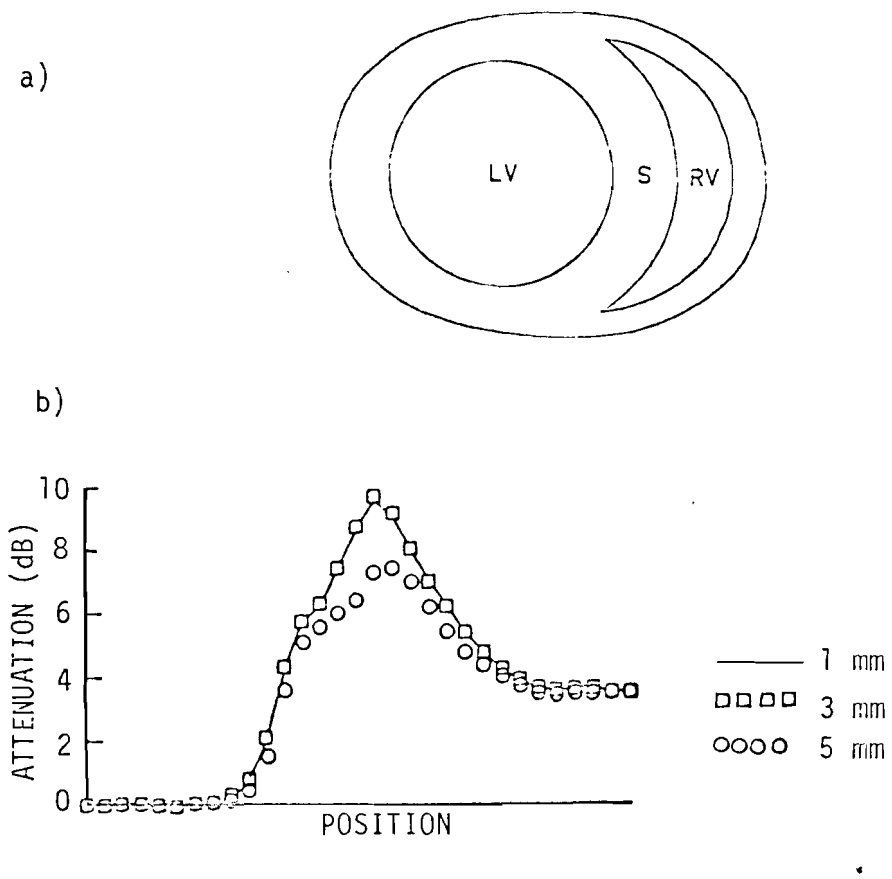

Figure 3.1. Panel a) depicts the approximate geometry of the heart during the experiment. Panel b) compares scan lines of the attenuation based on the zeroth spatial moment (M_0) over a two dimensional receiving array for 1, 3, and 5 mm element spacing in the array.

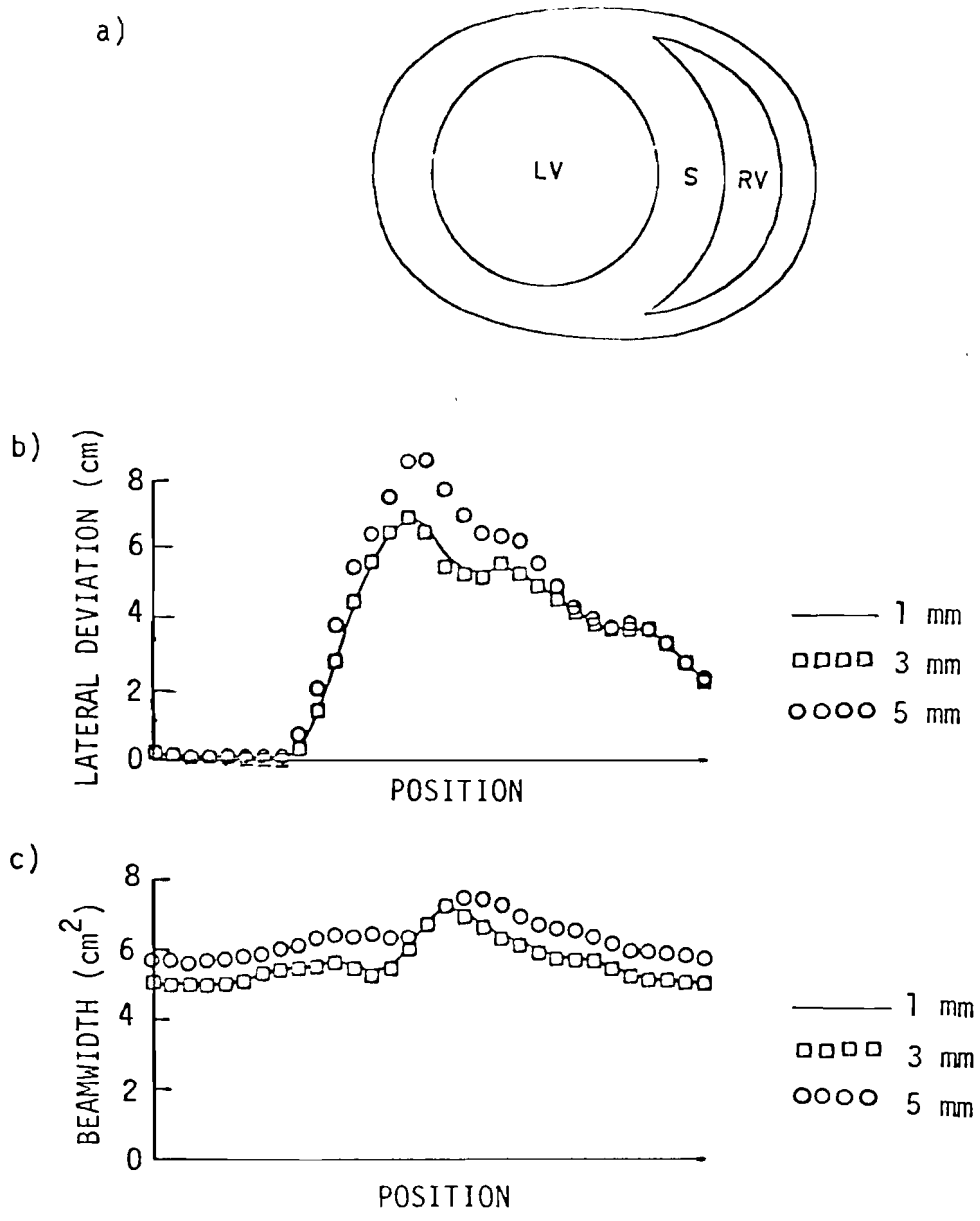

Figure 3.2. Panel a) depicts the approximate geometry of the heart. Scan lines of the lateral deviation (refraction) of the beam based on the first spatial moment (M_1) as shown in panel b). Results are presented for 1, 3, and 5 mm element spacing in the two dimensional receiving array. Scan lines of the mean square beamwidth based on the second spatial moment (M_2) are shown in panel c). Results are shown for 1, 3, and 5 mm element spacing in the receiver.

panel b) of Figure 3.2 we compare the lateral deviation introduced into the beam, as measured by M_1, for 1, 3, and 5 mm element spacing. Again there is quantitative agreement between results obtained with 1 and 3 mm spacing. Panel c) of Figure 3.2 compares the beamwidth as measure with M_2 for 1, 3, and 5 mm spacing. As before, the agreement between the 1 and 3 mm results is good. These results imply that the low order moments of acoustic fields which have propagated through inhomogeneous media may be accurately determined using a sparse receiver array.

The data used to calculate the scan lines shown in Figure 3.1 required far too much time to acquire for this approach to be used for practical investigations. Therefore, we have examined other techniques to simulate arrays of small elements. Initially we are proposing to simulate a two-dimensional array by using a small, fixed single element, and scanning a received beam across the receiver element, rather than scanning the element across the beam. This approach has been chosen in order to avoid the problems of fabricating multiple elements and associated electronics which need to be individually characterized. At the present time, the techniques we have examined introduce significant distortions in the phase fronts when the acoustic field is diverted by one centimeter. We are, however, confident that a technique which allows an incident acoustic field to be moved across a receiver element offers the most practical solution to studying techniques employing two-dimensional arrays without actually fabricating the arrays.

1. T. A. Shoup, G. H. Brandenburger, and J. G. Miller, "Spatial Moments of the Ultrasonic Intensity Distribution for the Purpose of Quantitative Imaging in Inhomogeneous Media," Proceedings of the 1980 IEEE Ultrasonics Symposium, pp. 973-978, 1980.

2. T. A. Shoup, "Quantitative Ultrasonic Imaging for Materials Characterization," Ph.D. dissertation, Washington University, St. Louis, Missouri, 1981.

B-4. A Pole-Zero Model for the Transfer Function of Soft Tissue

Personnel: R. M. Arthur, BCL

Support: RR 01362

Although soft tissue is both dispersive and inhomogeneous, conventional B-scan imaging systems focus signals received by phase-sensitive, linear arrays as if tissue were a homogeneous medium. Estimates of attenuation from such a beamformer are corrupted by the perturbation of wavefronts across the array caused by tissue inhomogeneities. Previously we described two nearly equivalent causal models for representing dispersion and inhomogeneity

in tissue. One, which is based on the Hilbert transform,[1] assumes attenuation is a linear function of frequency (PR 16, B-5). The other, a pole-zero model, can be synthesized from the magnitude of the frequency response of any experimental data (PR 17, B-4).

The pole-zero model was applied to three sets of experimental data reported in the literature. These were hemoglobin solutions,[2] dog myocardium at different temperatures,[3] and infarcted dog myocardium.[4] A single-pole matched the data to within a few percent. Phase velocity predicted by the single-pole model was within the measurement error for hemoglobin solutions. In contrast to the Hilbert model for which predicted phase velocity depends on the logarithm of frequency and consequently is not well-behaved at very low frequency, the phase velocity of the single-pole model has a sigmoid dependence on frequency.

Another advantage of the single-pole model is that it has an equivalent circuit representation. The equivalent circuit is a low-pass filter consisting of resistance in series with the parallel combination of resistance and capacitance. The input drives the whole circuit and the output is taken across the parallel network. This circuit gives the minimum-phase part of the transfer function of tissue. A pure delay serves as the all-pass function which completes the transfer function.

In almost every case, refinement of the single-pole model by the addition of either a zero or another pole resulted in the placement of the zero or pole, not on the negative real axis as expected, but well outside the range of the data on the frequency axis. Additional measurements below 1 MHz and above 10 MHz are needed to refine the tissue model beyond that of a single-pole model.

The pole location of the single-pole model is a relaxation frequency. This frequency was inversely proportional to the concentration of hemoglobin, directly proportional to the temperature of dog myocardium, and inversely proportional to the collagen content of dog myocardium. Furthermore, the single-pole model provided a fit of these data which was comparable to a straight line fit, i.e., to the slope of attenuation. Additional data are needed to determine whether or not relaxation frequency may be a more meaningful descriptor of attenuation of tissue than the slope of attenuation.

1. K. V. Gurumurthy, and R. M. Arthur, "A Dispersive Model for the Propagation of Ultrasound in Soft Tissue," Ultrasonic Imaging, vol. 4, pp. 355-377, 1982.

2. E. L. Carstensen, and H. P. Schwan, "Acoustic Properties of Hemoglobin Solutions," Journal of the Acoustical Society of America, vol. 31, pp. 305-311, 1959.

3. M. O'Donnell, J. W. Mimbs, B. E. Sobel, and J. G. Miller, "Ultrasonic Attenuation of Myocardial Tissue: Dependence on Time after Excision and on Temperature," Journal of the Acoustical Society of America, vol. 62, pp. 1054-1057, 1977.

4. M. O'Donnell, J. W. Mimbs, and J. G. Miller, "The Relationship Between Collagen and Ultrasonic Attenuation in Myocardial Tissue," Journal of the Acoustical Society of America, vol. 65, pp. 512-517, 1979.

B-5. Diffraction-Limited Lateral Resolution of Linear Phased Arrays

Personnel: R. M. Arthur, BCL

Support: RR 01362
Washington University

An important consideration in the production of an image based on ultrasonic tissue parameters is the size of the image element. The size of the region over which a given tissue parameter is characterized should be comparable to the resolution limit of the imaging system. A major factor in the determination of that resolution is the diffraction pattern of the transducer. The diffraction pattern is set by the geometry of the transducer and by the excitation used to drive the transducer.

After evaluation and correction of a simulated performance model for a linear phased array (PR 17, B-5), the simulation was used to map the lateral resolution in the field of view ($\pm$ 45 degrees) of a linear array.[1] The simulation included the effects of array geometry, form of the excitation (assuming a unity transfer function for the transducer), focus mode, and steering angle of the beam. The array was composed of rectangular elements. The dimension of the elements and the number of elements in the array was variable. We simulated the transmission, scattering, and reception of ultrasound in a homogeneous medium. All scatterers were point targets. Resolution was determined by scanning two point targets while varying their spacing until the received signals showed two peaks.

Resolution was calculated for a 2.25 MHz, 16-element array at ranges of 2, 5, 10, 15, and 20 cm from 0 to 45 degrees off the axis of the array. Element width and spacing were 0.9 and 1.8 wavelengths, respectively. Element height was 12 wavelengths. Excitation was a 2.25 MHz sine wave with an exponential envelope whose time constant was about one cycle of the center frequency. Both point focus on transmit and receive and axicon focus on transmit and receive were studied. Targets were scanned as their separation was increased from zero in 1/4 or 1/2 mm increments depending on their position in the field of view. From these scan data the separation required to distinguish the peaks in the received signal from the trough at the midpoint between the two targets can be estimated. Clearly resolution is dependent upon the size of the peak signal which can be distinguished from the surrounding scan. When this threshold was set at 3 dB, resolution for point focus ranged from less than 1.0 mm on axis at a range of 2 cm to 12 mm at 45 degrees off axis at a range of 20 cm. Resolution in the far field (> 7 cm) increased in inverse proportion to the square of the cosine of the angle of the field point offset by 20 degrees.

We plan to compare the results of our performance model with measurements on 32-element, 3.5- and 5-MHz linear arrays, which we are now evaluating. It is expected that the results of this study will provide us with important guidelines in the construction of images intended to show tissue properties.

1. R. M. Arthur, "Diffraction-Limited Lateral Resolution of Ultrasound Phased Arrays," Ultrasonic Imaging, vol. 5, p. 191, 1983 (abstract).

B-6. The Electroacoustic Transfer Function of Linear Transducer Arrays

Personnel: R. M. Arthur, BCL
M. L. Seiger, B.S., Electrical Engineering

Support: RR 01362
Washington University

Transducer behavior must be taken into account in order to make quantitative ultrasonic measurements. This work is intended to extend the description of transducer arrays for use in tissue characterization, which was begun with the study of the resolution of linear phased arrays used for ultrasonic imaging (PR 17, B-5; PR 18, B-3). In that earlier study we simulated the effects of array geometry, form of the excitation at the transducer surface, focus mode, and steering angle to assess the performance of a transducer array. Here we report the development of a phenomenological model for the transfer function of the transducer, i.e. the relation between the electrical excitation and the motion of the face of the transducer.

The transfer function of a transducer is dependent on frequency, the angle at which energy is propagated or received, and must include cross-talk from nearby elements. To characterize the transfer function of a given transducer we propose to model each element as a collection of facets or sub-elements. We plan to measure the pressure patterns generated at the transducer face by scanning across the face with a hydrophone in a water tank. We expect to be able to infer pressure at a distance from the motion of the facets, using the impulse-response method employed in the existing performance model (PR 17, B-5).

We are now attempting to find the transfer function for 3.5- and 5-MHz, 32-element linear arrays, composed of piezo-electric material. Mounting hardware and driver circuitry are complete. We are modifying our digital echo system (PR 15, A-17) to serve as receiver. With this system ultrasonic waveforms can be sampled at a 20-MHz rate with 8 bits of precision then sent to a TI 980B minicomputer. Using this approach, measurements can be readily compared to calculated behavior. The writing of FORTRAN programs to implement our phenomenological transducer model is underway.

B-7. The Processing Environment for Ultrasonic Tissue Characterization

Personnel: R. M. Arthur, BCL
R. W. Hagen, BCL
R. E. Hermes, BCL
P. H. Johnston, BCL
J. G. Miller, BCL
J. G. Mottley, BCL
D. W. Stein, Jr., BCL
L. J. Thomas, Jr., BCL

Support: RR 00396
RR 01362
RR 01380

A substantial effort went into modifying and upgrading the processing environment (PR 18, B-1) for the tissue-characterization project this year. Separate efforts were integrated into a single system which has much greater processing capability than existed previously. The two major systems which were combined were a scanner for tomographic reconstruction of ultrasonic tissue properties and a digital system for ultrasonic imaging. Both made use of a digital scan converter developed at the BCL and an electrostatic printer/plotter.

The scanner at BCL, which has a counterpart in the Department of Physics, was supported by two PC-1200 minicomputers. One was used for acquisition and analysis of scanner data. The other was used for off-line analysis. The digital imaging system consists of a dual-microprocessor acquisition system interfaced to a TI 980B minicomputer.

The new processing environment is built around a DEC LSI-11/23 microcomputer. Over the past year we interfaced the LSI-11/23 to: 1) two existing 50-megabit disk drives to provide operating system and programming storage; 2) an FPS 100E array processor to significantly improve execution time for both simulations and data analysis; 3) a 9-track, industry-compatible tape drive for mass storage; 4) the electrostatic printer/plotter; 5) an existing digital plotter; 6) an existing graphics terminal; and 7) an IEEE 488 bus for communication with peripherals such as the scanner. Four serial lines were added for a total of six for communication with, for example, the TI 980B, the USD (universal storage device), and to the TERRANET local-area network. Memory of the LSI-11/23 was increased from 96 K to 128 K bytes. A 16-bit parallel input/output interface was installed to give lines for experiment control and to interface to the scan converter.

Development of driver software for the Biomation recorder, the stepper motors, and other hardware of the scanning system continues. We hope to be able to fully support acquisition and analysis of scanner data on the LSI-11/23 and thereby retire the PC-1200 minicomputers next year. Simulations for the study of limitations of ultrasonic imaging such as the linear-array performance model, which were developed on the TI 980B, have been moved to the LSI-11/23. These simulations run about three times faster on the LSI-11/23 than on the TI 980B. The TI 980B system will still be used as

experimental controller and for intermediate analysis and storage in the linear-array studies. The single-channel digital acquisition system is being modified for use in the array studies (PR 15, A-17). Its previously fixed sample rate, and number of samples per ultrasonic pulse, and choice of its depth compensation function will be under control of the TI980B.

C. Quantitative Imaging: Radiation-Treatment Planning

About half of all cancer patients are treated with ionizing radiation during the course of their disease. The goal of radiation therapy is to control the malignant disease by delivering adequate radiation dose to the tumor volume while at the same time minimizing the dose to the surrounding normal tissues.

Treatment planning in radiotherapy is a procedure for appropriately selecting and placing sources of ionizing radiation so that their combined effect yields an optimal spatial distribution of absorbed dose in a particular region of the body. In the presence of tissues with inhomogeneous scatter and absorption properties, presently available methods of absorbed-dose calculation are approximate. Thus, their real utility in radiation-treatment planning is limited. We and several other groups have recognized for a number of years that computed tomography (CT) may provide a remedy for the shortcomings of present methods of absorbed-dose calculation. Accordingly, in 1977 we began the development of a new approach to absorbed-dose prediction that is based on fundamental physical principles and takes advantage of the information provided by CT scanning.

The general objectives of this project are to develop algorithms for computing three-dimensional dose distributions within inhomogeneous tissue regions valid for radiation fields of arbitrary shape and size, and to apply advanced computer technology in the implementation of these algorithms to render them clinically useful. A specific objective of our initial work was to investigate the validity of the physical basis of the mathematical model on which our method depends. For this purpose, we compared theoretical values of absorbed dose computed via our method with some published experimental results. We have largely completed this phase of our work, having obtained computed absorbed doses in excellent agreement with values obtained by measurements in phantoms. With the physical validity of our method thus established, we have shifted our attention to the second of our original objectives, that of applying advanced digital hardware to render our method useful in a clinical setting.

Work accomplished during the past year in developing accurate procedures based on fundamental physical principles for computing absorbed dose in clinical radiation-treatment planning is described in this section. An algorithm that is an extension of our previously validated model has been developed (C-1). This algorithm has been tested against demanding phantom measurements and its performance has been found to be superior even to that of its predecessor. Work accomplished and planned for an integrated-circuit implementation of the new algorithm is summarized (C-3). Finally, we describe (C-2) our efforts in developing clinically useful three-dimensional simultaneous displays of computed dose distributions superimposed on the corresponding CT-scan images.

C-1. Algorithm Development for Radiation-Treatment Planning

Personnel: F. U. Rosenberger, BCL and Computer Systems Laboratory
B. Emami, M.D., Radiology
K. B. Larson, BCL
C. A. Pérez, M.D., Radiology
J. A. Purdy, Ph.D., Radiology
D. W. Stein, Jr., BCL
J. W. Wong, Ph.D., Radiology

Support: RR 00396
RR 01380
Washington University

A new three-dimensional dose-calculation algorithm[1-3] has been implemented in RATFOR for the VAX-780. This new algorithm differs in several respects from the one reported previously (PR 13, I-3; PR 14, G-6; PR 15, G-4; PR 16, B-14; PR 18, B-8). The original delta-volume algorithm is shown in Equation 1 and the new one in Equation 2.

$$dose_i = primary_i + \sum_j atten_{ij} * primary_j * \rho_j * del3r_{ij} \quad (1)$$

$$dose_i = primary_i + \sum_j [atten_{ij} * primary_j * \rho_j * augfs_{ij}] + \frac{smm_i}{smw_i} \left[smw_i + \sum_j \frac{\bar{\rho} - \rho_j}{\bar{\rho}} * \Delta h_j \right] \quad (2)$$

In the above,
i is the point at which dose is calculated;
j is a volume element from which scatter contribution to point i is calculated;
$dose_i$ is the total dose at i;
$primary_i$ is the primary dose at i;
$atten_{ij}$ is the attenuation from j to i in the medium with respect to the attenuation in water;
$primary_j$ is the primary intensity at j;
$del3r_{ij}$ is the scatter contribution from a volume element at j to i in water;
$augfs_{ij}$ is the first scatter plus the part of second scatter that acts like first-scatter contribution from a volume element j to i in water;
smw_i is the residual multiple scatter contribution to dose at i in water due to a source at infinity;

smm_i is the residual multiple-scatter contribution to dose at i in a homogeneous medium with electron density equal to the average electron density of the medium due to a source at infinity;
$\bar{\rho}$ is the average electron density, relative to that in water, in the treatment medium;
ρ_j is the electron density, relative to that in water, at j; and
Δh_{ij} is the change, in water, of residual multiple scatter dose contribution at i due to a small void at j.

The first term, the primary contribution to dose, is the same in both equations. The second term has the same form in both equations but represents all scatter contribution to dose in Equation 1 and is based on measured data in water. The second term in Equation 2 represents the calculated first scatter and the part of the second-order scatter that behaves like first scatter. The third term in Equation 2 contains the residual multiple scatter in water and is obtained by subtracting the calculated values used in the second term from measured values in water. It is modified by the contribution to residual multiple-scatter dose of a small void at each volume element in water, and by the change in this dose with respect to water for a homogeneous medium with the same average electron density as the treatment medium. It thus matches measured data exactly for a homogeneous medium of any electron density or for water with a single small inhomogenity. For other conditions, small errors exist, but these are a small part of the residual scatter dose contribution which itself, for cobalt-60, is only about 10% of the total dose. The backscatter is calculated explicitly in Equation 2 instead of being lumped into the scatter from the level of the dose calculation as it was with implementations of Equation 1 that were reported previously.

Equation 2 is used to find correction factors by taking the ratio of the dose in the treatment medium to the dose in water. In this way systematic errors in the calculation are at least partially cancelled. Figure 1 shows a comparison between measured and calculated values for two different phantom geometries. In each case, except one for which changes of a few millimeters in position would give agreement, the maximum error in the correction factor is less than three percent and is usually less than one percent.

The VAX-780 implementation is an interactive program that calculates correction factors at user-specified points in the treatment medium. Facilities are provided for interactive specification of phantom densities and geometries, treatment volumes, and treatment beam parameters. A user's manual and programmer's guide have been completed to provide documentation for use and for maintenance of the system. It is programmed in RATFOR for ease of documentation and maintenance and uses the Q and A program (F-12) for user input and control. The system is particularly convenient for algorithm evaluation since dose at a few points can be easily and quickly calculated for comparison with measured values. About 40 hours are required to calculate all the doses on a 1-cm grid in a 25- by 25- by 25-cm treatment volume. However, dose at a single point is calculated in a few seconds.

Plans for next year include further verification of the dose-calculation accuracy on additional regular phantoms and on the RANDO Phantom, investigation

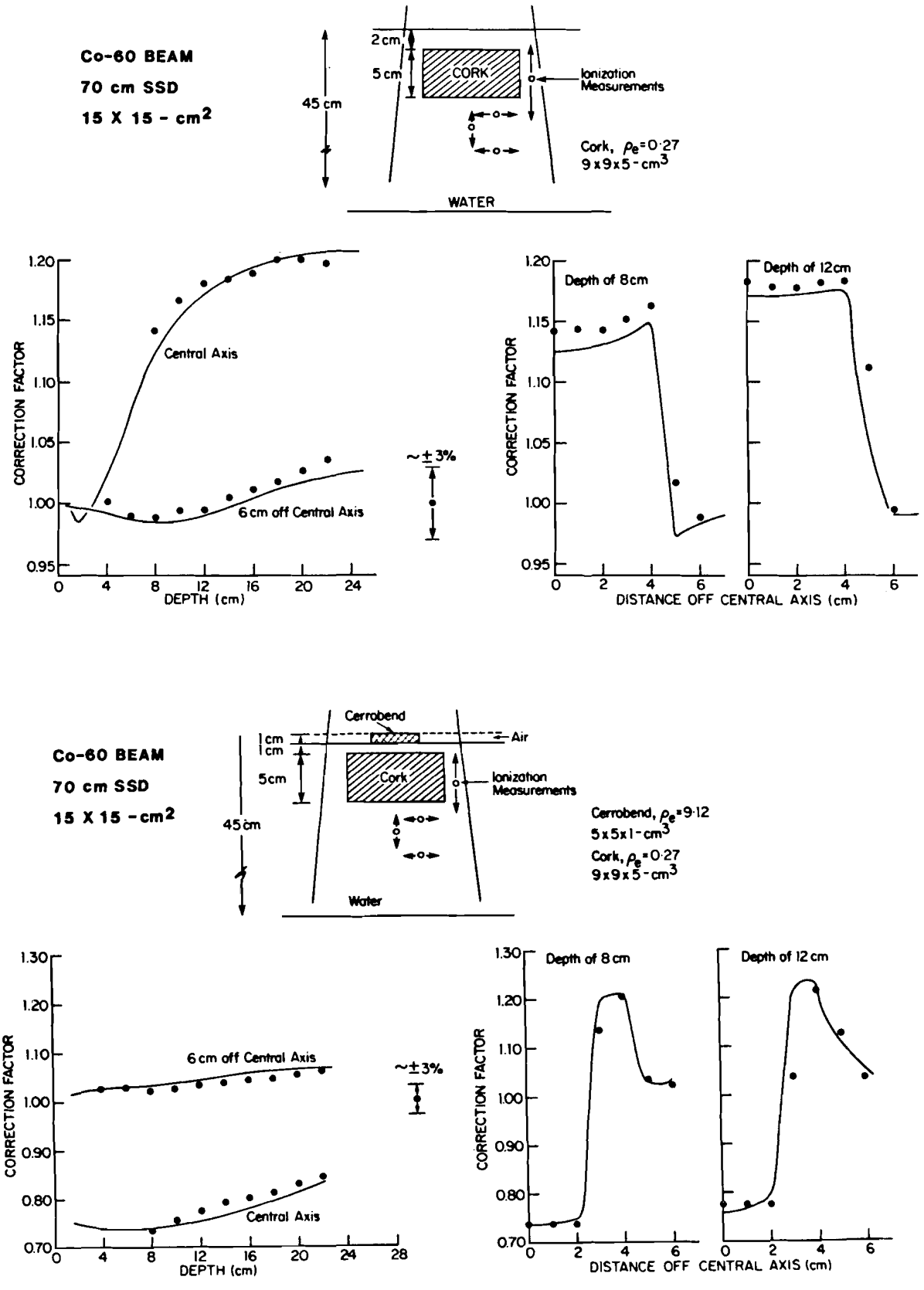

Figure 1. Comparison of Measured and Calculated Correction Factors

of a combination course-fine grid to reduce calculation time with small loss of accuracy, investigation of alternate methods for incorporating scatter angles to improve accuracy, investigation of methods to calculate multiple-beam dose with small increase in computation time, additional development of display capability (C-2), and completion of the Integrated Circuit (C-3) to decrease calculation time.

1. J. Wong, "A New Approach to Photon Dose Calculations in Radiotherapy Treatment Planning," Ph.D. Thesis, Department of Medical Biophysics, University of Toronto, July 1982.

2. J. W. Wong and R. M. Henkelman, "A New Approach to CT Pixel-Based Photon-Dose Calculations in Heterogeneous Media," Medical Physics, vol. 10, pp. 199-208, 1983.

3. J. Wong, E. Slessinger, D. Stein, F. Rosenberger, and J. A. Purdy, "Implementation and Verification of a New CT Based 3-Dimensional Photon Dose Calculation Algorithm," Medical Physics, vol. 10, p. 593, 1983 (abstract).

C-2. Three-Dimensional Display of Absorbed-Dose Computation for Radiation-Treatment Planning

Personnel: J. W. Matthews, D.Sc., Computer Systems Laboratory
B. Emami, M.D., Radiology
R. E. Hermes, BCL
C. A. Pérez, M.D., Radiology
J. A. Purdy, Ph.D., Radiology
F. U. Rosenberger, BCL and Computer Systems Laboratory
J. W. Wong, Ph.D., Radiology

Support: RR 00396
RR 01379
RR 01380
Washington University

A conventional treatment plan was entered into an MMS-X[1] system using the COMPOSE[2] program by manually tracing both anatomical features (from CAT data) and computed isodose contours for serial sections. This plan was then viewed on an MMS-X system having the capability of generating three-dimensional stereo scopic displays. We also investigated the stereoscopic display of a simulated isodose distribution as a "wire-mesh" of orthogonal contours superimposed on the same serial anatomical tracings. Software was extracted from the M3 molecular-modeling system[3] that will automatically prepare isodose-contour displays from an array of computed dose data.

Plans for the next year include: (1) computing such dose arrays using the algorithms described in (C-1) and preparing the isodose-contour displays; (2) further automating the entry of anatomical data into memory; (3) comparing display formats for accuracy and clarity; and (4) developing software that will allow display of the anatomical contours as seen from the source of the therapy machine ("beam's-eye view"[4]) - thus providing a tool for geometric optimization of the treatment plan.

1. C. E. Molnar, C. D. Barry, and F. U. Rosenberger, "MMS-X Molecular Modeling System," Technical Memorandum 229, Computer Systems Laboratory, Washington University, St. Louis, Missouri, January 1976.

2. J. P. McAlister, "Program COMPOSE," Technical Memorandum 291, Computer Systems Laboratory, Washington University, St. Louis, Missouri, December 1981.

3. C. Broughton, "M3 - Molecular Modeling and Fitting System," University of Alberta, Department of Biochemistry, Edmonton, Alberta, Canada, February 1980.

4. L. E. Reinstein, D. McShan, B. Webber and A. S. Glicksman, "A Computer-Assisted Three-Dimensional Treatment Planning System," Radiology, vol. 127, pp. 259-264, 1978.

C-3. Integrated-Circuit Implementation for Absorbed-Dose Computation in Radiation-Treatment Planning

Personnel: F. U. Rosenberger, BCL and Computer Systems Laboratory
G. J. Blaine, BCL
T. J. Chaney, M.S., Computer Systems Laboratory
A. D. Richardson, Computer Systems Laboratory
J. W. Wong, Ph.D., Radiology

Support: RR 00396
RR 01379
RR 01380
Washington University

We have identified three major goals to be achieved in the design of the Radiation-Treatment Planning Integrated Circuit (RTP IC) intended to perform part of the computation for absorbed-dose calculations using the algorithms described in (C-1). These goals are: (1) to reduce the dose-computation time to clinically useful values for large fields (The present implementation on a VAX-780 (C-1) requires about 40 hours to compute the dose for an entire cube 25 cm on an edge with 1-cm resolution. The integrated circuit will reduce the required time by a factor of about 60.); (2) to provide a large circuit for testing the CSL-imported design-aid programs for geometry generation, design rule checking, electrical rule checking,

and logic and electrical simulation; and (3) to provide design experience with a large and complicated circuit, which, having potential for real application, will provide an incentive for completing the project and for putting the resulting integrated circuit into service.

Approximately 30 cells including counters, arithmetic-logic-units, registers, and bus circuits, have been generated or modified for use in the RTP IC, primarily with a graphic editor[1] and color display terminal. A specification for the placement and connection of these cells has been written with a derivitive of LAP,[2] a geometry specification language that allows placement of cells with respect to other cells and makes changes and modifications relatively easy. The circuit is microprogrammed for ease of implementation and several procedures have been written to generate the instruction decoders from table input, to place the decoding logic, and to connect the decoder outputs to the other circuitry. Figure 1 shows a plot of the cell outlines for the arithmetic, storage, and control sections. The detailed design of the external bus connection, the pad placement, and the final circuit testing and simulation will be completed in the next few months.

The modifications to the original algorithm (PR 18, B-8; PR 13, I-3; PR 14, G-6; PR 15, G-4; PR 16, B-14; PR 18, B-8) described (C-1) do not affect the primary task of the RTP IC, which is to calculate the attenuation of scattered radiation along the path from each scatter point to each dose point, but they do change some of the auxiliary calculations. Since back-scatter is now calculated explicitly, approximately twice as many paths must be ray-traced, increasing the estimated computation time from that given before (PR 18, B-11).

The delta-h summation, although not as complex as the ray-tracing step, would drastically increase the required host computer time if carried out in that computer and would dominate the total time. It appears that this computation can be carried out by the integrated circuit with very little change to its design or complexity. Additional time, amounting to about 50% of that for the ray-tracing step, will be required to accommodate this computation. In addition, the irregular-field dose calculations required by the new algorithm will increase the computation time required by the host computer.

Design and fabrication of a card to support the integrated circuit and its associated memory will be completed during the next grant year. It will be designed to plug into the Unibus of a VAX or PDP-11 computer for use in further research and development of absorbed-dose computations, and also, possibly to plug into a Modulex radiation-treatment planning system for experimental and evaluation use in treatment planning.

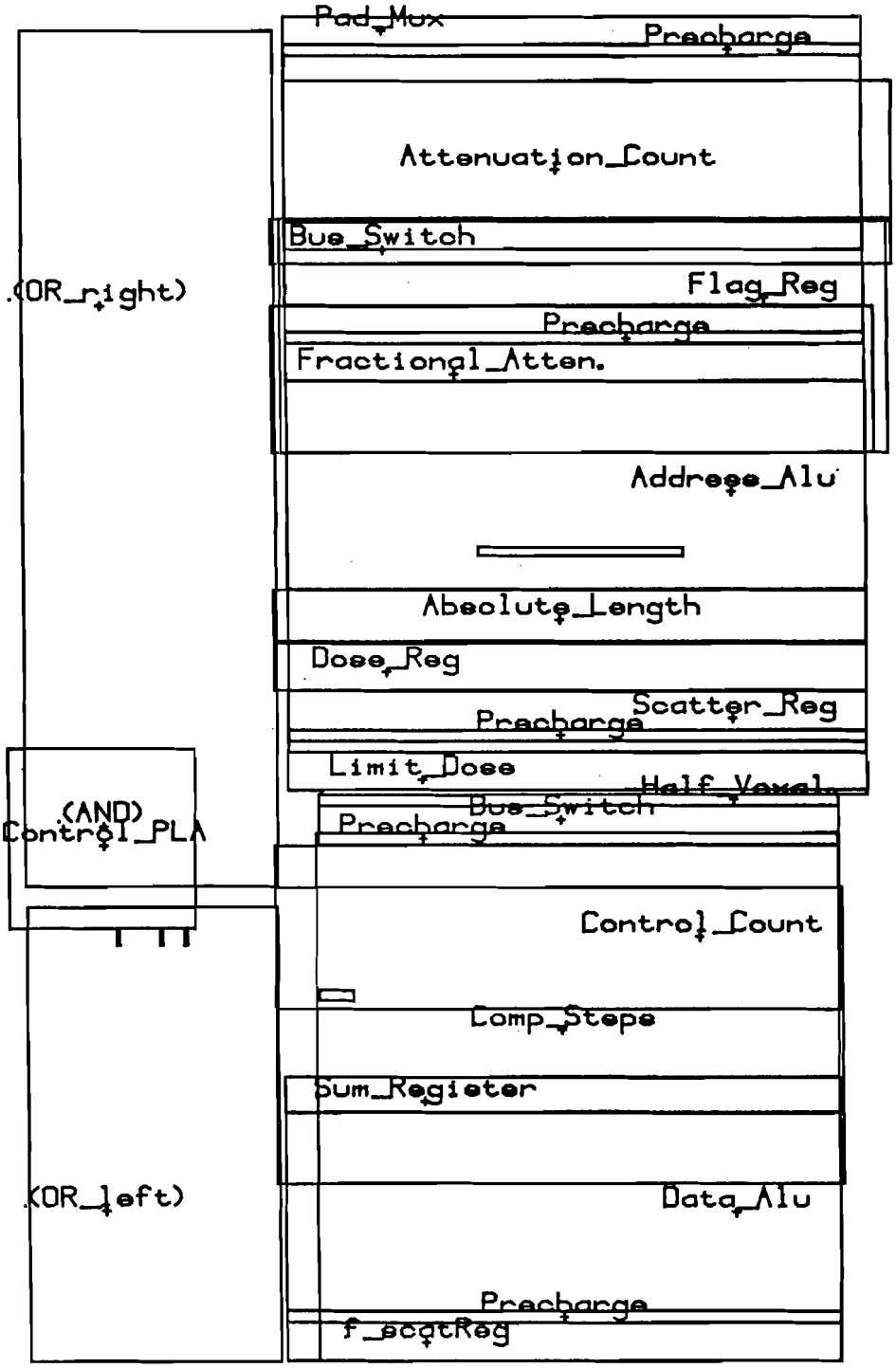

Figure 1. Cell outlines for the arithmetic, storage, and control sections of the Radiation-Treatment Planning Integrated Circuit.

1. J. K. Ousterhout, "Caesar: An Interactive Editor for VLSI Layouts," VLSI Design, vol. 2, no. 4, pp. 34-38, 4th Quarter, 1981.

2. S. Trimberger, J. A. Rowson, C. R. Lang, and J. P. Gray, "A Structured Design Methodology and Associated Software Tools," IEEE Transactions on Circuits and Systems, vol. CAS-28, no. 7, pp. 618-634, 1981.

D. Quantitative Imaging: Positron-Emission Tomography

Stimulated by the clinical impact of the EMI transmission tomographic scanner in 1973, experimental studies were initiated in collaboration with the Division of Radiation Sciences to evaluate positron coincidence-detection as a method for emission reconstruction tomography. This collaborative activity resulted in a prototype scanner called PETT (Positron-Emission Transaxial Tomograph). Extensive studies in patients and animals were conducted with the PETT III scanner in collaboration with the divisions of Neurology and Cardiology. A subsequent scanner, PETT IV, utilized concepts developed with its predecessor but incorporated a novel technique for the simultaneous collection of four tomographic slices from a single set of detectors. PETT IV is now located in the Cardiac Care Unit for use in the SCOR project for the quantification of regions of myocardial ischemia and infarction (D-1, D-2). Subsequent scanners have been developed that permit more rapid data collection and improved spatial resolution. One of these, PETT V, was used in experimental studies in dog hearts. PETT VI became operational during the summer of 1980 and employs fast detectors and an entirely circular motion for rapid data acquisition. Further experimental and clinical studies with this system occurred over this past year (D-3). One of the most exciting recent developments for emission tomography results because of new developments in crystal technology and high-speed electronics. These now permit the propagation time of each of the two photons created in an annihilation to be measured. Theoretical and experimental studies of tomography systems that utilize this new information continued, and the software and hardware needed to realize the predicted benefits were developed (D-4, D-5, D-7 to D-17); the new system is called SUPER PETT-I. Studies of ways to improve the detector electronics for the improved measurement of time-of-flight were initiated during the year (D-18), and some early consideration was given to specially designed VLSI circuits for PETT systems (D-19). An international workshop on time-of-flight tomography was hosted at Washington University and attracted participants from France, Japan, and several institutions in the United States (D-20).

D-1. PETT Experimental Studies

Personnel: S. R. Bergmann, Ph.D., Medicine
K. A. A. Fox, M.B., Ch.B., Medicine
J. Markham, BCL
B. E. Sobel, M.D., Medicine
M. M. Ter-Pogossian, Ph.D., Radiology
M. J. Welch, Ph.D., Radiology

Support: RR 01380
HL 13851
HL 17646

The overall goal of this project is to implement and evaluate procedures required to translate into intact animals the results obtained with selected positron-emitting tracers used to characterize myocardial metabolism and perfusion in isolated hearts and anesthetized, closed-chest dog studies performed with the Isolated Probe Data Acquisition System. Utilizing positron-emission tomography with PETT VI, the distribution of tracer and the time course of its uptake and clearance from the myocardium can be quantified. Such studies are intimately related to the clinical studies using positron-emission tomography (PET).

We have previously demonstrated the beneficial effects of intracoronary thrombolysis on the restoration of myocardial metabolism in vivo with ^{11}C-palmitate and positron-emission tomography, and the dependence of this recovery on the interval after coronary occlusion prior to reperfusion. In this previous study, coronary occlusion was produced in 23 closed-chest, anesthetized dogs with a copper coil prior to performance of cardiac PET with ^{11}C-palmitate. Jeopardized zones were calculated by summation of myocardial regions exhibiting less than 50% the peak left ventricular wall activity, and residual metabolic activity within jeopardized zones was quantified based on the average counts compared with counts in normal myocardium. After the initial tomography, streptokinase was infused into the coronary artery resulting in angiographically demonstrable restoration of patency. Repeat tomography was performed 90 minutes after the initial study following a second injection of ^{11}C-palmitate. If reperfusion was initiated within 1-2 hours (n=4) or 2-4 hours (n=6) the jeopardized zone was reduced by 51 $\pm$ 6%. When streptokinase was infused later after infusion, significant salutary metabolic effects did not occur. These results indicated that positron tomography is useful in the clinical delineation of the efficacy of thrombolytic therapy in the restoration of myocardial metabolism, and underscored the marked dependence of such efficacy on the duration of the interval of ischemia prior to the onset of reperfusion.[1]

Since non-invasive quantification of regional myocardial perfusion is desirable in order to make valid interpretation of restoration of metabolism, we extended our use of $H_2{}^{15}O$ for the measurement of myocardial perfusion in isolated hearts and open-chest dogs to intact dogs evaluated with PET. In studies completed this past year, $H_2{}^{15}O$ was injected intravenously

in 8 dogs (5 with coronary artery thrombosis) and its distribution quantified by cardiac positron tomography. Tomographic-data acquisition was obtained within 60 seconds after injection, and integrated regional $H_2{}^{15}O$ distribution was corrected for vascular $H_2{}^{15}O$ by subtracting vascular pool radioactivity (independently evaluated with $C^{15}O$). The distribution of $H_2{}^{15}O$ corrected for vascular radioactivity correlated closely (r=.89) with regional radioactivity in tomographic scans obtained in the same dogs after injection 6-10 mCi of ^{68}Ga-labeled macroaggregated albumin microspheres. Thus positron tomography after $H_2{}^{15}O$ using a vascular-pool-subtraction technique permits estimation of regional myocardial perfusion.[2]

Although coronary thrombolysis is a promising approach for the treatment of acute myocardial infarction, as currently practiced clinically, it requires coronary catheterization and induction of a systemic lytic state when conventional activators such as streptokinase or urokinase are employed. Tissue-type plasminogen activator is an active thrombolytic agent that does not induce systemic fibrinolysis or hemostatic breakdown because of its requirements for binding to fibrin. In a study completed within the past year, we showed that tissue-type plasminogen activator (t-PA) induced coronary thrombolysis within 8 minutes whether given intracoronarily (n=5) or intravenously (n=5). In contrast, streptokinase given intracoronarily induced thrombolysis in 31 $\pm$ 2 minutes, while intravenous streptokinase took 85 $\pm$ 19 minutes to cause thrombolysis. Evaluation of tomographs obtained after administration of ^{11}C-palmitate indicated a greater percentage reduction in the size of the jeopardized zone in dogs treated with t-PA compared to those treated with streptokinase, probably because of the more rapid induction of thrombolysis.[3]

In more recent studies, we evaluated 26 closed-chest anesthetized dogs with induced coronary thrombolysis with both regional perfusion evaluated with $H_2{}^{15}O$ (using $C^{15}O$ scan for correction of blood pool radioactivity) as well as ^{11}C-palmitate for assessment of myocardial metabolism. After initial PET was completed, thrombolysis was induced with intracoronary streptokinase. After thrombolysis, PET was repeated after a second administration of tracer. Thrombolysis within 4 hours of induction of ischemia resulted in flow restoration in the jeopardized zone of 72 $\pm$ 21% of flow in non-effected regions. Tomographically assessed myocardial metabolism recovered to 81% of normal. When thrombolysis was induced 6 to 12 hours after the onset of ischemia, myocardial perfusion averaged 65 $\pm$ 18% of normal, while myocardial metabolism recovered to only 27% of that seen in non-effected myocardium. Thus, metabolic salvage induced by thrombolysis is critically dependent on the time of reperfusion even though myocardial blood flow may be restored.[4]

The studies completed during the past year have demonstrated the utility of PET for the evaluation of myocardial metabolism and perfusion. Accordingly, patient studies designed to evaluate the efficacy of coronary thrombolysis are being implemented. During the past year we have also evaluated several factors such as partial volume effects and cardiac motion that may influence the absolute quantitation of regional radioactivity in the heart.[5]

During the coming year, we plan to continue our evaluation of the effects of coronary thrombolysis on the restoration of myocardial perfusion and metabolism with PET. In addition, we hope to define the usefulness of sequential (dynamic) cardiac PET after administration of ^{11}C-palmitate to demonstrate the restoration of myocardial metabolism after thrombolytic therapy using algorithms developed in open-chest dog studies. We further plan to evaluate the usefulness of cardiac and respiratory gating in obtaining quantitative tracer information. Finally, we hope to further refine the use of $H_2{}^{15}O$ in the measurement of myocardial perfusion so that not only regional measurements of myocardial perfusion can be defined, but also absolute quantitation of flow can be made.

1. S. R. Bergmann, R. A. Lerch, K. A. A. Fox, P. A. Ludbrook, M. J. Welch, M. M. Ter-Pogossian, and B. E. Sobel, "Temporal Dependence of Beneficial Effects of Coronary Thrombolysis Characterized by Positron Tomography," American Journal of Medicine, vol. 73, p. 573, 1982.

2. S. R. Bergmann, K. A. A. Fox, A. L. Rand, K. D. McElvany, M. M. Ter-Pogossian, and B. E. Sobel, "Non-invasive Measurement of Regional Myocardial Perfusion by Positron Tomography," Circulation, vol. 66, p. II-148, 1982 (abstract).

3. S. R. Bergmann, K. A. A. Fox, M. M. Ter-Pogossian, and B. E. Sobel, "Clot-selective Coronary Thrombolysis with Tissue-type Plasminogen Activator," Science, vol. 220, p. 1181, 1983.

4. S. R. Bergmann, K. A. A. Fox, A. L. Rand, M. J. Welch, M. M. Ter-Pogossian, and B. E. Sobel, "Assessment of Restoration of Myocardial Perfusion and Metabolism with Positron Emission Tomography After Coronary Thrombolysis," Journal of Nuclear Medicine, vol. 24, p. 5, 1983 (abstract).

5. M. M. Ter-Pogossian, S. R. Bergmann, and B. E. Sobel, "Influence of Cardiac and Respiratory Motion on Tomographic Reconstructions of the Heart: Implications for Quantitative Nuclear Cardiology," Journal of Computer Assisted Tomography, vol. 6, p. 1148, 1982.

D-2. PETT IV Cardiac Studies

Personnel: E. M. Geltman, M.D., Medicine
H. D. Ambos, BCL
T. R. Baird, Medicine
D. E. Beecher, BCL
A. S. Jaffe, M.D., Medicine
J. Markham, BCL
B. E. Sobel, M.D., Medicine
M. M. Ter-Pogossian, Ph.D., Radiology
M. J. Welch, Ph.D., Radiology

Support: RR 01380
HL 13851
HL 17646

This project was designed to determine whether positron-emission tomography (PET) permits a quantitative assessment of regional myocardial-metabolism in vivo in normal subjects and patients with cardiac disease of various etiologies. We have previously demonstrated that ^{11}C-palmitate accumulates avidly and homogeneously in normal myocardium, and its accumulation is depressed in areas of infarcted myocardium. The zones of depressed accumulation of palmitate correlate closely with the electrocardiographic locus of infarction and with the presence of regional wall motion abnormalities in patients with prior myocardial infarction. The extent of the zone of depressed accumulation of palmitate also correlates closely with enzymatic indices of infarction and with the extent of depression in left ventricular ejection fraction determined by radionuclide ventriculography.

During the past 12 months, activities have focused on several problems: 1) determining the natural history, the extent of distribution and myocardial injury during the first several weeks following myocardial infarction; 2) the assessment of the implications of "reciprocal" ST-segment depression associated with acute myocardial infarction; 3) assessment of the efficacy of interventions designed to salvage jeopardized myocardium (oral administration of nifedipine, a calcium antagonist, and intracoronary administration of streptokinase); 4) assessment of the characteristics of myocardial distribution of ^{11}C-palmitate metabolism in patients with mitral-valve prolapse to determine whether or not a myopathy underlies this valvular abnormality; and 5) an assessment of the distribution of ^{11}C-palmitate metabolism in patients with congestive cardiomyopathy due to ischemic heart disease compared to that caused by nonischemic congestive cardiomyopathy.

Before positron tomography can be employed as an endpoint for studies of interventions designed to salvage ischemic myocardium, one must first understand the natural history of tomographic indexes of myocardial ischemia and infarction in patients in whom acute intervention has not been employed. Accordingly, sequential PET was performed in 26 patients after the intravenous administration of ^{11}C-palmitate at selected time intervals after the onset of infarction. In 9 patients studied initially between 6 and

24 hours after the apparent onset of infarction and studied again 7 to 21 days later, PET infarct size did not change (60 ± 11 vs. 57 ± 12 PET-g-Eq). Similarly, in patients studied initially either 24 to 72 hours after onset or > 72 hours after onset of infarction, no changes between initial and repeat studies were detected. For patients studied late (> 72 hours after infarction) studies were highly reproducible with initial and repeat estimates of infarct size correlating closely ($r = 0.93$). Hence, it appears that the natural history of the region of myocardial metabolic derangement detected by tomography is stable in the absence of an intervention designed to salvage ischemic myocardium. This stability could reflect the inability to modify infarct size during this interval or the coexistence of zones of ischemia and infarction with evolution of the zones of ischemia to infarction over the intervals studied.

Based on the results of our studies on the natural evolution of tomographic estimates of infarct size, tomographic estimates of infarct size are being employed as endpoints for studies designed to test the efficacy of nifedipine, administered orally, and streptokinase, administered via the intracoronary route, as means of salvaging ischemic myocardium. At this time, a total of 42 patients have been studied acutely before and after therapy with nifedipine and 17 patients have been studied before and after the intracoronary administration of streptokinase. The results of these studies are presented in detail in Project A-8.

ST-segment depression is often observed in electrocardiographic leads potentially reflecting the electrical behavior of a myocardial segment distant from a primary zone of infarction. To determine whether the myocardium underlying these apparently "reciprocal" zones of ST-segment depression were truly ischemic, PET was performed after the intravenous injection of ^{11}C-palmitate in 20 patients with acute myocardial infarction. Infarction was anterior in 7 patients and inferior in 13 patients. Patients with anterior infarction did not show ST segment depression in the inferior leads and all of the patients exhibited normal homogeneous accumulation in palmitate in the inferior and posterior walls. Nine patients with inferior infarction (69%) exhibited ST-segment depression (apparently reciprocal or due to anterior ischemia) in the anterior precordial leads. Myocardial injury tended to be greater in the primary zones of necrosis among patients with inferior infarction and "reciprocal" ST-segment depression compared to those without anterior ST-segment depression. This was reflected by the greater total inferior ST-segment elevation (0.48 ± 0.35 vs. 0.07 ± 0.19 mv [± SD], $p < .05$), peak plasma MB creatine kinase activity (354 ± 134 vs. 80 ± 34 IU/ℓ, $p < .05$) and tomographically estimated infarct size (58 ± 13 vs. 13 ± 10 PET-g-Eq). Three of the 9 patients with inferior infarction and precordial ST-segment depression exhibited anterior tomographic defects underlying the ST-segment depression. Thus, although most of the patients with inferior infarction and precordial ST-segment depression had no anterior-wall metabolic compromise (67%), indicating that the anterior ST-segment changes were truly reciprocal phenomena. In some, the precordial electrocardiographic abnormalities reflected impaired metabolism in the anterior wall indicative of ischemia.

The pathogenesis of chest pain and arrhythmias observed in patients with mitral valve-prolapse (MVP), remains to be elucidated. To determine

whether myocardial metabolic abnormalities were associated with this clinical constellation, 31 mid-ventricular PET reconstructions obtained from 11 patients with MVP and chest pain or arrhythmias with angiographically documented normal coronary arteries were compared to 32 mid-ventricular PET slices obtained from 13 normal subjects after the i.v. injection of 15-20 mCi of ^{11}C-palmitate. Each tomographic slice was displayed at 7 selected isocount thresholds from 90 to 30% of maximum left ventricular mural radioactivity. The number of discrete zones of radioactivity was noted and summed for all thresholds (minimum = 7/slice). The number of discrete regions, a mark of the metabolic abnormalities of cardiomyopathy, were similar between patients with MVP and normal subjects [11.2 $\pm$ .6 (SE) vs. 11.8 $\pm$ .7, p = n.s.]. The frequency of radioactivity/pixel is shifted slightly towards higher levels of radioactivity among patients with MVP (67.5 $\pm$ 1.1 vs. 63.8 $\pm$ 1.1% of maximal myocardial radioactivity, $p < .05$). However, there was considerable overlap in the frequency distribution between normal subjects and patients with MVP. Thus, only subtle differences were found in the spatial and frequency distribution of myocardial accumulation of ^{11}C-palmitate between normal subjects and patients with MVP, insufficient to explain the clinical syndrome.

Differentiation of ischemic (ICM) from nonischemic (NICM) cardiomypathy is often difficult with conventional, noninvasive procedures. To determine whether PET offers powerful discrimination, we analyzed 103 transaxial reconstructions (all available mid-ventricular sections) from 7 patients with ICM and 17 patients with NICM documented at catheterization, and 13 normal subjects after 15-20 mCi of ^{11}C-palmitate, i.v. All patients with ICM exhibited at least one extensive region of homogeneously depressed ^{11}C-palmitate content compared with only 12% of patients with NICM ($p < .001$). Spatial accumulation of palmitate was more heterogeneous with NICM ($p < .01$), reflected by multiple discrete regions of uptake [17 $\pm$ .6 (SE), 11 $\pm$ .7, and 12 $\pm$ .7 for NICM, ICM and controls]. Mean radioactivity within apparently healthy zones in ICM and controls was similar (64 $\pm$ 2 and 64 $\pm$ 1% of maximal myocardial radioactivity) but greater than values with NICM (57 $\pm$ 1, $p < .01$). Thus, PET with ^{11}C-palmitate clearly distinguishes ischemic from nonischemic cardiomyopathy.

D-3. In-Vivo Measurements of Regional Blood Flow and Metabolism in Brain

Personnel: M. E. Raichle, M.D., Neurology and Radiology
D. C. Ficke, B.S., Radiology
P. T. Fox, M.D., Neurology
M. H. Gado, M.D., Radiology
R. L. Grubb, Jr., M.D., Neurological Surgery
P. Herscovitch, M.D., Neurology and Radiology
K. B. Larson, BCL
J. L. Lauter, Ph.D., Central Institute for the Deaf
J. Markham, BCL
M. A. Mintun, M.D., Neurology
W. J. Powers, M.D., Neurology and Radiology
D. L. Snyder, BCL
A. G. Swift, B.A., Radiology
M. M. Ter-Pogossian, Ph.D., Radiology
M. J. Welch, Ph.D., Radiology

Support: RR 01380
HL 13851
HL 25944
NS 06833
Washington University

We have continued our previously reported efforts (PR 18, B-16) in the study of central nervous system hemodynamics and metabolism using positron-emission tomography (PET). Several radiotracer techniques have been refined or implemented, and a variety of studies of cerebral metabolism and circulation in normal and diseased states have been pursued.

Our technique of measuring cerebral blood flow (CBF) regionally with PET and ^{15}O-labeled water,[1] based on the Kety autoradiographic method, has been validated in baboons.[2] Up to a mean CBF of 60 ml/(min hg), there was an excellent correlation of flow measured with PET and flow measured with standard tracer techniques using intracarotoid injection of tracer. At higher flows, there was a progressive decline in measured flow that was quantitatively accounted for by the limited brain extraction of water at higher flows. The use of ^{11}C-butanol as a flow tracer was investigated in baboons.[3] With this flow tracer, there was no decline in measured flow at higher flows, consistent with its complete extraction even at high flows. The use of ^{11}C-butanol as a PET flow tracer in humans was initiated and will be studied further.

Although the Kety method yields accurate estimates of flow when applied to 40-sec scans performed immediately after injection of tracer, disparities result when scan times differ in the same patients, and estimates of flow decline with scan duration or delays in the start of the scan after injection. These disparities have prompted the development of more complete models in which tissue is separated into several components, each with different kinetics, as opposed to the Kety model which assumes blood and tissue can be represented as a single compartment. In these models, as in the

original Kety model, accurate estimates of flow depend, to a great extent, on knowledge of the tracer capillary permeability-surface area product since water is not freely diffusible. Diffusion limitations are probably less significant immediately after injection of tracer, and may account for the disparities we have observed. A three-compartment model in which the vascular space, the extracellular fluid, and the cells were represented by different compartments yielded estimates of flow which declined less significantly with scan duration, but did not correct the discrepancies. Currently, a more detailed model is being tested.

An extensive analysis of an alternative PET CBF technique that involves the continuous inhalation of $C^{15}O_2$ has been completed.[4] It was shown that this method provides poor estimates of local flow in the face of tissue heterogeneity of flow and of partition coefficient for water. This heterogeneity is, of course, unavoidable with PET, given its limited spatial resolution.

A new model for the measurement of regional cerebral metabolic rate for oxygen with PET was developed, validated, and implemented.[5] The model permits calculation of regional oxygen-extraction fraction from scan data obtained following the bolus inhalation of oxygen-15 labeled oxygen. Measurements of regional cerebral blood flow and blood volume are also required for the calculation. The model accounts for recirculating labeled water of metabolism and corrects for unextracted oxygen-15 oxygen in the cerebral vasculature. An extensive error analysis of the model was performed and its accuracy was validated in baboons by comparison with oxygen extraction measured in the same animals using the intracarotid injection of tracer.

The recent development of reliable techniques to produce practical amounts of the radiolabeled compounds ^{11}C-glucose and ^{18}F-spiperone has allowed us to pursue the development of PET methods to measure brain glucose metabolism and brain dopamine-receptor distribution. Our major concerns have been the development of appropriate mathematical models for the biological systems under study, evaluation of the constraints and data requirements of the models in the context of use with PET acquired data, construction of software packages that estimate the physiologically relevant model parameters for any or all regions of interest from the PET-scan data.

Our work in glucose metabolism is a continuation of what has been previously reported,[6-8] (PR 10, B-12; PR 11, B-2; PR 12, B-4; PR 13, H-1; PR 14, F-4; PR 15, F-3; PR 16, F-3; PR 17, B-11; PR 18, B-16), with two significant extensions. The first is the introduction of the PET device for data collection to replace the single-detector probe. The second is an expansion of the glucose-metabolism model to include egress of ^{11}C-glucose metabolites, $^{11}CO_2$ in particular. While this creates a more complex modeling problem with an attendant increase in parameter-estimation time, we believe that the technique has the potential for becoming much more versatile in the range of brain physiologic and pathologic states that can be evaluated. Additionally, the resulting estimates of quantitative $^{11}CO_2$ production may provide information regarding the predominance of anaerobic vs. aerobic metabolism that will complement the conventional measurement of total regional glucose metabolism.

For the studies of brain receptors using PET, we have developed a three-compartment model that accounts for convective transport of spiperone into the region of interest, its diffusion across the blood-brain barrier, and its chemical interaction at the receptor site.[9] The model has been used to evaluate the PET-acquired time-activity curves of various regions of a baboon brain after injection of ^{18}F-spiperone. The model equations yield time-activity curves that resemble the experimental data; additionally, the estimated regional parameters of blood-brain-barrier spiperone permeability and of brain-receptor density agree closely with published values obtained by in vitro techniques. In progress is the development of the software to implement techniques for rapid parameter estimation for the temporal data in each pixel of the PET reconstruction images, such that an image, or map, of receptor distribution can be constructed and inspected. With completion of the final step, the method will be used to investigate diseases involving abnormalities in dopamine-receptor distribution such as Parkinson's disease and schizophrenia.

During the year, a variety of clinical studies on cerebral circulation and metabolism have been pursued in both normal subjects and patients with neurologic disease.[10] Quantitative PET methods for measuring regional cerebral blood flow (rCBF), regional cerebral metabolic rate for oxygen ($rCMRO_2$), regional cerebral blood volume (rCBV), and regional cerebral oxygen extraction fraction (rOEF) have been applied to the study of cerebrovascular disease in man. By studying a group of patients undergoing surgical revascularization of the brain, we have sought to identify and characterize the physiological differences between reversible ischemia and irreversible infarction. At this time we have analyzed data from approximately 20 patients and reached these preliminary conclusions: (i) Patients with reversible ischemia demonstrate normal $rCMRO_2$ in the face of decreased rCBF. (ii) Patients with irreversible stable infarction show slightly increased vascular transit time. Further studies to confirm these conclusions and to investigate the mechanisms by which ischemic brain responds to increased metabolic demands are in progress.

We have investigated cerebral blood flow with PET in premature infants with intraventricular hemorrhage and intraparenchymal hematoma.[11] This study, the first use of PET to measure CBF in the newborn, demonstrated wide-spread ischemia in the cerebral hemisphere containing the localized hematoma.

Considerable attention is being given to the functional mapping and activation of the normal human cerebral cortex as studied with PET. The local cerebral blood flow responses to a variety of physiological stimuli - visual, auditory, somatosensory, and motor - are being studied. A clear-cut relationship between stimulus frequency and local flow response in the visual cortex has been demonstrated. Similar stimulus-response relationships are being studied in other systems.[12]

Studies are being performed on patients with major depression, and with anxiety attacks, in conjunction with members of the Department of Psychiatry. The study of depressed patients involves measurement of CBF and oxygen metabolism before, shortly following, and six months after a course of electroconvulsive therapy (ECT) as treatment for the depression. Cerebral blood

flow and metabolism of oxygen was found to be decreased in depressed patients both immediately before, and just after the ECT, while it had returned to normal at six months. Other investigators have demonstrated that in subjects with a prior history of anxiety attacks, these can be precipitated by infusion of sodium lactate. This observation has motivated our study of the response of cerebral blood flow and metabolism to sodium lactate infusion in anxiety patients and in normal subjects.

As part of our study of cerebral circulation and metabolism in dementia and in elderly normal patients, we examined the effect of cerebral atrophy on global-hemisphere or whole-brain PET measurements. Because of volume averaging over metabolically inactive cerebral spinal-fluid spaces, such global measurements can be erroneously low. Using anatomical information from the CT scan, a technique to correct for such errors was developed.

1. P. Herscovitch, J. Markham, and M. E. Raichle, "Brain Blood Flow Measured with Intravenous $H_2{}^{15}O$. I. Theory-and Error Analysis," Journal of Nuclear Medicine, in press.

2. M. E. Raichle, W. R. W. Martin, P. Herscovitch, M. A. Mintun, and J. Markham, "Brain Blood Flow Measured with Intravenous $H_2{}^{15}O$. II. Implementation and Validation," Journal of Nuclear Medicine, in press.

3. M. E. Raichle, W. R. W. Martin, P. Herscovitch, M. R. Kilbourn, and M. J. Welch, "Measurement of Cerebral Blood Flow with C-11 Butanol and Positron Emission Tomography," Journal of Nuclear Medicine, vol. 24, p. 63, 1983 (abstract).

4. P. Herscovitch and M. E. Raichle, "Effect of Tissue Heterogeneity on the Measurement of Cerebral Blood Flow with the Equilibrium $C^{15}O_2$ Inhalation Technique," Journal of Cerebral Blood Flow and Metabolism, in press.

5. M. A. Mintun, M. E. Raichle, W. R. W. Martin, and P. Herscovitch, "Brain Oxygen Utilization Measured with O_{15} Radiotracers and Positron Emission Tomography," Journal of Nuclear Medicine, in press.

6. M. E. Raichle, K. B. Larson, M. E. Phelps, R. L. Grubb, Jr., M. J. Welch, and M. M. Ter-Pogossian, "In Vivo Measurement of Brain Glucose Transport and Metabolism Employing Glucose-^{11}C," American Journal of Physiology, vol. 228, pp. 1936-1948, 1975.

7. K. B. Larson, M. E. Raichle, M. E. Phelps, R. L. Grubb, Jr., M. J. Welch, and M. M. Ter-Pogossian, "A Mathematical Model for In Vivo Measurement of Metabolic Rates Using Externally-Monitored Radiotracers," in Information Processing in Scintigraphy, C. E. Metz, S. M. Pizer, and G. L. Brownell, eds., U.S. Energy Research and Development Administration Publication No. CONF-780687, National Technical Information Service, Springfield, Virginia, pp. 28-61, 1975.

8. M. E. Raichle, M. J. Welch, R. L. Grubb, Jr., C. S. Higgins, M. M. Ter-Pogossian, and K. B. Larson, "Measurement of Regional Substrate Utilization Rates by Emission Tomography," Science, vol. 199, pp. 986-987, 1978.

9. M. A. Mintun, M. E. Raichle, M. R. Kilbourn, G. F. Wooten, and M. J. Welch, "A Quantative Model for the In Vivo Assessment od Drug Binding Sites with Positron-Emission Tomography," Annals of Neurology, in press.

10. W. J. Powers, W. R. W. Martin, P. Herscovitch, M. E. Raichle, and R. L. Grubb, Jr., "The Value of Regional Cerebral Blood Volume Measurements in the Diagnosis of Cerebral Ischemia," Journal of Cerebral Blood Flow and Metabolism, vol. 3, pp. S598-S599, 1983.

11. J. J. Volpe, P. Herscovitch, J. M. Perlman, and M. E. Raichle, Positron Emission Tomography in the Newborn: Extensive Impairment of Regional Cerebral Blood Flow with Intraventricular Hemorrhage and Hemorrhagic Intracerebral Involvement," Pediatrics, in press.

12. J. L. Lauter, C. Formby, P. T. Fox, P. Herscovitch, and M. E. Raichle, "Tonotopic Organization in Human Auditory Cortex as Revealed by Regional Changes in Cerebral Blood Flow," Journal of Cerebral Blood Flow and Metabolism, vol. 3, pp. S248-S249, 1983.

13. P. Herscovitch, M. A. Mintun, M. H. Gado, and M. E. Raichle, "The Necessity for Correcting for Cerebral Atrophy in Global Positron Emission Tomography Measurements," Journal of Nuclear Medicine, vol. 24, p. 106, 1983 (abstract).

D-4. PETT Time-of-Flight Data Acquisition System Development

Personnel: T. J. Holmes, BCL
G. J. Blaine, BCL
D. C. Ficke, B.S., Radiology
S. J. Phillips, BCL
D. A. Schwab, BCL
M. M. Ter-Pogossian, Ph.D., Radiology

Support: RR 01380
HL 13851
HL 25944

The prototype slice processor (PR 18, B-17) is fully operational, and two collection modes have been implemented. The first mode, collection of conventional projections, utilizes a TOF windowing technique to reduce the contribution of random coincidences. This mode is necessary to obtain

calibration factors for detector-pair efficiency and attenuation. The second mode implements a "hybrid list mode" concept by which the slice processor converts the raw machine event (PR 18, B-19) into a corrected event, containing angle, displacement, and time-of-flight (TOF). In addition to performing corrections, presorting of events into slices also occurs.

The slice processor[1] consists of approximately 270 ICs and is implemented in wire wrap technology. The wire list has been transferred to a commercial automated system which has produced another slice processor which is now being evaluated. Upon completion, the remaining five slice processors will be generated for the system.

Future developments with the slice processor will involve microprogramming to implement additional modes of operation. The first will be estimation of the TOF offset for each detector pair (D-17) which is then used to correct all subsequent measurements. Another operational mode would be a reduced angle reconstruction algorithm (D-7) to assist in reconstructing data collected in the "hybrid list mode."

If processing times available by the above are considered excessively long, an enhancement will be developed to speed reconstruction and to allow prospective on-the-fly processing.

1. T. J. Holmes, R. E. Hitchens, G. J. Blaine, D. C. Ficke, and D. L. Snyder, "A Dedicated Hardware Architecture for Data Acquisition and Processing in a Time-of-Flight Emission Tomography System (Super-PETT)," IEEE Transactions on Nuclear Sciences, vol. NS-30, no. 1, February 1983.

D-5. Data Acquisition Software for SUPER PETT I

Personnel: D. E. Beecher, BCL
D. C. Ficke, B.S., Radiology
T. J. Holmes, BCL

Support: RR 01380
HL 13851
HL 17646
HL 25944

The development of data-acquisition software for SUPER PETT I has continued over the past year. Several different modes of data acquisition have been identified and successfully implemented in response to research needs.

Patient studies performed on SUPER PETT I have demonstrated that list-mode data collection is particularly useful. This was the first mode of collection implemented simply because it was straightforward and provided a quick method for verifying some basic scanner operations (PR 18, B-18). Some enhancements have been made to the interrupt structure of the main collection routine which make the software faster and more storage efficient. The implementation sustains a nearly continuous transfer of list-mode events from SUPER PETT I.

The recently developed slice processors (D-4 and PR 18, B-17) support additional data-collection modes for SUPER PETT I. Because the slice processors can perform on-the-fly calculations on the list-mode data, the host processor can be relieved of some of the work. The slice processors (each of which contains a CPU and local memory) have the capability of correcting the list-mode data for attenuation and building projection arrays on-the-fly. This capability necessitated the development of a projection-array collection mode. It involves sending a small number of command sequences to each slice processor, and waiting for the scan to end. When the scan has terminated, the host computer then prompts each slice processor for the transfer of its projection array. Although this mode is useful for attenuation scans and a quick-look capability, it is not the preferred mode since the time-of-flight information is not utilized.

Another data-collection procedure, called "hybrid list-mode," is being implemented to utilize the slice processors more effectively. In the hybrid list-mode, each slice processor collects and corrects each list-mode event on-the-fly and stores it in one of its two buffer memories. When one of the memories becomes full, the host is prompted by that particular slice processor for transfer of its set of corrected list-mode events. This mode is useful in that the host now receives list-mode events which have been partially corrected and separated according to the slice in which they occurred.

Software is also under development which will allow the slice processors to be utilized as off-line array processors to speed up the image reconstructions. The previously collected list-mode data will be down-loaded to the slice processors which will then compute seven reconstructions simultaneously.

D-6. Three-Dimensional Image Construction and Display

Personnel: D. E. Beecher, BCL

Support: RR 01380
HL 13851
HL 17646

During the past year, studies have been initiated for three-dimensional image construction and display using data obtained from positron-emission transaxial tomography (Super PETT I). In what follows, the volume construction section is exclusive to the Super PETT I geometry, however the display algorithms considered are more general and can be applied to many different types of picture data.

Three-Dimensional Image Construction. The major problem in visualizing PETT data in three dimensions is the need for interpolating the missed intervening slices of data when PETT images are reconstructed. The first (and probably optimal) method is a true three-dimensional reconstruction of the list-mode data obtained from Super PETT I. This problem is quite complex and since the main thrust of this research involves fast display algorithms, an alternative algorithm was used. This alternative uses an interpolation scheme based on Super PETT I geometry to reconstruct the missing slices from the known slices.

The scheme used was a weighted-linear interpolation based on the Super PETT I detector geometry. By using the assumed slice responses as shown in Figure 1, we can construct any arbitrary slice within the reconstruction zone denoted the Figure. This scheme has obvious drawbacks since no matter how intelligent we try to make the interpolation scheme, some real information cannot be recovered. Even though this approach is not optimal, it is easy to implement and the volumes generated provided a good test set for the new display algorithms to be discussed in the next section.

Three-Dimensional Image Display. The new three-dimensional display techniques to be presented are variations of the work done by Herman et al. A search of the current literature revealed the major work done on three-dimensional visualizations using voxel models is that of Herman and associates,[1-8] and Farrell.[9] Although Herman's technique can produce excellent visualizations, it has several disadvantages:

1. The algorithm is not directly context preserving. Herman's algorithm operates on a voxel space composed of one or more objects. The surface detection algorithm can identify only one object per invocation. Recognition of multiple objects requires multiple passes and a merge to reconstruct all objects in the scene. Identification of the object to be detected is usually done from a visual inspection of arbitrary transverse slices.

RECONSTRUCTED SLICES:

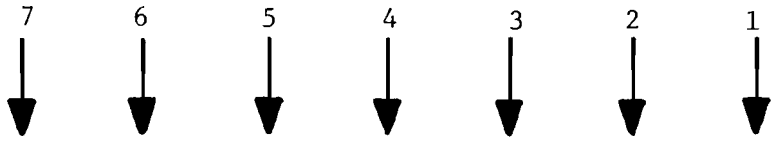

[.78(SLICE 4) + .22(SLICE 5)] (1)

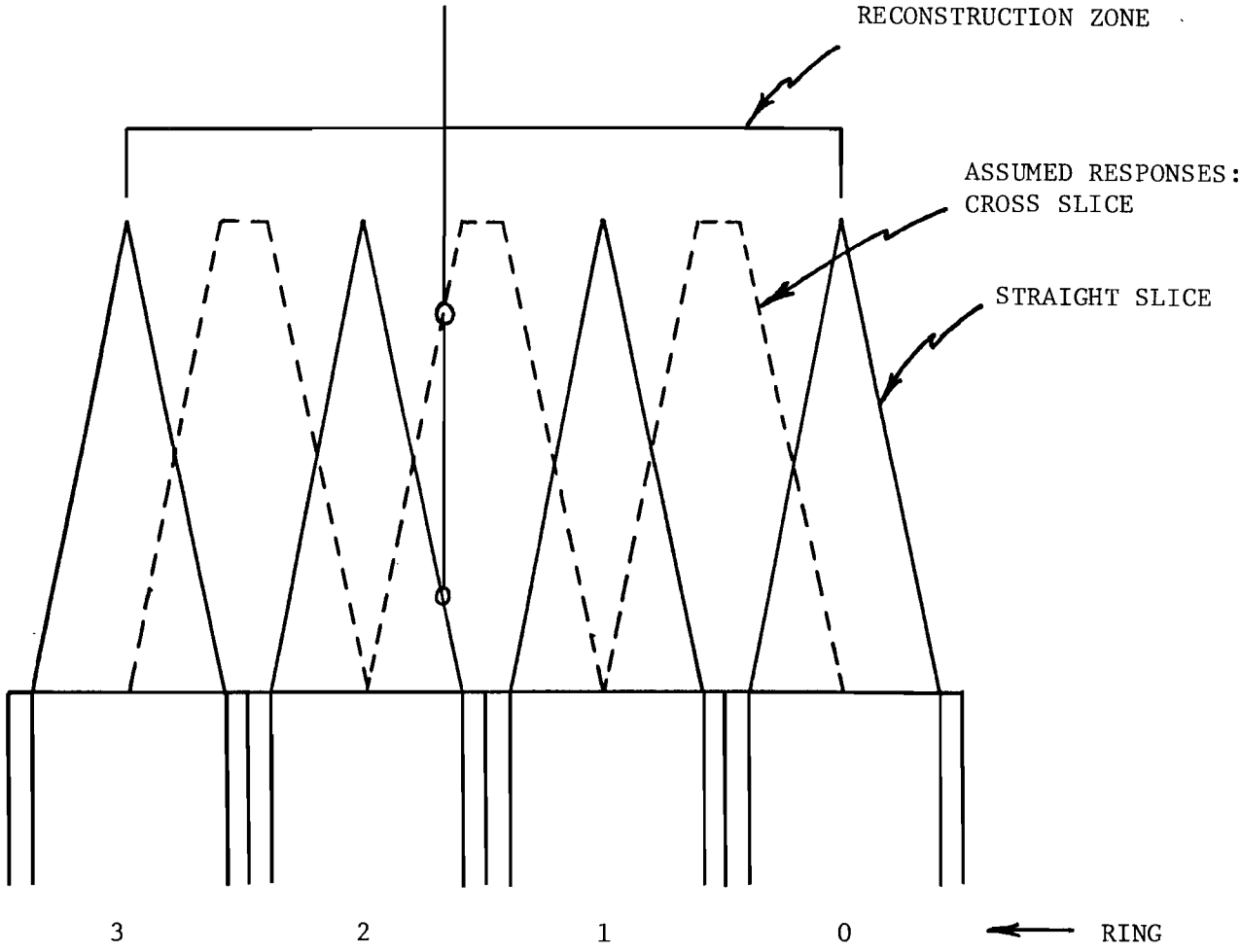

Figure 1. This figure illustrates the straight-slice and cross-slice responses for Super PETT I. Any given intermediate slice can be formed with a variation of equation (1).

2. Surface-detection time for a given object depends on the connectedness of the surface to be detected. This time can be prohibitive as it may range from "a few minutes to an hour."[8]

3. The result of the surface detection is a list of faces which must be stored. This list usually contains around 10,000 faces requiring a minimum of 2 bytes/face. Even though the faces may not be necessary for the particular view needed, they must still be stored.

After studying Herman's work and understanding the z-buffer algorithm, a scheme was devised for arbitrary visualizations of the voxel space which involve less memory and reduced computational complexity. For this method, the time to generate any view of any given object(s) will be a constant, the algorithm is context preserving, and it is not necessary to generate and store large lists of faces.

Conceptually, the algorithm involves passing a perpendicular plane through the voxel space on a line parallel to the line of sight. The plane begins at the rear of the view and proceeds to the viewer in increments of the voxel separation. At each location, the voxel space is sampled at locations specified by the coordinates derived from the view plane and these sample values are shaded on-the-fly (distance and angle coordinates are known because the current position in the plane is known). The final view plane is updated only if the current pixel distance is greater than the distance just computed for that pixel (all pixels initially have a distance value of infinity assigned to them). Only voxels which fall in the object space are eligible to replace a pixel value in the view plane. After the plane has passed completely through the voxel space we have the desired view, which was being formed on-the-fly. This technique offers several advantages over Herman's surface detection technique. First, it is context preserving since separate objects in the scene need not be connected in order to be part of the visualized scene. Regardless of the view being generated, the time to final view will be bounded by a constant. Internal views are easily generated by simply restricting the distance which we allow the plane to travel through the voxel space.

A prototype system has been implemented to generate the orthogonal views of the voxel volume. Photographs of four of these views are shown in Figure 2. The time for each view generation was approximately 20 seconds on a Perkin Elmer 3242 system with hardware floating point, even though the current implementation has not been optimized for speed or space efficiency. Object definition was implemented via a 50% threshold cutoff.

Obviously, orthogonal view generation is the most simplistic case. Future efforts will address modification of the existing system in order to generate arbitrary views of the given voxel space. Generalization of this technique to arbitrary views will require the development of time-efficient techniques to determine which voxels intersect a plane of arbitrary orientation. New object definition techniques will also be researched in hopes of finding an alternative to simple thresholding.

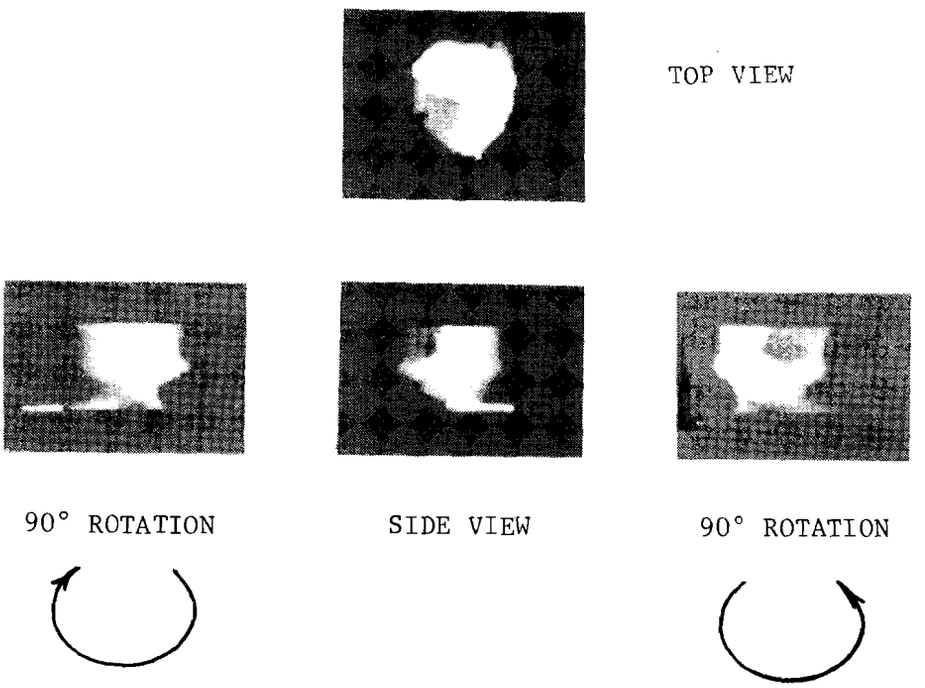

Figure 2. Shown above are four orthogonal views using the display technique described in D-6. The final volume contained 18 total slices which were formed from five transverse slices reconstructed with data from Super PETT I.

1. E. Artzy and G. T. Herman, "Boundary Detection in 3-Dimensions with a Medical Application," Technical Report No. MIPG9, Medical Image Processing Group, State University of New York at Buffalo, Buffalo, New York, November 1978.

2. E. Artzy, G. Freeder, and G. T. Herman, "The Theory, Design, Implementation, and Evaluation of a Three Dimensional Surface Detection Algorithm," Computer Graphics and Image Processing, vol. 15, pp. 1-24, January 1981.

3. G. T. Herman and H. K. Liu, "Display of Three-Dimensional Display of Human Organs from Computed Tomograms," Journal of Computer Assisted Tomography, vol. 1, pp. 155-160, 1977.

4. G. T. Herman and H. K. Liu, "Three-Dimensional Display of Human Organs from Computed Tomograms," Computer Graphics and Image Processing, vol. 9, pp. 1-21, January 1977.

5. G. T. Herman and H. K. Liu, "Dynamic Boundary Surface Detection," Computer Graphics and Image Processing, vol. 7, pp. 130-138, 1978.

6. G. T. Herman, "Representation of 3-D Surfaces by a Large Number of Simple Surface Elements," Technical Report No. MIPG26, Medical Image Processing Group, State University of New York at Buffalo, Buffalo, New York, March 1979.

7. J. K. Udupa, S. N. Srihari, and G. T. Herman, "Boundary Detection in Multidimensions," Technical Report No. MIPG31, Medical Image Processing Group, State University of New York at Buffalo, Buffalo, New York, July 1979.

8. J. K. Udupa, "DISPLAY82 - A System of Programs for the Display of Three-Dimensional Information in CT Data," Technical Report No. MIPG67, Medical Image Processing Group, University of Pennsylvania, Philadelphia, Pennsylvania, April 1983.

9. E. J. Farrell, "Color Display and Interactive Interpretation of Three-Dimensional Data," IBM Journal of Research and Development, vol. 27, pp. 356-366, July 1983.

D-7. A Reduced Angle Reconstruction Algorithm for Super PETT I

Personnel: D. C. Ficke, B.S., Radiology
D. E. Beecher, BCL
G. R. Hoffman, B.A., Radiology

Support: RR 01380
HL 13851
HL 17646

Two recent developments in image reconstruction using Super PETT I, a time-of-flight assisted positron emission tomograph, have improved the speed and architectural simplicity of the reconstruction process.

The first development is that of a "sparse triangle" weighting function which is applied when constructing a preimage on an event-by-event basis. With this modality, a detected event is placed at its measured position on the preimage and updated along the angle of detection by a weighting function corresponding to the error distribution of the time-of-flight measurement system. If the intersection lengths of the weighting function with the preimage matrix along the flight line are used to determine the coefficients for updating each preimage cell, the result is an angularly dependent set of coefficients. However, if the weighting function is sampled sufficiently at regular intervals to obtain the updating coefficients, no such angular dependence exists. Furthermore, if a triangular-weighting function, as opposed to a Gaussian weighting function is used, successive coefficients are obtained by subtraction of a constant as opposed to multiplication of a variable. A prototype implementation of this technique has been found to produce equivalent quality images to those obtained using the Gaussian-weighting function.

The second development is a direct implementation of techniques presented by Tanaka[1] and Tomitani.[2] These ideas suggest that the angular sampling requirements may be greatly reduced when time-of-flight information is available. Also presented is a method involving angular reduction of the event data to produce a storage-efficient, three-dimensional, measurement array which updates one cell for each detected event. Using these ideas, data from Super PETT I have been organized into a reduced no-loss array, 16 (angle) × 128 (distance) × 40 (TOF), and reconstructed to produce equivalent quality images. This technique represents a substantial savings in storage requirements when compared to the conventional no-loss array requiring 96 (angle) × 128 (distance) × 40 (TOF).

The design and implementation of a new software reconstruction system is currently underway which will include the enhancements discussed above. Use of the reduced-angle no-loss arrays will enable the new system to reconstruct all seven slices of a single scan simultaneously. This technique will represent a substantial savings in time since the list mode data will only need to be scanned once instead of several times, as present methods dictate.

1. E. Tanaka, "Line Writing Data Acquisition and Signal-to-Noise Ratio in Time-of-Flight Positron Emission Tomography," Proceedings of the Workshop on Time-of-Flight Tomography, IEEE Catalog No. CH1791-3, St. Louis, Missouri, pp. 101-108, May 17-19, 1982.

2. T. Tomitani, "Simulation Study of Reconstruction with Practical Weighting Function and Noise Evaluation in Time-of-Flight-Assisted Positron Computed Tomography," Proceedings of the Workshop on Time-of-Flight Tomography, IEEE Catalog No. CH1791-3, St. Louis, Missouri, pp. 117-124, May 17-19, 1982.

D-8. Image-Reconstruction Algorithm Using List-Mode Data of Super PETT I

Personnel: G. R. Hoffman, B.A., Radiology
D. E. Beecher, BCL
D. C. Ficke, B.S., Radiology
T. J. Holmes, BCL

Support: RR 01380
HL 13851
HL 25944

The reconstruction of PETT images from list mode data, using Super PETT I as previously described (PR 18, B-19), has been used with only minor modifications for 45 patient studies and various phantom studies. This procedure has been found to be extremely slow and tedious. Speed enhancements will be provided by the "hybrid list-mode" collection using the slice processors (D-4), and by reduced angle reconstruction (D-7). The ability to retrospectively analyze list-mode data has, however, proven to be a valuable tool. This is especially true when such constraints as cardiac gating and time segmenting are imposed.

It is possible to select for reconstruction a desired phase of the scan, such as diastole, retrospectively by recording cardiac cycle information in the control words, which occur at a rate of 96 per second. Since the raw data are preserved, other phases, such as systole, can also be selected for reconstruction. Additionally, irregular cardiac cycles, which often occur in diseased patients, can be rejected.

The list-mode data can also be used to reduce artifacts in gated data due to gantry motion. These artifacts arise as a result of unequal sampling of the desired cardiac phase during the 96 gantry states. A history of the 96 gantry states for a particular cardiac phase can be constructed, however, and used to generate corrections for artifact reduction by analyzing the list-mode data.

Any desired time segment of a scan can be isolated and reconstructed separately. This is accomplished by determining which records of the data correspond to the desired time segment and then processing only that portion of the list-mode data.

D-9. Maximum-Likelihood Estimation of Images

Personnel: D. L. Snyder, BCL
D. G. Politte, BCL

Support: RR 01379
RR 01380
HL 13851
HL 25944

List-mode data collected in the Super-PETT emission-tomography system are three dimensional, but reconstruction algorithms utilizing the time-of-flight information operate on two-dimensional data derived from the three-dimensional data. A study was initiated to develop a reconstruction algorithm that would utilize the three-dimensional data. This was accomplished. The algorithm and its derivation have been published.[1]

1. D. L. Snyder and D. G. Politte, "Image Reconstruction from List-Mode Data in an Emission-Tomography System Having Time-of-Flight Data," IEEE Transactions on Nuclear Science, vol. NS-20, no. 3, pp. 1843-1849, June 1983.

D-10. Utilizing Side Information in Image Reconstruction

Personnel: D. L. Snyder, BCL

Support: RR 01379
RR 01380
ECS-8215181

There is an increasing variety of imaging modalities becoming present in modern radiology departments, and with the general trend toward digital instrumentation, many of these produce data in a compatible, digital format. Considerable throught has already been given to the transmission, archiving, and display of digital images from a wide variety of sources so that a radiologist can view and manipulate them conveniently with computer aids

at a common viewing station.[1] It will become more and more important to be able to combine data acquired with different modalities in the study of a patient so that better images might be produced than would be possible with each modality alone.

Included in these modalities are instruments that acquire transverse tomographic sections through the body, such as x-ray CT scanners, emission scanners, and the newer NMR scanners. While the information provided with these instruments has some overlap, there are important, complementary differences. The x-ray and NMR scanners produce high-resolution images showing remarkable anatomical detail, while the emission scanners yield physiological and biochemical information more flexibly because of the large number of biologically active compounds that can be labeled radioactively.

The reduced resolution of an emission scanner compared to an x-ray scanner is quite evident when images of the same transverse section in a patient are compared. For example, in neurological studies, the emission image commonly indicates amounts of radioactivity in regions where it is clear from the x-ray image that there can be none, such as in regions that lie outside the brain or inside the ventricles. Because of this, and because of the longer term goal of being able to combine images from different modalities, we have been motivated to initiate the development of an approach for utilizing the anatomical information available in an x-ray image of a transverse section to improve an emission image of that same section, with the expectation that this will provide more accurate quantification of the radioactivity, and thereby the physiological and biochemical function, in those regions of the emission image that are of real importance and interest.

There are some significant practical problems in combining x-ray and emission tomography images. One is that of registering the two images so that the orientation, size, and location of anatomical structures coincide. The degree of accuracy with which this might have to be accomplished is difficult to specify at this time, but it is conceivable that registration to within a few millimeters will be of interest. For example, in many neurological studies, it is the radioactivity in gray matter that is of most interest. In a tomographic section, the region containing gray matter appears as a serpentine structure a few millimeters wide. An NMR tomographic image can delineate this region, delineate the region outside the brain and inside the ventricles where there is no activity, and delineate the region containing white matter where the activity is thought to be approximately uniform and so might be estimated throughout the region by-examining a subregion in it away from interferring structures. The full utilization of this side information derived from the NMR image as an aid in the formation of the emission image would presumably require that the images be registered to within some fraction of the region containing gray matter.

It is only recently that reconstruction algorithms have been derived for emission tomography that suggest how side information might be incorporated during the image formation process. Shepp and Vardi[2] used the maximum-likelihood method of statistics to develop a recursive algorithm for reconstructing distributions of radioactivity in a conventional emission-tomography instrument. This was extended by Snyder and Politte[3] to include

instruments currently under development which measure the differential time-of-flight of annihilation photons in addition to their line-of-flight as measured in conventional instruments. The recursive algorithm is derived by maximizing a particular function of the acquired data called the "likelihood function." The approach used in this study is to include side information as a constraint during the step of maximizing the likelihood function. Additionally, side information available in some regions of interest might be best modeled statistically; this is included by generalizing the likelihood function through the addition of the prior statistics of the side information. The recursive algorithm which results should provide improved quantitative images of radioactivity distributions, particularly in low count situations. Present efforts include the processing of simulated and experimental data to evaluate this new approach.

1. J. R. Cox, G. J. Blaine, R. L. Hill, and R. G. Jost, "Study of a Distributed Picture Archiving and Communication System for Radiology," Proceedings of the 1982 PACS Conference, SPIE vol. 318, pp. 132-142, 1982.

2. L. A. Shepp and Y. Vardi, "Maximum Likelihood Reconstruction for Emission Tomography," IEEE Transactions on Medical Imaging, vol. MI-1, no. 2, pp. 113-121, October 1982.

3. D. L. Snyder and D. G. Politte, "Image Reconstruction from List-Mode Data in an Emission Tomography System Having Time-of-Flight Measurements," IEEE Transactions on Nuclear Science, vol. NS-30, no. 2, April 1983.

D-11. A Comparative Study of Image-Reconstruction Approaches

Personnel: D. G. Politte, BCL
D. L. Snyder, BCL

Support: RR 01379
RR 01380
HL 25944
ECS-8215181

In this study, we are comparing the performance of two image-reconstruction algorithms for time-of-flight tomography, the confidence-weighting (CW) algorithm[1] and the estimated posterior-density weighting (EPDW) algorithm.[2] The algorithms differ fundamentally in that the CW algorithm is linear and the EPDW algorithm is a nonlinear, iterative approach. Further, the nonlinearity of the EPDW algorithm makes analytic performance predictions difficult. Therefore, our approach for comparison has been to implement both algorithms on real and simulated data (D-16) in order to compare specific performance metrics.

We find that the EPDW algorithm improves the signal-to-noise ratio in the myocardium of a simulated left ventricle by 2.1 db over the CW reconstruction.[2] Further, resolution improvement and background-artifact reduction are observed for the EPDW algorithm.

The choice of a reconstruction algorithm is also influenced by the total reconstruction time, however. In this respect the CW algorithm is preferable. For a final choice to be made, it will be necessary to consider possible methods to speed the execution time of the EPDW algorithm, and then carefully consider the choice of reconstruction fidelity versus reconstruction time.

1. D. L. Snyder, L. J. Thomas, Jr., and M. M. Ter-Pogossian, "A Mathematical Model for Positron-Emission Tomography Systems Having Time-of-Flight Measurements," IEEE Transactions on Nuclear Science, vol. NS-28, no. 3, pp. 3575-3583, June 1981.

2. D. L. Snyder and D. G. Politte, "Image Reconstruction from List-Mode Data in an Emission Tomography System Having Time-of-Flight Measurements," IEEE Transactions on Nuclear Science, vol. NS-30, no. 3, pp. 1843-1849, June 1983.

D-12. Preimage Selection

Personnel: D. L. Snyder, BCL

Support: RR 01379
RR 01380
HL 13851
HL 25944

The confidence-weighted preimage, used in processing time-of-flight emission-tomography data, has been shown to have a "minimax" property in that it minimizes the worst case reconstruction-error among all two-dimensional preimages derived linearly from three-dimensional, list-mode data, including the most likely position and profile preimages.[1]

1. D. L. Snyder, "Preimage Selection in Time-of-Flight Emission Tomography," IEEE Transactions on Nuclear Science, vol. NS-30, no. 1, pp. 701-702, February 1983.

D-13. Count Normalization for Conventional and Time-of-Flight Tomography

Personnel: T. J. Holmes, BCL
D. C. Ficke, B.S., Radiology
D. L. Snyder, BCL

Support: RR 01380
HL 25944

Two of the fundamental operations of a positron-emission tomography instrument are the sorting and counting of discrete recordings of positron annihilation events according to measurement vectors which they carry. Part of the reconstruction process includes the normalization of these counts with respect to scintillation-detector efficiency, spatial-sampling density, and photon absorption. There are several possible ways to combine and normalize these counts during the image-reconstruction process. We have performed a theoretical statistical analysis on these methods to determine their relative performances. The combined, normalized counts are treated as parameter estimators, and the metrics of their performances are their biases and variances. The results, which are to appear,[1] have some implications on the complexity of the reconstruction process.

This analysis was performed under the ideal assumption that the efficiency, sampling density, and photon absorption parameters are known quantities. In reality, these are estimated parameters, and their biases and variances would also have an effect on the reconstructed image quality. We have begun a theoretical statistical analysis of this effect. The preliminary results show that, as expected, when the variances in the normalization parameters decrease, the signal-to-noise ratio increases in the final image. However, there is a point at which any additional decrease in the variance of the normalization parameter will result in a minimal increase in the signal-to-noise ratio. Where this point occurs, as well as its implications on the complexity of data-processing, are issues which will receive further research.

1. T. J. Holmes, D. L. Snyder, and D. C. Ficke, "A Statistical Analysis of Count Normalization Procedures Used in Positron-Emission Tomography," to be presented at the 1983 IEEE Nuclear Science Symposium, San Francisco, October 20-22, 1983.

D-14. Modeling of Random-Coincidence Detections in Time-of-Flight Tomography

Personnel: T. J. Holmes, BCL
D. C. Ficke, B.S., Radiology
D. L. Snyder, BCL

Support: RR 01380
HL 25944
ECS 8215181

Mathematical predictions of the improvement in signal-to-noise ratio that results when time-of-flight information is used in emission tomography are smaller than the improvement observed experimentally. It has been conjectured that the additional performance gain is due to the way in which random coincidence detections are treated by the time-of-flight reconstruction process. Random coincidence detections are a phenomenon in which fictitious annihilation events are erroneously detected and recorded by the instrument.[1] In this study we have developed an extended mathematical model which includes the effects of this phenomenon. The analytical results show a significant additional gain which increases with the level of radioactivity. By comparing these results to the experimental results, we have determined that this additional gain is due to the way in which time-of-flight techniques suppress the effects of the erroneous detection.

1. T. J. Holmes, D. L. Snyder, and D. C. Ficke, "Modelling of Random-Coincidence Detections in Time-of-Flight Tomography," to be presented at the 1983 IEEE Nuclear Science Symposium, San Francisco, California, October 20-22, 1983.

D-15. Effects of Quantization of Time-of-Flight Measurements in PETT

Personnel: T. J. Holmes, BCL
D. G. Politte, BCL
D. L. Snyder, BCL

Support: RR 01380
RR 07054
HL 13851
HL 25944

Most of the existing mathematical models of time-of-flight (TOF) positron-emission tomography have suppressed the sampling issues by assuming that all measurements are known with arbitrary precision. We have examined the effect on final image quality of quantizing the TOF information, with

a varying number of bits in the time-to-digital converter (TDC), while letting all other measurements be known with much greater precision.

The main analytic conclusion, which is based on the algorithm-performance study[1] and some mathematical approximations, is that four or more bits of quantization should be adequate for tomographs with a 190 picosecond standard deviation in the TOF measurement error.

To verify these analytic results, the simulations described in D-16 have been performed.[2] These, likewise, show neglegible signal-to-noise ratio degradation for four or more TDC bits, but show significant degradation for three or less bits. Severe image artifacts are also present when three or less bits are used. The Super PETT I system uses seven bits, which provide a comfortable margin above the acceptable minimum.

1. D. L. Snyder, L. J. Thomas, Jr., and M. M. Ter-Pogossian, "A Mathematical Model for Positron-Emission Tomography Systems Having Time-of-Flight Measurements," IEEE Transactions on Nuclear Science, vol. NS-28, no. 3, pp. 3575-3583, June 1981.

2. D. G. Politte, T. J. Holmes, and D. L. Snyder, "Effects on Quantization of Time-of-Flight (TOF) Measurements on Image Signal-to-Noise Ratio in TOF Emission Tomography," IEEE Transactions on Nuclear Science, vol. NS-30, no. 1, pp. 720-722, February 1983.

D-16. Simulation of Time-of-Flight Emission Tomography Systems

Personnel: D. G. Politte, BCL
D. L. Snyder, BCL

Support: RR 01380
RR 07054
HL 13851
HL 25944

A time-of-flight tomography simulator has been written in the form of a modular, user-friendly software package. The user is allowed to study the effects of the hardware, such as detector width and timing quality. The simulations also provide much insight into the appropriate selection of a reconstruction algorithm and the manner in which it should be implemented.

The simulation package is organized as shown in Figure 1. Note that there are two possible processing paths, depending on which reconstruction algorithm is selected.

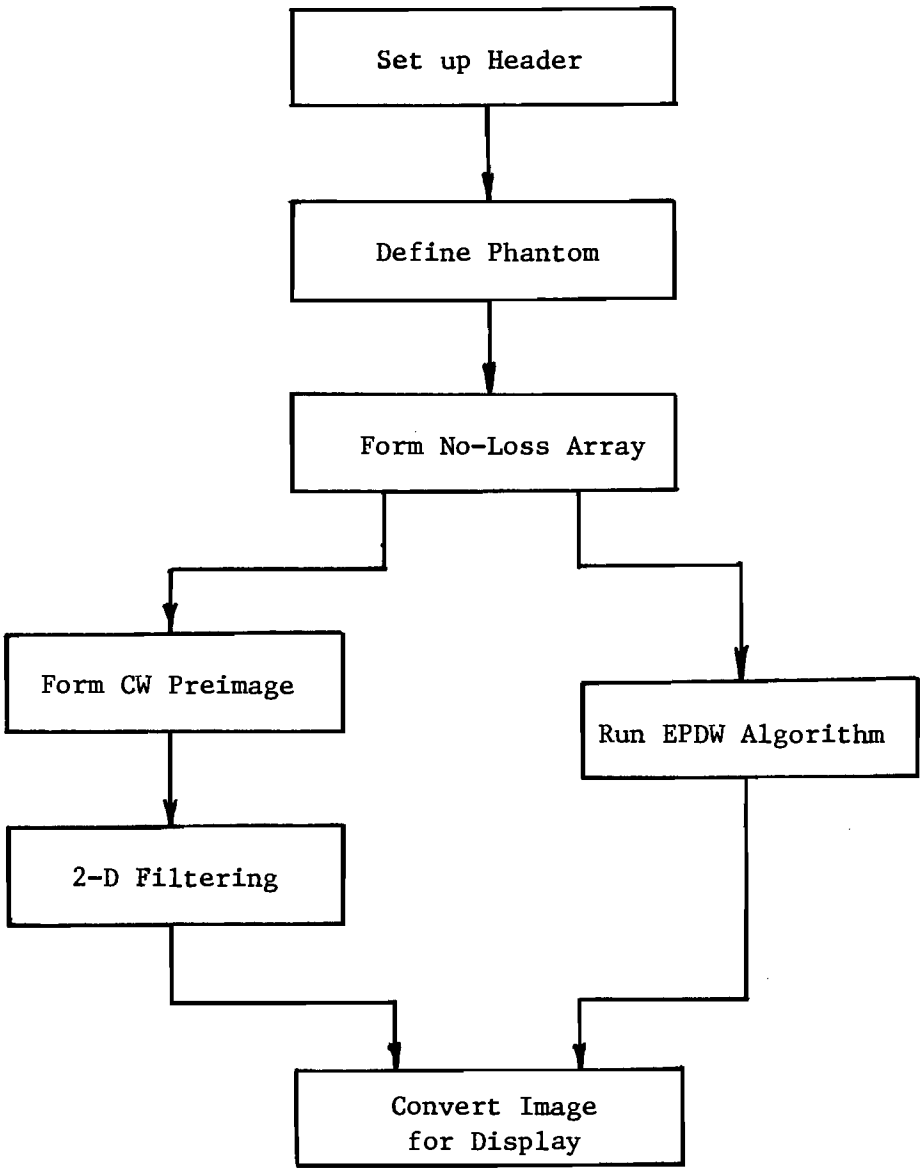

Figure 1. The flow diagram shown above depicts the time-of-flight tomography simulator. The processing stream proceeds from top to bottom. Each box represents a different program unit.

The user is first asked for information pertinent to the simulation, such as the detector size, timing measurement quality, and the total number of measurement counts to be registered over the duration of the scan. This information is stored in a header record which is appended to the data file and subsequently modified at each step of the processing path.

The radioactive object to be scanned is next delineated in the phantom definition step. The user may choose an existing phantom (heart-liver model, left-ventricle model, uniform disk) or create his own, by constructing a simple program.

The no-loss array data resulting from a simulated scan is then obtained by performing the annihilation point process[1,2] and translating each annihilation by a random vector from the measurement error density. The result is a three-dimensional array of simulated measurement points, including the position and angle information. Note that the effects of random and scattered radiation are not addressed here.

These data may be reconstructed in two ways. The first method is the linear reconstruction algorithm called confidence-weighting (CW).[1,2] In this technique, a two-dimensional preimage array is formed from the three-dimensional no-loss array by convolving the measurement point array at each angle with the measurement error density at the same angle and summing the results. This preimage is then filtered to yield the final image. The second method is a nonlinear iterative reconstruction algorithm called estimated posterior-density weighting (EPDW).[3] This algorithm also requires, in a portion of the processing, that various image arrays be convolved with the measurement error density at each angle. Two implementations are available; one uses a space-domain based discrete convolution, the other a Fourier-transform based convolution. Only the first convolution technique has been implemented for the confidence-weighting processing.

Finally, the images are readied for display by the standard display programs of the Radiation Sciences department of the Mallinckrodt Institute of Radiology.

New results obtained from the simulations are reported elsewhere in this progress report (D-11 and D-15).

1. D. L. Snyder, L. J. Thomas, Jr., and M. M. Ter-Pogossian, "A Mathematical Model for Positron-Emission Tomography Systems Having Time-of-Flight Measurements," IEEE Transactions on Nuclear Science, vol. NS-28, pp. 3575-3583, June 1981.

2. D. G. Politte and D. L. Snyder, "A Simulation Study of Design Choices in the Implementation of Time-of-Flight Reconstruction Algorithms," Proceedings of the Workshop on Time-of-Flight Tomography, IEEE Catalog No. 82CH1791-3, St. Louis, Missouri, May 17-19, 1982.

3. D. L. Snyder and D. G. Politte, "Image Reconstruction from List-Mode Data in an Emission Tomography System Having Time-of-Flight Measurements," IEEE Transactions on Nuclear Science, vol. NS-30, pp. 1843-1849, June 1983.

D-17. Calibration Problems in Time-of-Flight Emission Tomography

Personnel: T. J. Holmes, BCL
D. C. Ficke, B.S., Radiology
D. L. Snyder, BCL
M. Yamamoto, M.S., Radiology

Support: RR 01380
HL 25944

Positron-emission Tomography (PET) systems having time-of-flight (TOF) data require calibration of the TOF measuring electronics on a daily basis. The calibration process is performed on the instrument through a separate data collection prior to the tomographic data collection. In this study we have examined approaches to processing the calibration data in order to detect and estimate a fixed offset in the TOF measurements. Bias, variance and processing complexity were considered as metrics for various proposed estimators. A computer simulation of calibration data was performed to determine the biases and variances.

The results of the study have appeared[1,2] and are summarized as follows:

1. The most intuitive approach to estimating the offset, simply averaging all of the TOF measurements in the calibration data, results in extremely poor performance.

2. An estimator which achieves maximum-likelihood under the ideal condition that no random-coincidence detections (D-14) are present in the calibration data performs better than any other proposed estimator under this ideal condition. However, its complexity and inability to deal with random-coincidence detections make it infeasible.

3. An estimator which is quite similar to the maximum-likelihood estimator, but which is able to suppress the effect of random coincidences, performs adequately and has been implemented on the instrument.

This study has given us a fundamental understanding of some of the calibration requirements of a practical TOF PET instrument.

Additional plans to study various estimators which result when random coincidences are assumed to be present were deemed unnecessary due to the performance of the implemented estimator. Plans were also made to study various methods of detecting and estimating the scale factors in TOF measurements. However, Super PETT I has proven to be insensitive to changes in the scale factor, making further studies unnecessary. Additional efforts are not expected unless the next generation instrument has special calibration requirements.

1. T. J. Holmes, D. L. Snyder, D. C. Ficke, and M. Yamamoto, "Some Calibration Problems in Time-of-Flight Tomography," Proceedings of the Workshop on Time-of-Flight Tomography,-IEEE Catalog No. 82CH1791-3, St. Louis, Missouri pp. 161-166, May 17-19, 1982.

2. M. Yamamoto, G. R. Hoffman, D. C. Ficke, and M. M. Ter-Pogossian, "Imaging Algorithm and Image Quality in Time-of-Flight Positron Computed Tomography: Super PETT I," Proceedings of the Workshop on Time-of-Flight Tomography, IEEE Catalog No. 82CH1791-3, St. Louis, Missouri, pp. 125-129, May 17-19, 1982.

D-18. Studies of Detector Electronics for Time-of-Flight Tomography Systems

Personnel: D. C. Ficke, B.S., Radiology
R. O. Gregory, BCL
J. T. Hood, B.S., Radiology
M. M. Ter-Pogossian, Ph.D., Radiology

Support: RR 01380
HL 13851
HL 25944

For future PET systems utilizing TOF information it is desirable to improve spatial resolution, sensitivity, and the TOF measurement uncertainty. To this end, studies with new scintillation detectors and photomultiplying devices have been undertaken. Barium fluoride is a recently discovered[1] scintillation detector for use in TOF measurements. Its density, decay constant, and nonhygroscopic characteristics are all improvements over previously used cesium fluoride and will no doubt be the prime detector choice in future systems.

As an alternative to photomultiplier tubes (PMTs) for scintillation detection, work is in progress to develop a multistage detector using microchannel plates (MCPs). Early results show that simply substituting MCPs for PMTs gives somewhat inferior timing resolution, however the work demonstrates that a single stage MCP followed by a solid state amplifier solves the problem of MCP saturations. In the planned multistage configuration,

the MCP-based detector should out perform current PMT-based detectors. More research is required before the MCP approach can be considered practical.

A newly developed photomultiplier tube (Hamamatsu R1450Q) is the best currently available device for this application. The TOF measurement error is comparable to the larger devices previously used, but due to its inherent size, improved spatial resolution can be achieved. At present, the best candidate for a future system would be small barium fluoride detectors packed tightly in pairs under the new tube using coding information provided by another tube, for detector identification. This arrangement is expected to yield a spatial resolution of 4.5 mm, about 50% of maximum sensitivity, and a TOF uncertainty of 500 psec.

1. R. Gariod, R. Allemand, E. Cormoreche, M. Laval, and M. Moszynski, "The 'LETI' Positron Tomograph Architecture and Time of Flight Improvements," Proceedings of the Workshop on Time-of-Flight Tomography, IEEE Catalog No. 82CH1791-3, St. Louis, Missouri, pp. 25-29, May 17-19, 1982.

D-19. VLSI Systems for Time-of-Flight PET

Personnel: C. E. Molnar, Sc.D., Computer Systems Laboratory

Support: RR 01379
RR 01380

Over the past several years, it has become practical for university research groups to design and have fabricated specialized silicon chips with a high level of complexity (Very Large Scale Integration). The developments that have made this possible and some possible opportunities for application in the design of time-of-flight positron-emission tomography systems have been briefly reviewed and reported.[1]

1. C. E. Molnar, "VLSI Systems for Time-of-Flight PET," Proceedings of the Workshop on Time-of-Flight Tomography, IEEE Catalog No. 82CH1791-3, St. Louis, Missouri, pp. 167-170, May 17-19, 1982.

D-20. International Workshop on Time-of-Flight Tomography

Personnel: D. L. Snyder, BCL
G. J. Blaine, BCL
J. R. Cox, Jr., BCL
M. E. Raichle, M.D., Neurology
M. M. Ter-Pogossian, Ph.D., Radiology
L. J. Thomas, Jr., BCL

Support: RR 01358
Washington University

An international workshop on time-of-flight tomography was held at Washington University during May 17-19, 1982. During the past year, the proceedings of this workshop were edited and then published by the IEEE Computer Society.[1] A portion of the introduction to these proceedings follows.

> "It is safe to state that this is the first scientific meeting devoted to the utilization of photon time-of-flight information in positron emission tomography. The concept of utilizing such information in the localization of positron annihilation events for biomedical purposes is not new. A number of authors, some who are contributing to this symposium, particularly Dr. Gordon Brownell, have speculated about this possibility and carried out experimentation, the results of which were encouraging but which also indicated that better temporal resulition in time-of-flight measurements was needed to utilize effectively such measurements in the biological tracing of positron emitters. The first concept of utilizing time-of-flight information to improve signal-to-noise ratio in PET should be credited to a French group (Laboratoire d'Electronique et de Technologie de l'Informatique) who reported encouraging results in 1979. It is to the credit of this interesting concept and also to the intense commitment of a segment of the scientific community to PET that sufficient interest and useful studies have been carried out in the past three years to warrant the gathering of this symposium.
>
> Several facets of the present meeting deserve mention. The invited participants come from several countries extending as far from St. Louis as Japan and France. They represent a number of scientific disciplines including medicine, biology, mathematics, physics, electronic engineering, computer science and others. Of course, they share the common interests of positron emission tomography and the utilization of time-of-flight for this modality. Because it is important to consider future research directions in the context of application needs, specific attention was given to biomedical issues as well as to technical issues in an atmosphere that fostered useful dialogue between users and developers of time-of-flight systems.

The structure of the symposium was developed to emphasize strongly the active involvement of the participants both in the scientific presentations and discussions of the material presented, for which ample time was allocated. Assigned discussion leaders and chairmen of the corresponding scientific sessions developed short summaries which were then presented to the full body of the workshop for their approval in a final session. Those summaries are included at the beginning of the respective sections of these proceedings."

1. L. J. Thomas, Jr. and M. M. Ter-Pogossian (co-chairman), Proceedings of the Workshop on Time-of-Flight Tomography, J. R. Cox, Jr. (ed.), IEEE Catalog No. 82CH1791-3, Washington University, St. Louis, Missouri, May 17-19, 1982.

D-21. A Computer System to Support Super PETT I in the Coronary Care Unit

Personnel: D. E. Beecher, BCL

Support: RR 01380
HL 17646

Plans are now underway to transport Super PETT I, a time-of-flight assisted positron camera, to the Coronary Care Unit where it will be used routinely to study critically ill patients with cardiac disorders. Technical aspects of this device are discussed at length in other sections of this report and in the literature.

Super PETT I requires a very specialized and powerful computer system to support its high data-transfer rates and the software development needed to interpret and analyze the data it generates. Initially, many different configurations were considered before choosing the Perkin Elmer 3230 system as the host for Super PETT I. The configuration for this system is shown in Figure 1.

The 3230 processor is particularly advantageous in that it is totally compatible with the 3242 processor on which Super PETT I was initially developed and tested. All software which was designed on the 3242 is directly transferrable to the 3230 without modification. The 3230 processor has various options including: a hardware floating point unit to enable fast floating point operations, 2K bytes writable control store to enable fast execution of time-critical sections of code, and cache memory to enhance the overall system performance.

Central to the successful support of Super PETT I are data transfer from the PETT device and storage of the data received in real time. The

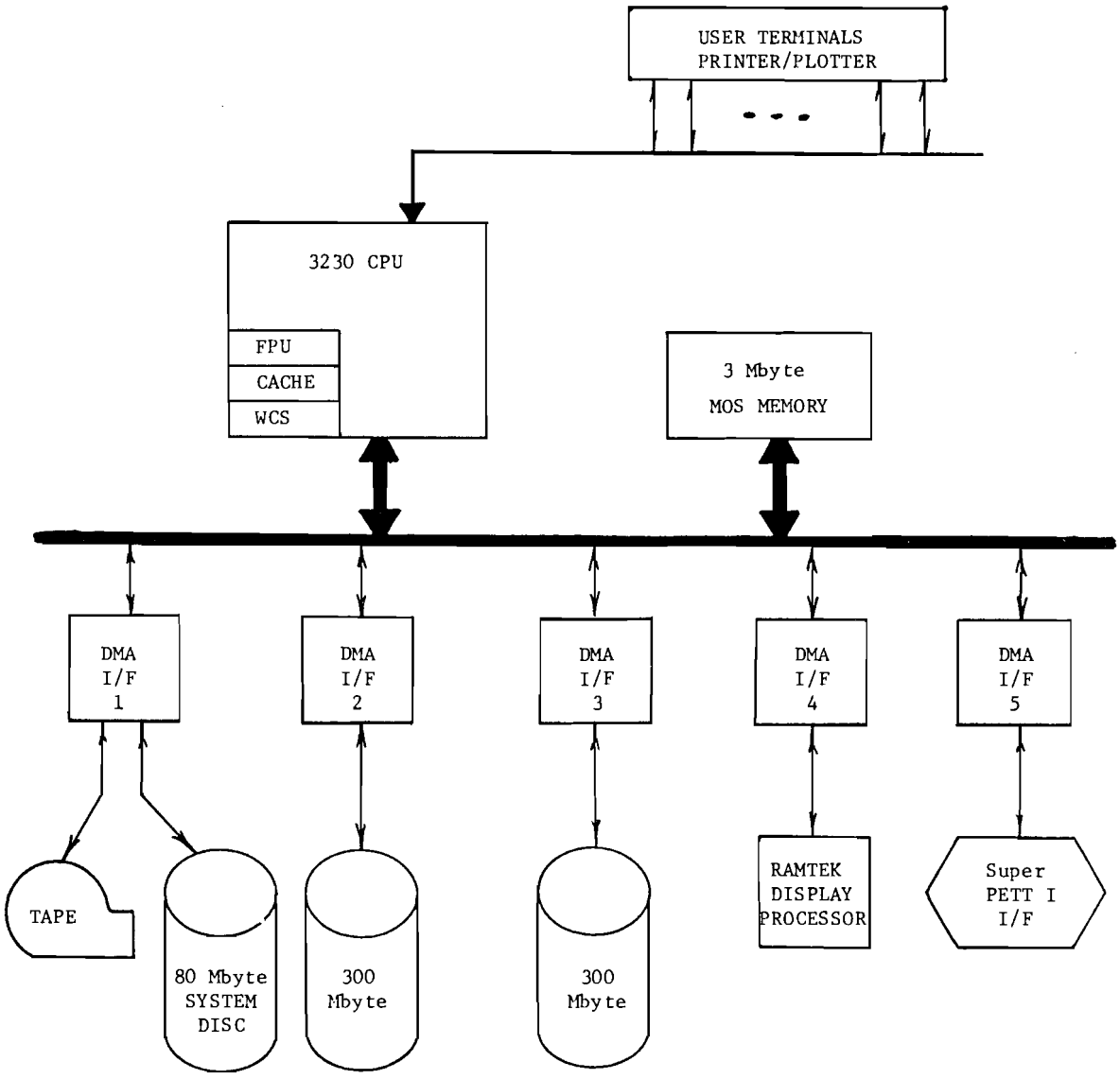

Figure 1. The hardware configuration to support Super PETT I in the Coronary Care Unit.

3230 is equipped with 3 Mbytes of main storage to accommodate the large data spaces required for the collection software and the new reduced-angle reconstruction technique (D-7). As fast as the data are collected from Super PETT I it must be stored in real time on rigid disks for later retreival and processing. Two 300-Mbyte disks on separate DMA channels ensure that we can handle the expected data transfer rates. The current configuration is capable of storing 550 Mbytes of data and sustaining an average transfer rate of approximately 1.6 Mbytes/sec.

The system also includes several user terminals, an 80-Mbyte fixed system's disk, a dual-density 75 i.p.s. tape drive to archive the data, and a custom built Super PETT I interface to allow communications with the PETT device. The bulk of the image processing work is handled by a Ramtek 9450 image processing system with an interactive trackball.

E. Systems for Specialized Biomedical Studies

This section is characterized by a diverse range of topics: as in previous years the common factor is that each relates to the transformation, transduction and display of physiologic variables.

Two of the projects involve neurophysiology. A system for the acquisition of potentials recorded from many sites on and in the exposed human brain is undergoing refinement and clinical testing (E-9). For the study of long periods of EEG recording a very low cost and easily portable multiple channel tape recorder has been developed (E-3). Apart from its primary use it is expected to have value in other experimental situations where commercially available recorders are not cost effective.

Work continues on methods designed to improve understanding and diagnosis of a variety of visual problems. Assessment of the effects of elevated intraocular pressure on visual fields (E-6) and the use of color as a parameter in perimetry (E-5) are examples. Since not all glaucoma patients persist with their drug treatment regimen, evaluation of treatment is difficult. A simple and convenient device (E-6) to measure compliance with the prescribed treatment has been made.

Work on the mapping of the yeast genome which has important implications for genetics is continuing (E-2) and a mathematical and pathophysiologic model of the ways in which albumin permeates the kidney is under test (E-7).

E-1. An Automated Autoradiographic Analysis System for Neuroanatomical Studies

Personnel: R. E. Hermes, BCL
A. J. Gray, BCL
E. G. Jones, M.D., Ph.D., Anatomy
S. R. Phillips, BCL
J. L. Price, Ph.D., Anatomy

Support: RR 00396
RR 01380
NS 15070

The automated silver-grain counter developed and revised during the past few years (PR 16, F-4; PR 17, C-1; PR 18, C-1) has proven to be a useful research tool not only for analysis of neuroanatomical autoradiographs but also in a variety of other areas which require acquisition of digital images.

The system is capable of obtaining silver-grain counts for large fields, with accuracies on the order of 92%. Good performance has been partially attributed to the use of auto-thresholding and auto-focus algorithms. The system has proven to be easy to use, and to provide accurate data presented through the use of pseudocolor and gray-scale grain-density maps produced in color or black and white photographs on Polaroid or 35 mm film.

The high degree of flexibility of this system which incorporates a Lexidata display system and a TN 2500 CID solid-state camera has made the configuration useful for obtaining image data for use in image compression studies, digitizing cells undergoing division, and has aided the study of retina images obtained from diabetic patients.

E-2. DNA Restriction Mapping Studies

Personnel: J. G. Dunham, BCL
D. E. Beecher, BCL
A. J. Gray, BCL
J. Markham, BCL
M. V. Olson, Ph.D., Genetics

Support: RR 00396
RR 01380
GM 28232

The preparation and analysis of hundreds of electrophoretic gels is required in the construction of a complete physical map of a yeast genome. The rationale and background of this project has been previously reported (PR 16, G-10; PR 17, C-2). Subsequently, the hardware for a semi-automated system for extracting the DNA fragment-size data from these electrophoretic gels was completed. The system consists of an Eikonix EC 78/99 solid-state image digitizer, a Digital Equipment Corporation LSI 11/23 with a 30-Mbyte disk drive, and a Lexidata 3400 raster display system. A block diagram of the hardware configuration was shown in PR 18, C-2, Figure 1. The data acquisition and analysis software which has been completed during the past year consists of three main modules: Creation, Gel Reading, and Update and Review. Two heuristic band-detection algorithms were developed and one was chosen for the initial version of the system. A working version of the system is currently being evaluated in Dr. Olson's laboratory.

We have begun to study the feasibility of using partial digestion techniques to obtain both order and length information about the fragments in each clone sample. A probabilistic mathematical model has been developed that predicts the time course evolution of the partial digestion fragment concentrations as a function of cleavage reaction rates. Experiments are being developed to verify the feasibility of the model. To detect the numerous low-concentration bands found in a partial digestion, a probabilistic model was developed for the band intensities obtained from a electrophoretic gel photograph. From this model an optimal estimation approach was developed that suggests using a spatially varying parabolic matched filter to detect the location of each band. We propose to implement and study this band-detection algorithm in the coming year to determine its feasibility and usefulness. We also propose to study the statistics of the overall gel-reader system to determine their overall impact on the band detection accuracy problem.

In previous reports (PR 17, G-10; PR 18, C-2) it was indicated that a probabilistic model of DNA base pairs was developed to aid in the reconstruction of the genome from the experimental clone data and that the validity of the model would be tested on a 100-clone sample prepared by Dr. Olson. Work is continuing on this project and we anticipate it will be completed in the early part of the next year. We propose to begin to develop sequential algorithms for the actual construction of the physical map from the experimental clone data.

E-3. Development of Multi-Channel Analog Data Recorder

Personnel: H. W. Shipton, BCL

Support: RR 00396

Multi-channel tape recorders that are capable of DC or very low frequency recording are expensive (circa $30K for 16 channels), heavy, and in some cases, hard to adjust. Many have been developed for military and/or aerospace applications where near absolute reliability and fidelity are mandatory. For many biomedical applications occasional loss of data ("drop-outs") can be tolerated and balanced against the system cost and complexity. Examples of such fault-tolerant data are polysomnographic recordings and EEG data for topologic analysis.

The home video cassette recorder (VCR) suggests itself as a convenient low cost instrument for analog data recording because mass production has reduced their retail cost to less than $500. Their use as data recorders is however, not entirely straightforward. They cannot easily be used in an "open-loop" mode because speed variations are then intolerable and the electronics are specifically conditioned to the requirements of network television.

The system under development converts the analog signals to "false" video so that no modifications to the VCR are needed and so that data may be recorded in any of the available tape formats.

As a consequence of the TV system the video signal is interrupted for approximately 1.3 ms every 16.6 ms. The spectrum of this signal lies within the desired signal passband and it is this artifact that has restricted the use of VCR machines for data storage. The solution adopted is to reduce the number of TV "lines" from 525 to 512 and to divide this into 32 segments. One segment is used as the frame-sync pulse (which also controls, via a PLL, tape speed in the VCR). The next segment contains 16 pulse-position modulated signals and the next is blank. The arrangement is shown in Figure 1.

Signals are sampled at equal intervals and thus no frequency components related to the frame rate are spuriously added to the signal spectrum and in principle signals in the range 0 to 250 Hz can be recorded. Conventional multiplexing and demultiplexing methods are used to route signals to and from their appropriate time slots.

The system has been tested in "breadboard" form on three different VCRs and show encouraging results. A final version should be available in Fall 1983.

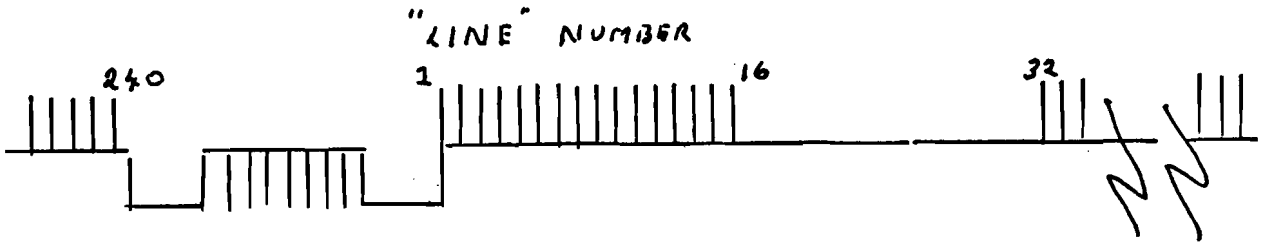

Figure 1. The synchronizing pulses are similar to those used in (American) T.V. The interval between frame pulses (16.67 ms) is divided into 256 equal intervals. Analog signals are converted to P.W.M. code during the first 16 of these intervals, the next 16 are blank and so on until "line" 260 is reached whereupon a serrated frame synchronizing pulse is formed.

E-4. Visual Fields and Ocular Hypertension

Personnel: W. M. Hart, Jr., M.D., Ph.D., Ophthalmology
D. E. Beecher, BCL

Support: RR 00396
EY 02044

This project, which was originally established to support the study of the long-term effects of elevated intraocular pressure on the visual field, has evolved over the past year to include the use of the microprocessor-based visual-fields data-acquisition system for the static perimetric examination of patients with a broader variety of ophthalmic diseases.[1,2,3,4] Three-dimensional static perimetry has been used to examine the topography of the central visual field in patients with a variety of primary macular disorders, as well as diseases of the optic nerve. A significant feature which has been detected by this technique is the tendency of visual field defects arising from macular disease to produce annular depressions in the visual-field surface placed concentrically about the point of fixation. Thus, there is a generic tendency for foveal sensitivity to be relatively preserved at the center of relative scotomas arising from macular disease. This phenomenon has not been detected in central scotomas resulting from optic nerve disorders.

Continued study of patients with elevated intraocular pressure to detect the earliest manifestations of visual field depression associated with the onset of glaucoma have demonstrated that in those patients who have definite pathologic changes in their optic disks, yet who show no evidence of visual field defect by conventional forms of perimetry (kinetic perimetric examination with a Goldmann perimeter), have shown the presence of transient, shallow localized depressions in that portion of the visual field referred to as the Bjerrum region. This area has long been known to be the location of initial glaucomatous visual field defects which are,

under ordinary circumstances, more dense when first detected. Although threshold static perimetry with this form of three-dimensional examination appears to be the most sensitive visual function test we now have for the detection of the early stages of glaucoma, it is thought still to be inadequate, since anatomic changes in the optic nerve can be observed ophthalmoscopically prior to the onset of detectable functional defects in the visual field.

1. W. M. Hart, Jr. and A. E. Kolker, "Computer-generated Display for Three-dimensional static Perimetry: Correlation of Optic Disc Changes with Glaucomatous Defects," Documenta Ophthalmologica, in press.

2. W. M. Hart, Jr., "Three-dimensional Topography of the Central Visual Field, Proceedings of the XXIV International Congress of Ophthalmology, in press.

3. W. M. Hart, Jr. and R. M. Burde, "Three-dimensional Topography of the Central Visual Field: Sparing of Foveal Sensitivity in Macular Disease," Ophthalmology, in press.

4. W. M. Hart, Jr., R. M. Burde, G. P. Johnston, and R. C. Drews, "Static Perimetry in Chloroquine Retinopathy: Perifoveal Patterns of Visual Field Depression," Archives of Ophthalmology, in press.

E-5. Color Perimetry Studies

Personnel: W. M. Hart, Jr., M.D., Ph.D., Ophthalmology
K. W. Clark, BCL
A. J. Gray, BCL
R. W. Hagen, BCL

Support: RR 00396
EY 03703

Over the past year hardware development work on the color perimeter was completed. The device now consists of an Aydin color video monitor driven by a custom video controller, which is connected by an IEEE-488 bus to a Motorola Exorset microcomputer. In addition, a Hewlett-Packard 9111A graphics tablet is also interfaced through the bus into the system. Operator interaction with this system is by way of the graphics tablet. Manipulation of the magnetic stylus on the tablet, which includes 16 soft keys as well as a high-resolution digitizing area, allows the selection of menu choices, as well as real-time kinetic presentation of perimetric test objects on the color video monitor screen. A Tektronix video photometer with BCD output has also been incorporated into the system to permit use of an automated calibration routine.

The instrument system has been installed in a laboratory-in the McMillan Hospital where it is now being used in initial clinical trials to evaluate the visual fields of patients with known or suspected glaucoma. The color video monitor has been placed on an adjustable-height table equipped with a sliding platform to allow adjustment of the monitor position in front of the patient to be examined. Steady support of the patient's head during the examination is accomplished through use of a conventional ophthalmic chin rest device. A small surveillance vidicon camera has been placed on top of the color video monitor, and is focused at close range on the face of the subject to be examined. A closed circuit image of the patient's face is provided on a 9-inch monitor in front of the operator to permit continuous assessment of patient fixation on the center of the color video monitor screen.

Colored test objects are matched to a constant-luminance white surround through the use of heterochromatic flicker photometry, following which presentation of colored test objects of varying saturation (but constant luminance) are used to explore the peripheral portions of the central visual field. Initial studies have demonstrated that isopters (contours of isosensitivity in the visual field) for variably saturated colored targets of constant luminance, are qualitatively identical to those obtained for conventional perimetric targets of varying luminance but constant color (white).

A series of 24 patients with early though well-established glaucomatous visual field defects have been examined by this technique, and formal comparisons have been made to the results of conventional forms of perimetric examinations on the same individuals. Initial results indicate that color defects in the visual field are spatially identical to those for luminance defects. There is no apparent tendency for color defects to extend spatially beyond those defined by luminance techniques. Studies are currently underway to evaluate the possibility that early visual field defects (prior to the onset of conventional luminance defects) might be more sensitively detected with the use of variably saturated colored test objects.

E-6. Compliance with Ophthalmic Therapy

Personnel: M. A. Kass, M.D., Ophthalmology
D. E. Beecher, BCL
M. E. Gordon, Ph.D., Ophthalmology
D. W. Meltzer, M.D., Ph.D., Ophthalmology

Support: RR 01380
EY 03579

In recent years it has become obvious that compliance is an important limiting factor in many clinical situations.[1] Glaucoma is an asymptomatic disease that often requires chronic medical therapy. We have designed an eyedrop medication monitor to study compliance with topical ophthalmic medications.

This monitor records a use in any 15 minute period if the patient removes the bottle cap and inverts the bottle. The monitor has memory for approximately six weeks. The data are read via direct hardware interface with a PDP 11/34 and stored on rigid disk for future reference. The software system which resides on the PDP 11/34 has remained essentially unchanged from the functional description in PR 18, E-13. Some minor changes were made to accommodate an operating system upgrade to RSX-11M version 4 earlier this year.

Our initial studies have concentrated on compliance with topical pilocarpine therapy. Data on the first 108 patients indicate many patients omitted a substantial number of pilocarpine doses - 19.6% of the patients administered fewer than 50% of the prescribed doses and 37% of the patients administered fewer than 75% of prescribed doses. The time scheduling for pilocarpine administrations was suboptimal in many patients. Patients skipped entire days and compressed the doses during the daytime hours.

Less than 50% of the patients were following a 4-dose/day administration pattern. Physicians were unable to distinguish patients with high rates of compliance from patients with low rates of compliance.

1. M. A. Kass, D. W. Meltzer, and M. E. Gordon, "The Compliance Factor" in The Pharmacology of Glaucoma, S. Drance and A. Neufeld, eds., in press.

E-7. Assessment of Albumin Permeation in Glomerular and Postglomerular Capillaries in Diabetic Kidneys Using Mathematical Models of Mass Transport to Interpret Kinetic Radiotracer Data

Personnel: J. R. Williamson, M.D., Pathology
K. C. Chang, Ph.D., Pathology
K. B. Larson, BCL
J. S. Marvel, B.S., Pathology
R. G. Tilton, Ph.D., Pathology
J. R. Udell, B.S., Pathology

Support: RR 00396
RR 01380
AM 07296
The Kilo Diabetes and Vascular Research Foundation

The objective of this project is to develop procedures for assessing albumin permeation of both the glomerular and of the postglomerular capillaries in the isolated perfused rat kidney under normal as well as under pathophysiological conditions. Methodologically, the project is related in its aims to those of our studies of the pathophysiology of ischemic injury to the heart (A-7).

Estimates of albumin permeation of glomerular capillaries obtained in intact kidneys by conventional techniques (for radiolabeled albumin and other tracer molecules) are markedly influenced by alterations in postglomerular tubular epithelial function; estimates of postglomerular capillary permeability properties are difficult if not impossible to obtain by conventional approaches. By the use of residue detection and mathematical modeling techniques in isolated perfused kidneys, it should be possible to circumvent the effects of altered tubular epithelial cell function and to assess albumin permeation f glomerular and postglomerular capillaries individually.

For these studies, we remove the kidney from the rat and perfuse it via a cannula in the renal artery with Krebs-Ringer phosphate buffer containing 1% albumin. A cannula is also placed in the ureter to monitor urine production. After a 30-min stabilization period, a bolus of ^{125}I-BSA and ^{57}CoEDTA is injected via a port in the arterial cannula and the washout history of the isotope in the kidney is monitored by external detection of the emitted radiation. The detector response is fitted to the parameterized function

$$r(t) = A_1 e^{-\alpha_1 t} + A_2 e^{-\alpha_2 t} + A_3 e^{-\alpha_3 t}. \qquad (1)$$

In the above, t denotes elapsed time after bolus administration; r(t), the radioactivity counting rate registered by the external detector at time, t. The A's and α's represent modal parameters related to the physiological parameters of the compartmental model. A maximum-likelihood method of parameter estimation for radiotracer kinetic data, developed some years ago at BCL,[1] has been implemented and applied in order to obtain estimates of the six modal parameters in Equation (1). We are now initiating experiments to test the model and to examine the impact of diabetes and other pathophysiological states on the integrity of glomerular and postglomerular capillaries.

1. J. Markham, D. L. Snyder, and J. R. Cox, Jr., "A Numerical Implementation of the Maximum-Likelihood Method of Parameter Estimation for Tracer-Kinetic Data," Mathematical Biosciences, vol. 28, pp. 275-300, 1976.

E-8. System Support for Isolated Probe Data Acquisition System Utilizing Altair 8080's

Personnel: D. E. Beecher, BCL
H. D. Ambos, BCL

Support: RR 01380
HL 13851
HL 17646

An identical pair of Altair 8080 computer systems is used to support open-chested canine preparations and isolated-heart rabbit preparations in the Cardiology Laboratory located on the sixth floor of Wohl Clinic. Each consists of eight Nuclear Instrument modules and an Altair 8080 microcomputer and is capable of collecting, formatting, and storing data from four probes directly. The Altair 8080 microcomputer system consists of 32 Kbytes of memory, dual floppy-disk drive and controller, real-time clock, seven A/D converter channels, seven D/A converter channels, a custom probe-data interface, and a dot-matrix printer/plotter. In the past year it became necessary to replace one of the printer/plotters due to a malfunction which could not be repaired. The printer/plotter replacement was a PRISM model 80 which proved to be somewhat compatible with the discarded device. Modifications were made to several system-level device handlers in order to adequately support the new printer/plotter.

These multiprobe detection systems are still being used to validate tracer methods for noninvasive measurement of myocardial perfusion and metabolism. However, the two Altair microcomputers are no longer manufactured and spare parts are unavailable, making maintenance virtually impossible. For these reasons we have purchased a replacement system consisting of an LSI 11/23 with dual floppy disks, memory management, floating point, and a VT103 video terminal. The recently purchased PRISM printer/plotter will be moved to the new system near the end of the development cycle. Also purchased was a SELANAR raster-graphics display board which will allow real-time monitoring of the time-activity curves while the experiment is in progress.

The software system to support this work will be completely redesigned to incorporate protocols not practical with the existing system configuration. The retired Altair system will be used for spare parts to maintain the remaining Altair system for as long as is practicable.

E-9. An Automated System for the Monitoring of Patients with Epidural Electrode Arrays

Personnel: J. S. Massey, BCL
S. Goldring, M.D., Neurological Surgery
E. M. Gregorie, M.D., Neurological Surgery
P. Lombardo, B.A., Neurological Surgery
B. A. Pearson, B.S., Neurological Surgery
K. Socha, Neurological Surgery

Support: RR 00396
RR 01380
NS 14834
McDonnell Center for Studies of Higher Brain Function
Washington University

The purpose of this project is to develop a system which will permit simultaneous recording of the EEG and somatosensory evoked responses (SER) from patients in whom epidural electrode arrays have been implanted for the purpose of localizing an epileptogenic focus.

The system consists of three parts, as shown in the block diagram (Figure 1). An automated switching matrix allows us to select EEG or SER data from up to 52 electrodes and to switch rapidly from one set of input signals to another. The system for computer-assisted extraction of somatosensory evoked responses (CAESER) is used to acquire, store, and display the SER. The system will be able to monitor the patient's EEG activity, detect a seizure, and generate a videotape showing the patient behavior and corresponding EEG data. It will also be able to produce a conventional paper recording of the EEG. This will give us the ability to store, index, and display on command the EEG activity and patient behavior for a period of several minutes before, during, and after each seizure.

As reported before (PR 18, E-14), the automated switching matrix is now in routine use. It continues to perform satisfactorily.

Initial hardware development of the CAESER system was completed in September 1982. It consists of a sixteen-channel EEG amplifier, a sixteen-channel analog-to-digital converter, a Digital Equipment Corporation (DEC) MINC microcomputer, and a video module which displays the evoked responses on standard television monitors.

The initial system uses sixteen Grass Instrument Company 8A5 EEG amplifiers which are part of our EEG machine. Because of this, EEG and SER cannot be acquired simultaneously. In May 1983 sixteen Grass Model 12 Computer Interface Neurological Amplifiers were ordered. These should be installed and usable under-manual control by September 1983.

The MINC software, which performs signal averaging, data manipulation, and storage, is written in the RATFOR structured dialect of FORTRAN and in PDP-11 MACRO assembly language. It runs under the RT-11 operating system. Development and testing of the initial software package was completed in December 1982, and enhancements were added in May of 1983.

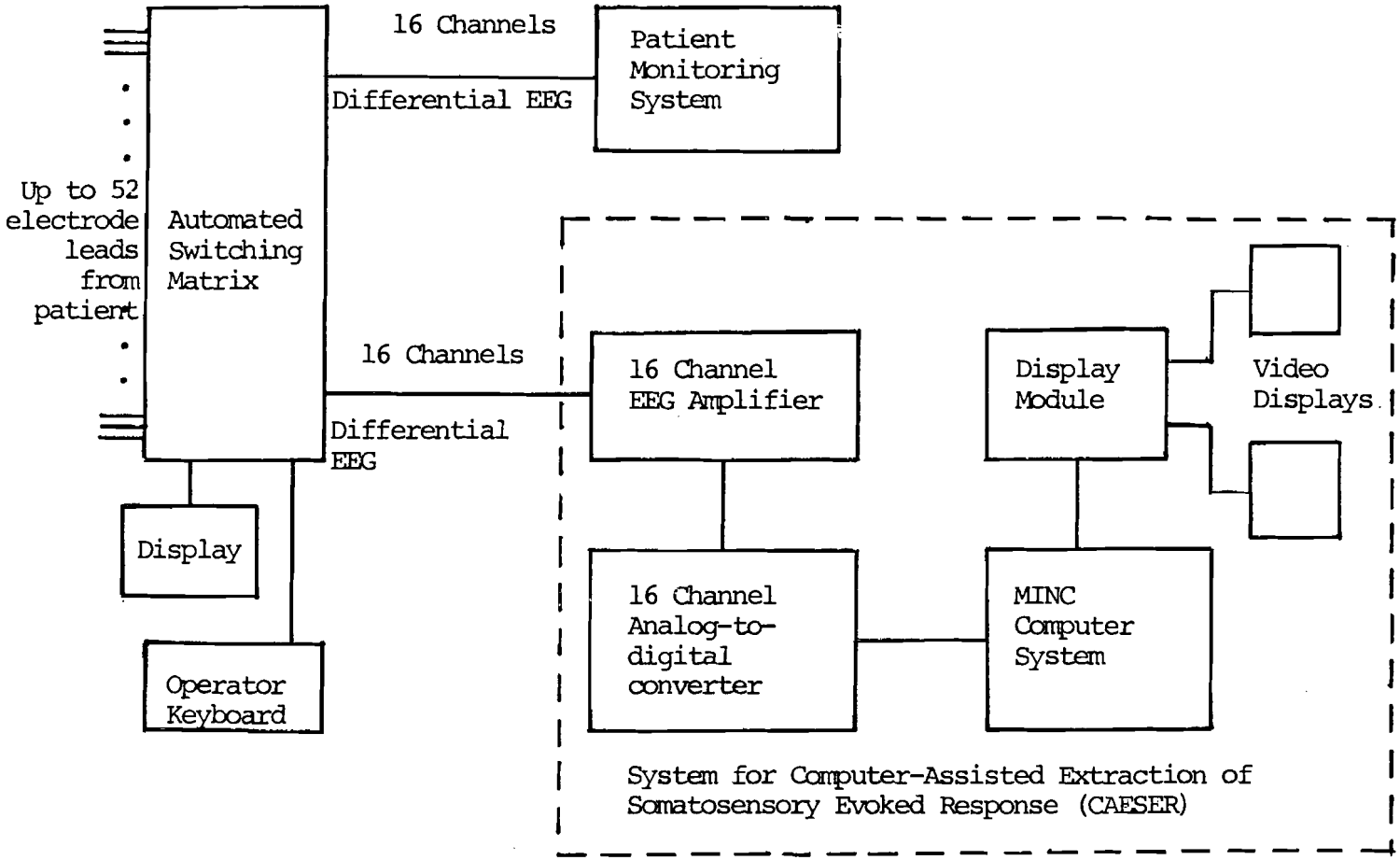

Figure 1. Block diagram of automated system for the monitoring of patients with epidural electrode arrays.

The system has been used to gather SER data from six patients since December 1982. While it has performed according to specification, several improvements are desired to make the system more useful. These include better control of data acquisition, easier manipulation and comparison of the displayed waveforms, and the ability to better view SER data as it is being acquired.

Currently, we are in the process of making the necessary hardware upgrades to accomplish these improvements. These include upgrading the MINC with a DEC VT125 graphics terminal and LSI-11/23 processor, and obtaining a new sixteen-channel analog-to-digital converter.

In addition to making the software upgrades necessary to obtain these improvements, we would like to make the programs easier and faster to use, so that the system can be run by medically-oriented users. The sudden death of Ms. Barbara Pearson, our software engineer, in May 1983 has proved a serious setback to our efforts. Currently, we are searching for a replacement, and hope to have software development efforts underway again by September 1983.

Initial plans called for the patient monitoring system to be based on a DEC PDP-11/34 minicomputer located in McMillan Hospital and linked to equipment near the patient via a digital communication system. The PDP-11/34 was installed in December 1981 and has been used since then in software development for the CAESER system. Recent studies indicate that using one of the new powerful microcomputers with Winchester storage, such as the DEC MICRO/PDP-11, may provide the same amount of computing power as the PDP-11/34 while being sufficiently small and rugged to be moved to the patient bedside. Full scale design and development of this system would begin upon completion of the CAESER system upgrades.

F. Resource Development Activities

Resource development activities are those which contribute to the goals of more than one major program of the laboratory, address the needs of individual users who can benefit from the expertise of the BCL staff and the inventory of computing and specialized test equipment, or identify new technologies which may become appropriate foundations for new experimental tools. Service to users does not follow the usual computation-center pattern with an established fee schedule and a highly centralized facility. Rather, senior laboratory staff members consider requests for assistance from investigators who must address a particular biomedical computing problem. If an appropriate technology exists, investigators may be referred to commercial vendors or fee-for-service organizations when these are available. In other cases, problems may be approached by the laboratory provided that the effort complements other activities of the laboratory. Many times the project can be assigned to a staff member with appropriate experience and completed in a short time. The investigator then has his or her results, and a short note describing the work will appear in the annual report and perhaps the open literature. A few projects, however, may develop into major initiatives within the laboratory. Most of the major projects began in this fashion and the opportunities that supporting activities provide are valued.

The broad spectrum of projects reported on in this section may be categorized as biomedical applications, system development aids, digital hardware designs, and ad hoc studies. The biomedical applications represent new initiatives in which basic explorations are being conducted, some having potential for becoming major, long term programs. An example is the DNA restriction mapping work which was previously reported in this section, but which has matured to the point where it is reported under Systems for Specialized Biomedical Studies (E-2). Even when an extended collaboration does not develop, the relationships cultivated and the experiences gained frequently prove beneficial to future work.

System development aids primarily benefit BCL staff, but may also be used by others. Examples include microprocessor development support and RSX-11 system enhancements. System software developments reported here also are widely utilized in a variety of projects.

Many digital hardware designs are one-time, special purpose projects. Others may have wide appeal and construction of multiple copies is envisioned, an example being the TERRANET local network.

The topics of the studies reported in this section are quite varied. Some are theoretical and address a highly specific problem; others are more properly thought of as feasibility studies.

F-1. Microprocessor Development Support

Personnel: G. J. Blaine, BCL
M. W. Browder, BCL
K. H. Haserodt, M.S., Computer Science
R. E. Hermes, BCL
R. E. Hitchens, BCL
S. M. Moore, BCL

Support: RR 00396
RR 01380
HS 03792

Software and hardware development of 8-bit microprocessor-based systems continues to be supported by locally-developed FORTRAN-based cross-assemblers (FOCRAS) and intelligent consoles (Inc). FOCRAS is available on PDP-11/RSX, PDP-11/RT-11, and TI-980/MIST 980 host environments. A Data I/O universal PROM/PLA programmer has been added to facilitate custom firmware and hardware design. Support for bit-slice processors based on the AMD 2900 series-components is supported with an Advanced Micro Computers System 29 development system (D-4).

Progress toward hardware and software support facilities for development of systems based on the Motorola M68000 (M68K) 16-bit microprocessor continues. Assembly language as well as high-level language (C language compiler) software development is available on a variety of machines (PDP-11, VAX 750) throughout the Washington University Computer Laboratories.

Installation and augmentation of a UNIX (a trademark of Bell laboratories) based cross-compilation system developed at Massachusetts Institute of Technology provides a sophisticated development support facility for M68K systems. UNIX has been successfully transported to a Motorola M68K Versamodule system. Distributed access for both program generation and downloading is provided by TERRANET.

F-2. Information Systems Group

Personnel: J. R. Cox, Jr., BCL and Computer Science
G. J. Blaine, BCL
M. W. Browder, BCL
R. E. Hitchens, BCL
M. M. Maurer, Jr., M.D., St. Louis Children's Hospital
P. Moore, BCL
S. M. Moore, BCL
S. R. Phillips, BCL
L. J. Thomas, Jr., BCL

Support: RR 00396
HS 03792
Washington University

The Information Systems Group provides the collaborative structure within which participants from the Department of Computer Science, the Computer Systems Laboratory, the School of Medicine, and the Biomedical Computer Laboratory are addressing the development of a methodology for the design of composite medical-information systems. The development activities can be divided into four major categories: model, design studies, implementation and Neonatology Database. The more theoretical portions of the work on a design methodology fall in the first category and the more applied tasks in the second. The design-studies category also includes architectural studies and custom LSI design experiments. Implementation activities are to establish an adaptable, experimental environment for the support of a trial implementation of a medical-information system designed according to the methodology specified by the Abstract Database System (ADS) data model. The Neonatology Database undergirds the entire effort by providing a relevant context for testing concepts, models and implementations.

The tightly knit interdisciplinary team ensures an environment based on direct experience with the operation of a complex medical-information system which contains data on actual patients and which is useful to clinically active decision-makers. Such an environment facilitates realistic model development and architectural considerations.

Properties of the data model (ADS) have been refined and extended to include abstraction on symbols as a primitive concept. ADS is believed to be an appropriate model of sufficient power to allow translation between other existing data models. A database design aid has been implemented in MUMPS which provides an environment for the construction of an ADS description of the Neonatology Database. Design studies of pattern-matching architectures suited to VLSI implementation have continued.

Implementation activities include developing an ADS system in the C programming language on a PDP-11/34 computer. The C-based implementation has been transported to Motorola 68000 (M68K) experimental configuration.

A coprocessor for high-speed pattern matching is designed and under construction (F-3). Specific details of these activities are summarized elsewhere.[1]

1. J. R. Cox, Jr., "A Medical Information Systems Design Methodology," HS 03792 Final Report, September 1983.

F-3. Studies in the Design of a Coprocessor for Pattern Matching

Personnel: S. M. Moore, BCL
G. J. Blaine, BCL
J. R. Cox, Jr., BCL, and Computer Science

Support: RR 00396
HS 03792

The search mechanism in the current implementation of ADS is done in software (F-2). To determine how much gain could be realized from a hardware searcher, a study in the design of a coprocessor for pattern matching was begun. Algorithm development was done using the current ADS implementation and the C programming language on a PDP-11/34.

An algorithm of time complexity O(N) was found, where N is the size of the database. Several architectures for implementing this algorithm were studied. One of the architectures is used as the basis for a processor currently being built using commercially available MSI parts. This unit will serve as a coprocessor in the Motorola 68000 Versabus system (F-10). Debugging and evaluation of the system should be completed in the next two months.

F-4. MUMPS-Based Applications

Personnel: P. Moore, BCL
F. Arias, M.D., Ph.D., Obstetrics and Gynecology
L. S. Hillman, M.D., Pediatrics
J. E. Knobbe, Obstetrics and Gynecology
S. P. Leara, Obstetrics and Gynecology
S. J. Salmons, C.P.N.P., Pediatrics

Support: RR 00396
HD 09998
HS 03792
St. Louis Children's Hospital

Prior activity in the Laboratory has included the development and operation of several information systems for the support of ongoing research projects. Almost all of these databases have concentrated on longitudinal information because of its importance to clinical investigations of chronic diseases. During the past year, the development and operation of such databases has been deemphasized as a research activity because such services are now provided by other organizations within the University.

The four MUMPS-based systems of note in the past two years have been Neonatology, Mineral-Homeostasis and Mineralization, Obstetrics, and Premature Rupture of Membranes. All four used the same table-driven software. Experience with these databases influenced the development of the data model called Abstract Database System (ADS). In particular a specification of key features in the Neonatology Database was completed this year to aid the evaluation and implementation of ADS (F-2).

The Neonatology Database (2728 infants) contained clinical data collected from a Neonatal Intensive Care Unit. The Mineral-Homeostasis and Mineralization Database (273 infants) emphasized the collection and manipulation of quantitative data. The Obstetrics Database (8375 mothers) contained data on all deliveries performed at Barnes Hospital since March 15, 1981 and on some deliveries done at Jewish Hospital. The Premature Rupture of Membranes Database (458 mothers) contained data on both mothers and their newborn infants. The Neonatology and Obstetric Databases were used primarily to respond to ad hoc questions concerning patient care and research issues.[1] The other two databases addressed specific research questions.

Economic constraints have changed the operation of these databases. The Neonatology Database was archived on tape because funds were unavailable to continue its on-line operation. Support of the remaining databases was shifted to the appropriate users.

In the current grant year, the remaining three databases were transferred to other computing systems prior to the departure of the database manager. The Mineral-Homeostasis and Mineralization Database was installed on a Digital Equipment Corporation MINC system. Programs, in BASIC, will

be written to perform any further analyses. The two obstetric applications were transferred to the University's IBM System/370 where the database features of SAS are utilized.

The operation of these databases has provided experience in maintaining data collected to respond to specific research issues as well as to ad hoc data searches. The operational experiences and the actual data sets coupled with the theoretical data model developments have provided a realistic substrate for work toward medical information systems which are capable of dynamic system evolution (F-2).

1. D. M. Main, E. K. Main, and M. M. Maurer, Jr., "Cesarian Section Versus Vaginal Delivery for the Less than 1500 Gram Breach Fetus," American Journal of Obstetrics and Gynecology, in press.

F-5. Optical Communication Experiment

Personnel: D. L. Snyder, BCL
G. J. Blaine, BCL
M. L. Peterson, M.S., Electrical Engineering

Support: RR 00396
ECS-8113266

The feasibility of an optical atmospheric-communication link between the Hilltop Campus and the Medical School Campus of Washington University was investigated and documented.[1] Included is an overview of the existing literature about optical propagation through clear-air turbulence. This was compared to experimental results observed using a HeNe laser over a 4.19 km path from Lopata Hall in the Engineering School to the Computer Systems Laboratory in the Medical School; the agreement between theory and experiment was good. The performance of M-ary pulse-position modulation and convolution coding was predicted based on the experiments, and a feasible communication system was described. The results of this study should be useful to those contemplating alternatives to telephone service for supporting digital communication at low to modest data rates.

1. M. L. Peterson, "A Feasibility Study for an Optical Atmospheric Communication Link," BCL Monograph No. 420, Washington University School of Medicine, December 1982.

F-6. An Experimental Local-Area Network: TERRANET

Personnel: G. J. Blaine, BCL
A. J. Gray, BCL
R. E. Hermes, BCL
S. M. Moore, BCL
S. R. Phillips, BCL
M. J. Rainey, BCL
D. A. Schwab, BCL

Support: RR 00396
RR 01380
Washington University

Development and utilization of a modest local-area network, TERRANET,[1] to support computing via remote terminals and medium-speed inter-computer communication has continued. Cost and actual availability of commercial local-area networks (LANs) have mitigated against their application at this laboratory, and provided the rationale for this experiment. Insights developed during the implementation phase should lead to the definition of design and evaluation aids for LAN protocols.

As presently designed, TERRANET provides up to 15 full-duplex virtual-circuit data channels between a maximum of 30 stations at a speed of 9600 bps using time-division-multiplexing. Alternatively, TERRANET may be configured to support more stations if lower data rates per channel are permissible (e.g. 60 stations at 4800 bps). The network consists of two principal functional elements: a microprocessor-based "tap unit" which implements data-link level functions and end-to-end connection supervision, and a cable-insert unit which provides access to the coaxial cable trunk through which TERRANET transports data and synchronization signals. Tap units are connected through a system of optically isolated RS-422 lines to their corresponding cable inserts. Network synchronization is achieved using asynchronous packet transmission within globally synchronized transmission slots. Although synchronization is centralized, control of the TERRANET system is a fully distributed peer protocol.

The coaxial trunk cable was installed through all three levels of BCL and through the basement, to the second and third floors of the Computer Systems Laboratory (CSL). This pilot system has been operated successfully, providing both a needed utility and a test bed for development of network protocol.

A second cable was installed and is utilized as a test bus. A network test program was developed to facilitate loop-back testing and development of error statistics.

TERRANET has been successfully utilized to "download" M68000 systems from UNIX-based hosts and transfer files between RT-11 microcomputers and RSX-11 hosts. Revisions to cable-insert hardware and tap-unit software

enhanced the reliability of TERRANET virtual circuits under conditions of power-line transients and radiated interference.

1. A. J. Gray and G. J. Blaine, "TERRANET: A Modest Terminal-Processor Interconnect for the Laboratory Environment," 7th Conference on Local Computer Networks, Minneapolis, Minnesota, October 11-13, 1982.

2. A. J. Gray, "TERRANET Tap Unit Post-Assembly Checkout Procedure," BCL Working Note 33, January 1983.

3. A. J. Gray, "TERRANET Reliability Tests: Recent Results," BCL Working Note 37, January 1983.

4. S. R. Phillips and G. J. Blaine, "TERRANET: Four-Port Insert Unit," BCL Working Note 38, January 1983.

5. A. J. Gray, "TERRANET: Tap Unit Software Manual," BCL Working Note 39, January 1983.

6. S. R. Phillips, "TERRANET: 60 Channel Configuration," BCL Working Note 46, May 1983.

F-7. Electronic Radiology Studies

Personnel: J. R. Cox, Jr., BCL, Computer Science and Computer Systems Laboratory
G. J. Blaine, BCL
J. G. Dunham, BCL and Electrical Engineering
R. L. Hill, BCL and Radiology
R. G. Jost, M.D., Radiology
C. D. Shum, BCL

Support: RR 00396
RR 01380
RR 01379
Mallinckrodt Institute of Radiology
Washington University

The transformation of radiographic image sequences to the digital domain provides opportunities for enhancing both interpretation and management of diagnostic information. Integration of the various imaging and diagnostic modalities to provide an environment capable of delivering the promised medical benefits holds considerable challenge for both the medical and technological communities.

The basic activities and equipment related to the acquisition, transport, display and archiving of the radiological information can be viewed as a picture archive and communication system (PACS). The canonic form of a

PACS includes three classes of nodes interconnected by a high-bandwidth digital network. The first class of nodes includes all image sources: computed tomography (CT), nuclear medicine, ultrasound, digital subtraction angiography and eventually chest and other radiographs. The picture archive may be centralized or distributed, but it seems likely that this second class of nodes will be heavily dependent on the new technology of optical disks to provide the dense packing of information required. Picture-viewing stations that incorporate image processing responsive to the radiologist's needs represent the third class of nodes on the network. The functional characteristics of these stations are just emerging, but rapid response seems to be a high priority requirement whether the image to be viewed is in a distant archive or has already been retrieved but needs to be processed before viewing.

Preliminary design studies have been carried out for a distributed picture archiving and communication system (PACS) for the Mallinckrodt Institute of Radiology.[1,2] Estimates of current image generation and retrieval activity at MIR underpin the studies.

A functional partitioning of the picture network into two portions, specifically, the message network (short messages and small packets) and the service network (images and large packets) simplifies the analyses. Primary attention has been focused on the image service network candidate organizations for the service network, based on a bus architecture, include point-to-point channels, single shared-transmit/receive channel, multiple shared-receive channels and multiple shared-transmit/receive channels. Appropriate queueing models have been postulated and analyzed. A cost function defined in terms of the channel bandwidth is used to estimate the network cost for each organization. Engineering design curves are being formulated to assist design and development of our prototype PACS network (F-8).

1. J. R. Cox, Jr., G. J. Blaine, R. L. Hill, and R. G. Jost, "Study of a Distributed Picture Archiving and Communication System for Radiology," Proceedings of the First International Conference and Workshop on Picture Archiving and Communications Systems (PACS) for Medical Applications, Proceedings of SPIE, vol. 318, pp. 133-142, January 1982.

2. J. R. Cox, Jr., G. J. Blaine, R. L. Hill, R. G. Jost, and C. D. Shum, "Some Design Considerations for Picture Archiving and Communication Systems," IEEE Computer Magazine, August 1983.

F-8. A Broadband Cable Distribution System for Radiology

Personnel: G. J. Blaine, BCL
J. C. Chabut, BCL
R. L. Hill, BCL and Radiology
R. G. Jost, M.D., Radiology
S. R. Phillips, BCL
M. J. Rainey, BCL

Support: RR 01380
RR 01379
Washington University

A pilot cable system to transport analog and digital radiology pictures and support terminal-to-computer digital data transmission was designed.[1] A dual-cable system, separate inbound and outbound cables, (sub-split on the outbound cable) with a head-end configured at the 12th floor of the Mallinckrodt Institute of Radiology (MIR) provides a trunk system which traverses the core of the MIR building and extends through the steam tunnels to a junction point near the power plant. The junction point allows branches to the future site of a remotely located film library and to the Biomedical Computer Laboratory.

Initial installation includes branches to radiology resources located within the West Pavilion of Barnes Hospital, the 3rd and 4th floors of MIR, the BCL, and the Computer Systems Laboratory. A diagram is shown in Figure 1.

The dual-cable 400 MHz system utilizes "off-the-shelf" cable television components to provide approximately 50 channels, based on frequency multiplexing and an allocated bandwidth of 6 MHz for each channel. The system will provide an environment for the evaluation of commercial digital transmission equipment in addition to supporting experiments related to digital picture networking and archiving studies. Evaluation of the locally developed design aids and modeling of the cable channel continue.

1. G. J. Blaine, R. L. Hill, J. R. Cox, and R. G. Jost, "PACS Workbench at Mallinckrodt Institute of Radiology (MIR)," SPIE, vol. 418, pp. 80-86, May 1983.

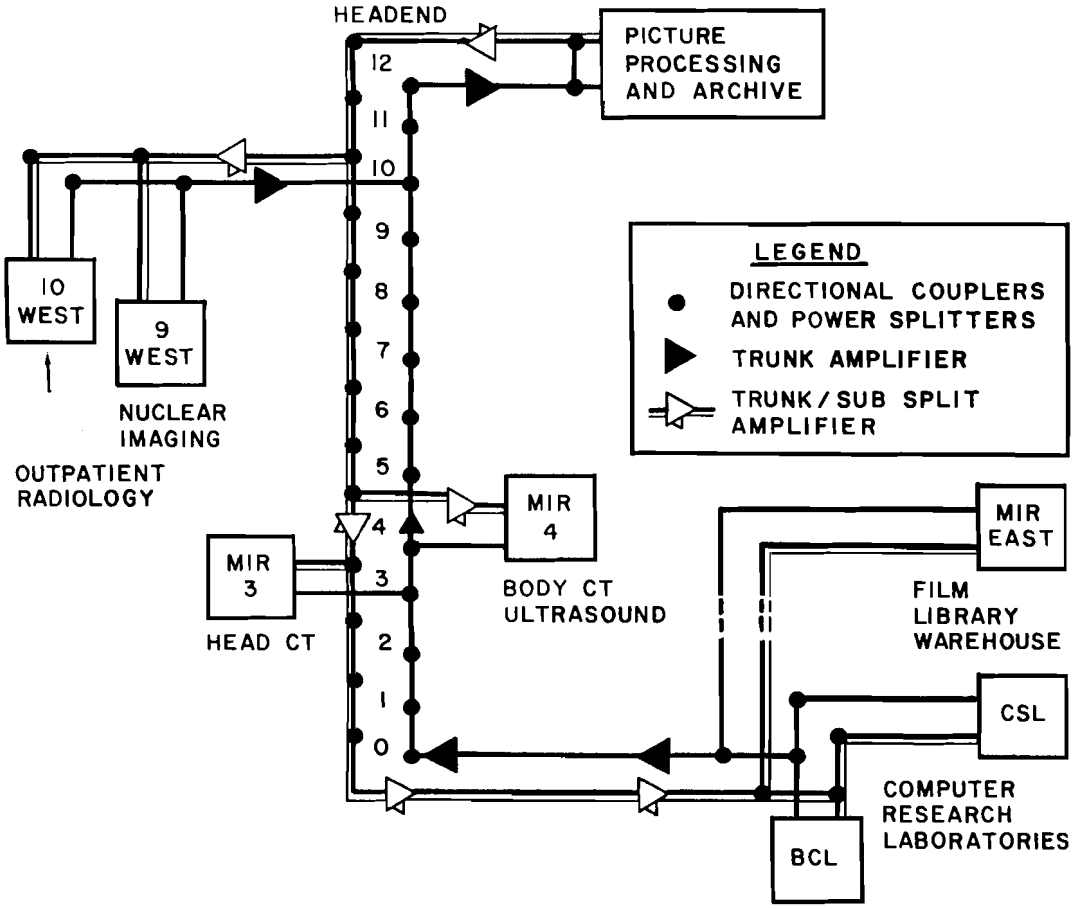

Figure 1. PACS workbench picture network block diagram illustrating topology of the MIR broadband local area picture network.

F-9. Data Compression Studies

Personnel: J. G. Dunham, BCL and Electrical Engineering
K.-H. Tzou, M.S., Electrical Engineering

Support: RR 01380
RR 07054
Washington University

Data compression or source coding is useful in situations where the amount of storage for a given biomedical data set is limited or the rate required to transmit the biomedical source is constrained as in the case of a telephone line. The study for compression of silver-grain images (PR 18, E-11) indicated the need for a better understanding of the human visual system for establishing compression fidelity criteria. An in-depth study was made of mathematical models for the human visual system. These models were predominantly psychophysical-based models that treated the human visual system as a black box and used a limited set of input-output relationships obtained from psychophysical experiments to characterize it. As a result, they are useful only over a limited range of situations. A new physiological-based model[1] was developed in which the signals at each stage are accurately modeled and the overall anatomical structure of the human visual system is closely followed. The physiological data used are from humans and monkeys, if available, and otherwise from cats. To test the validity of the new model, we propose to apply it along with optimal signal detection theory to predict the results of various standard psychophysical tests such as contrast sensitivity and visual acuity. Next we propose to apply the model to image data compression situations and to other image-processing applications.

Recently there has been an increase in the number of digital imaging modalities in radiology including CT, ultrasound, DVI and NMR. In the foreseeable future, it is likely that many standard radiographic images will also be available in digital form. As a result, there has been considerable interest in Picture Archive and Communication Systems (PACS) that are capable of storing, transmitting and displaying large numbers of digital radiographic images. Since the quantities of image data are large, it is important to consider techniques for data compression to minimize, where possible, the burdens of storage and transmission.

A preliminary investigation[2] indicated that the data compression requirements for PACS are varied and that different solutions are likely for different aspects of the problem. Algorithms which are computationally efficient or which are easily implemented in hardware will be preferable. In most situations it is not important how long it takes to compress an image for archival storage, but clinical image retrieval demands will often require prompt decompression. In collaboration with the Mallinckrodt Institute of Radiology, we propose to do a detailed study of linear predictive coding of CT images as they are readily available. Next we propose to develop an extensive database of radiological images for general compression studies. Then we propose to apply the algorithms to the images in the database and then apply the model of the human visual system to develop a visual fidelity criteria for radiology applications.

Finally, we note that many data compression systems operate in a casual, real-time manner as do differential pulse code modulation (DPCM) systems. We have begun to develop the structure of optimal casual systems and have studied the optimal delta-modulation system for first-order Gauss-Markov sources.[3] We propose to study higher rate systems in the future and adaptive systems for sources with unknown parameters.

1. K.-H. Tzou and J. G. Dunham, "A Physiological-Based Human Visual System Model for Image Processing," Biomedical Computer Laboratory Monograph No. 435, July 1983.

2. J. G. Dunham, R. L. Hill, G. J. Blaine, D. L. Snyder, and R. G. Jost, "Compression for Picture Archiving and Communication in Radiology," Proceedings of the 2nd International Conference and Workshop on Picture Archiving and Communication Systems (PACS II) for Medical Applications, SPIE vol. 418, Kansas City, Missouri, pp. 201-208, May-1983.

3. J. G. Dunham, "Optimal Delta Modulation Systems," Biomedical Computer Laboratory Monograph No. 432, June 1983.

F-10. M68K/VERSAbus Hardware Support

Personnel: R. E. Hitchens, BCL
M. W. Browder, BCL
K. H. Haserodt, M.S., Computer Science
S. M. Moore, BCL
S. R. Phillips, BCL

Support: RR 00396
HS 03792

To form a complete computer system capable of running UNIX V7 (F-2), a Winchester Disk, Memory Management Unit (MMU) adapter and 384 kbytes of memory were added to the Motorola 68000-based VERSAmodule system. The Winchester Disk system consists of a Charles River Data Systems CC-1 VERSAbus to SASI bus interface board, Shugart Associates model 1404D disk controller, Shugart 4008 Winchester drive and Shugart 801 floppy drive. Testing showed the disk system to be relatively slow, but still suitable for our purpose. The 1404D disk controller is the limiting element in the disk system due to microcode which causes seemingly unnecessary rotational latency and a slow SASI bus byte-transfer rate of 357 kbytes per second. I/O operations with no seek required approximately three disk revolutions for a minimum delay of 60 ms.

The object of the MMU adapter was to provide effective memory management in order to port UNIX without resorting to an extensive design effort. The MC68451 was chosen as the basis for the adapter. The adapter uses one

MC68451 and interfaces to the VERSAmodule board only through the processor socket. Installation of the MMU adapter required minor modifications to the VERSAmodule I Computer and memory boards. The MMU adapter adds 125 ns to memory operations.

Two VERSAmodule chasses were connected using a VERSAbus expansion kit to provide enough backplane slots for the additional memory, CC-1 interface board and coprocessor to be added later (F-3). Tests showed that the extension of the bus lengthened memory read and write operations by less than 2%. The difference approaches 1% when the additional time caused by the MMU is considered. The system is currently operational and requires no external host except when booting.

F-11. System Support for Programming and Image Processing

Personnel: R. E. Hermes, BCL
A. J. Gray, BCL
R. E. Hitchens, BCL
S. R. Phillips, BCL
D. W. Stein, Jr., BCL

Support: RR 00396
RR 01380

Computer support for diverse research projects continues to be provided by two PDP 11/34s (PR 18, E-2, E-3). To enhance this support many system improvements have been added during the past year.

The operating system for both systems has been upgraded to RSX11M V4.0 providing complete software compatibility between the two computers. In addition, existing software for the Lexidata display system which originally was supported by RT-11 has been revised for use with RSX11M. Other software packages which have been added or improved include: software for controlling a DATA I/O Prom Programmer, software for intermachine communication, an M68000 cross assembler, and a variety of general purpose algorithms for signal processing.

Many system hardware improvements have been made to enhance system performance and to improve compatibility with computer systems in other research departments within the university. A UNIBUS to Q-Bus adapter has been installed on the primary PDP 11/34. This adapter now allows the use of low-cost Q-Bus peripherals of which we have added a DZV-11 four-line asynchronous multiplexor, an RX02 compatible floppy disk controller with two disk drives, and a 10-megabyte RL02 disk controller and disk drive. To enhance data transfers between each PDP 11/34, a high speed parallel interprocessor link has been installed. In addition, the primary processor now supports two tape drives and 13 terminal ports including three connections to TERRANET. Both computer systems now include high-speed cache

memory, floating-point processors, and two 5-Mbyte RK05 equivalent disk drives each. The systems also are capable of storing large amounts of data on 80-megabyte disk drives, of which there are two on the primary system and one on the other.

F-12. A Machine Portable Question and Answer (Q and A) Display System

Personnel: D. W. Stein, Jr., BCL

Support: RR 01362
RR 01380

Several projects currently in progress (B-7, C-1) require extensive software systems to support the investigations. Although the nature of the investigations are quite diverse, the supporting software systems often have several functions in common. One of the most frequently required functions is the ability to interactively query the user for needed information.

The Machine Portable Question and Answer Display System is a flexible menu-driven interactive display system. The system is composed of two parts. The first is a subroutine library to control the display of the menus and the querying for information. The second part is an editor to ease the task of generating and altering the menus.

The subroutine package has three major user interfaces. There is a routine to display text not requiring user response and two slightly different routines to display a menu and allow the user to input and edit responses. The program has control of such useful parameters as menu placement, size and screen clearing. A special feature of the subroutine package is the ability to associate "help-text" screens with the information prompts in the menus. After reviewing the help-text screen(s) the user requests that the original menu be redisplayed for continuing the Q & A sequence.

A special editor (QANTXT) was designed to facilitate the generation and revision of the menus and their associated help-text screens. QANTXT has two distinct modes. The first is used to create and maintain menu screens. The second is used to create and maintain help-text screens. Menu screens are created by allowing the QANTXT user to generate prototype screens defining the question and answer fields of the menu. Help-text screens are created by allowing the user to generate the actual help-text screen. QANTXT stores both types of screens in an encoded form. When the user is satisfied with the screen contents, QANTXT is used to generate "include" files which can be incorporated into the main program. The "include" files contain the necessary data-structure declaration and initialization statements to allow the user to simply pass the data structures to the desired subroutines.

The Q and A subroutine package and the QANTXT editor are written to be easily portable to different machines and different operating systems. This is accomplished by writing the programs in Ratfor which is translated to Fortran and by separating the machine-dependent functions from the machine independent functions.

The Q and A package has been completed and is implemented on a VAX 11/780, a PDP-11/34 and a LSI-11/23. The code for the subroutine package is approximately 1200 Ratfor source lines (not counting documentation). The QANTXT editor is approximately 1000 Ratfor lines. Using the Q and A subroutine package with programs of even modest length on the PDP-11s required extensive overlaying. A user's guide to the subroutine package is available.[1] A user's guide to the QANTXT editor is in preparation.

1. D. W. Stein, Jr., "QANDA Q and A Package Programmer's Reference Manual and User's Guide," BCL Working Note No. 48, St. Louis, Missouri, July 1983.

VI. INDUSTRIAL COLLABORATION

Industrial collaboration provides a mechanism for the deployment of laboratory developments and benefits the staff by keeping abreast of the practical considerations of reliability, maintainability, and cost.

The TERRANET system (F-6), which provides a simple low-cost interconnect to support terminal-to-computer and computer-to-computer communications for modest (up to 9600 bps) speeds, is currently being produced and marketed in Japan under a licensing agreement with Computer Services Corporation (CSK), a major facilities management consulting firm headquartered in Tokyo. As part of the agreement, CSK supplied two evaluation systems of 10 tap-units each for installation in the Computer Science and Electrical Engineering Departments at Washington University.

During the past year we have digitized several tens of long-term ECG recordings for IBM Biomedical Systems (Hopewell Junction, New York) on a fee-for-service basis. We have also digitized several recordings for Medicomp (Melbourne, Florida).

We have continued to analyze long-term ECG recordings on the Argus/2H arrhythmia analysis system for the Cardiology Division of Jewish Hospital of St. Louis. That division is involved in the multicenter "Multiprotocol Study of Encainide Hydrochloride (Encainide)" sponsored by Mead Johnson (Evansville, Indiana) (PR 18, VI). Encainide is an antiarrhythmic agent.

The Argus algorithms for rhythm analysis of ECG waveforms had been implemented in the real-time environment by Mennen-Medical (Clarence, New York) several years ago. More recent improvements developed at BCL are being implemented at Mennen. In addition, Mennen has installed a duplicated Argus/2H system to facilitate rapid testing of cataloged waveforms. BCL personnel have worked closely with Mennen to facilitate the implementation of their testing system.

BCL personnel have worked closely with Biosensor Corporation (Brooklyn Center, Minnesota) to implement Argus algorithms in a "real time analyser," a device to analyze ECG rhythm of a patient who wears the small device and goes about normal activities.

Laboratory personnel are cooperating with Dr. James Atkins, University of Texas Health Science Center at Dallas, who is developing an Advanced Cardiac Life Support (ACLS) video program. BCL is furnishing long-term ECG recordings collected and analyzed for the Multicenter Investigation of the Limitation of Infarct Size (A-12). Events of specific interest are copied from the recordings, and the recordings returned to BCL.

VII. TRAINING ACTIVITIES

Training activities of the Biomedical Computer Laboratory are directed toward the goals of informing the local and national scientific communities about resource projects and facilities and of instructing a broad spectrum of people in the application of advanced computer-techniques to problems in clinical medicine and biological research. Training activities include the teaching of formal courses at the School of Medicine and the School of Engineering as well as supervision of graduate students by Laboratory staff, seminars relating to resource projects and applications, individual and small-group training about resource facilities, and national workshops and symposia on topics of interest and importance to the resource and community.

The bringing together of biomedical scientists, engineers, and computer scientists provides important cross-fertilization between disciplines. In these settings, students and staff find the need and opportunity to test the relevance of theory and the usefulness of technology in applications to real problems. Also, the biomedical scientists are aided in learning new techniques for acquiring useful information. To this end, some of the courses offered are addressed to biologists without strong technical backgrounds who want and need a below-the-surface appreciation of biomedical computing. Laboratory personnel also participate in regularly scheduled conferences in the clinical departments where both the biological and technological issues are examined.

The establishment of a fee-for-service facility, the Medical Computing Services Group, provides comprehensive support to biomedical investigators for research database activities. The focus of that facility has fostered a natural transition to their sponsorship of the non-credit MUMPS course previously conducted by our Laboratory. Other non-credit courses continue to be offered by the Laboratory. These include "Introduction to Programming the Laboratory Computer" and "Computers in Medicine." Also, research-training electives in biomedical computing are offered to medical students in their junior and senior years.

VIII. SEMINARS

During the year the following seminars were sponsored by the Biomedical Computer Laboratory:

"Tutorial on the FPS 100E Floating Point Processor" August 25-26, 1982	Floating Point Systems, Inc. Schaumberg, Illinois
"Ventricular Arrhythmia Detector Performance Evaluation" September 8, 1982	Russell E. Hermes Biomedical Computer Laboratory Washington University St. Louis, Missouri
"Image-Reconstruction Algorithms for Positron-Emission Tomography Systems" September 15, 1982	Shirley Cheng Department of Electrical Engineering Washington University St. Louis, Missouri
"Single Chip Microprocessors - The Micro/T-11 and Micro J-11" January 25, 1983	Jim Ford Digital Equipment Corporation St. Louis, Missouri
"Three Dimensional Image Display" January 28, 1983	David Beecher Biomedical Computer Laboratory Washington University St. Louis, Missouri

IX. PUBLICATIONS AND ORAL PRESENTATIONS

Arthur, R. M., "Diffraction-Limited Lateral Resolution of Ultrasonic Phased Arrays," Ultrasonic Imaging, vol. 5, p. 191, 1983 (abstract).

Barzilai, B., Perez, J. E., Madaras, E. I., Miller, J. G., and Sobel, B. E., "The Influence of Contraction on Ultrasonic Backscatter of Normal and Ischemic Myocardium," Circulation, vol. 66, p. II-30, 1982 (abstract).

Beecher, D. E., "Three-Dimensional Image Construction and Display," seminar presented to Electronic Radiology Group at the Mallinckrodt Institute of Radiology, St. Louis, Missouri, February 25, 1983.

Bergmann, S. R., Fox, K. A. A., Collen, D., and Sobel, B. E., "Coronary Thrombolysis Achieved with Human Extrinsic Plasminogen Activator, a Clot Selective Activator, Administered Intravenously," Journal of American College of Cardiology, vol. 1, p. 615, 1983 (abstract).

Bergmann, S. R., Fox, K. A. A., Rand, A. L., Markham, J., and Sobel, B. E., "Quantitation of Myocardial Perfusion with Radiolabeled Water," presented at the 32nd Annual Scientific Session of the American College of Cardiology, New Orleans, Louisiana, March 20-24, 1983.

Bergmann, S. R., Fox, K. A. A., Rand, A. L., Markham, J., and Sobel, B. E., "Quantitation of Myocardial Perfusion with Radiolabeled Water," Journal of American College of Cardiology, vol. 1, p. 577, 1983 (abstract).

Bergmann, S. R., Fox, K. A. A., Rand, A. L., McElvaney, K. D., Ter-Pogossian, M. M., and Sobel, B. E., "Non-Invasive Measurement of Regional Myocardial Perfusion by Positron Tomography," Circulation, vol. 66, p. II-148, 1982 (abstract).

Bergmann, S. R., Fox, K. A. A., Rand, A. L., Welch, M. J., Ter-Pogossian, M. M., and Sobel, B. E., "Assessment of Restoration of Myocardial Perfusion and Metabolism with Positron Emission Tomography after Coronary Thrombolysis," Journal of Nuclear Medicine, vol. 24, p. 5, 1983 (abstract).

Bergmann, S. R., Fox, K. A. A., Ter-Pogossian, M. M., and Sobel, B. E., "Clot-Selective Coronary Thrombolysis with Tissue-Type Plasminogen Activator," Science, vol. 220, pp. 1181-1183, 1983.

Bergmann, S. R., Lerch, R. A., Fox, K. A. A., Ludbrook, P. A., Welch, M. J., Ter-Pogossian, M. M., and Sobel, B. E., "Temporal Dependence of Beneficial Effects of Coronary Thrombolysis Characterized by Positron Tomography," American Journal of Medicine, vol. 73, pp. 573-581, 1982.

Bergmann, S. R., Mathias, C. J., Sobel, B. E., and Welch, M. J., "Evaluation of Thrombolytic Therapy in Coronary Artery Thrombosis: Scintigraphic Detection with the Use of In-111-Labeled Platelets," Proceedings of the Third World Congress on Nuclear Medicine and Radiation Biology, Pergamon Press, pp. 65-68, 1982.

Bergmann, S. R., Nomura, H., Rand, A. L., Sobel, B. E., and Lange, L. G., "Externally Detectable Changes in Fatty Acid Utilization by Perfused Hearts from Rabbits Exposed to Alcohol," Circulation, vol. 66, p. II-109, 1982 (abstract).

Blaine, G. J., "Networks and Distributed Systems: A Primer," invited tutorial to be presented at MEDINFO 83, Amsterdam, The Netherlands, August 21-26, 1983.

Blaine, G. J., "Network Tutorial," seminar presented to Electronic Radiology Group at the Mallinckrodt Institute of Radiology, St. Louis, Missouri, April 1, 1983.

Blaine, G. J., Hill, R. L., Cox, J. R., and Jost, R. G., "PACS Workbench at Mallinckrodt Institute of Radiology (MIR)," Proceedings of the Second International Conference and Workshop on Picture Archiving and Communication Systems (PACS II) for Medical Applications, Proceedings of SPIE, vol. 418, pp. 80-86, 1983.

Cheng, S. N. C., "Image-Reconstruction Algorithms for Positron-Emission Tomography Systems," Department of Electrical Engineering, Washington University, St. Louis, Missouri, December 1982 (D.Sc. Dissertation).

Clark, K. W., Geltman, E. M., Miller, J. P., Moore, P., Madden, K. A., Thomas, Jr., L. J., Hartwell, T. D., Jaffe, A. S., Raabe, D. S., Stone, P. H., Gold, H. K., Rude, R. E., and the MILIS Study Group, "Reproducibility of Dysrhythmia Findings by a Centralized Laboratory within a Major Multicenter Trial," Proceedings of the IEEE Conference on Computers in Cardiology, IEEE Catalog No. 82CH1814-3, Seattle, Washington, pp. 55-60, October 12-15, 1982.

Clark, K. W., Hart, W. M., Hagen, R. W., Hartz, R. K., and Zelenka, M., "A Microprocessor-Based System for Color Contrast Perimetry," accepted for presentation at the Seventh Annual Symposium on Computer Applications in Medical Care," Baltimore, Maryland, October 23-26, 1983.

Coben, L. A., Danziger, W. L., and Berg, L., "Frequency Analysis of the Resting Awake EEG in Mild Senile Dementia of Alzheimer Type," Electroencephalography and Clinical Neurophysiology, vol. 55, pp. 372-380, 1983.

Coben, L. A., Danziger, W. L., and Hughes, C. P., "Visual Evoked Potentials in Mild Senile Dementia of Alzheimer Type," Electroencephalography and Clinical Neurophysiology, vol. 55, pp. 121-130, 1983.

Cohen, R. D., Mottley, J. G., Miller, J. G., Kurnik, P. B., and Sobel, B. E., "Detection of Ischemic Myocardium in vivo Through the Chest Wall by Quantitative Ultrasonic Tissue Characterization," American Journal of Cardiology, vol. 50, pp. 838-843, 1982.

Corr, P. B., "Potential Arrhythmogenic Role of Biochemical Factors in Sudden Cardiac Death," in Electrophysiological Mechanisms Underlying Sudden Cardiac Death, Futura Publishing, Mount Kisco, New York, pp. 105-130, 1982.

Corr, P. B., Ahumada, G. G., and Sobel, B. E., "Membrane Active Metabolites: Potential Mediators of Sudden Cardiac Death," in Cardiovascular Medicine, vol. 1, J. H. K. Vogel, ed., Raven Press, New York, pp. 161-175, 1982.

Corr, P. B., Gross, R. W., and Sobel, B. E., "Arrhythmogenic Amphiphilic Lipids and the Myocardial Cell Membrane," invited editorial for the Journal of Molecular and Cellular Cardiology, vol. 14, p. 619, 1982.

Corr, P. B., and Sharma, A. D., "Alpha-Adrenergic Mediated Effects on Myocardial Calcium" in Calcium, Calcium Antagonists and Cardiovascular Disease, L. H. Opie and R. Krebbs, eds., Raven Press, New York, in press.

Corr, P. B., and Sharma, A. D., "α- Versus β-Adrenergic Influences on Dysrhythmias Induced by Myocardial Ischemia and Reperfusion," in Advances in β-Blocker Therapy II, A. Zanchetti, ed., Excerpta Medica, Amsterdam, p. 163, 1982.

Corr, P. B., Snyder, D. W., Lee, B. I., Gross, R. W., Keim, C. R., and Sobel, B. E., "Pathophysiological Concentrations of Lysophosphatides and the Slow Response," American Journal of Physiology, vol. 243, no. 2, pp. H187-H195, August 1982.

Corr, P. B., and Sobel, B. E., "Amphiphilic Lipid Metabolism and Ventricular Arrhythmias," in Early Arrhythmias Resulting from Myocardial Ischemia, Mechanisms and Prevention by Drugs, J. R. Parratt, ed., Macmillan Press Limited, London, pp. 199-218, 1982.

Corr, P. B., and Sobel, B. E., "Arrhythmogenic Properties of Phospholipid Metabolites Associated with Myocardial Ischemia," Federation Proceedings, vol. 42, no. 8, pp. 2454-2459, 1983.

Corr, P. B., and Sobel, B. E., "Biochemical and Metabolic Factors Contributing to Malignant Ventricular Arrhythmias," in Ventricular Tachycardia - Mechanisms and Management, M. E. Josephson, ed., Futura Publishing, Mount Kisco, New York, p. 97-150, 1982.

Corr, P. B., and Sobel, B. E., "Membrane Active Metabolites: The Concentration Dependence of the Electrophysiological Effects of Amphiphiles," in Myocardial Ischemia and Protection: Possibilities and Strategies, O. D. Mjos, ed., Churchill Livingstone Co., Edinburgh/London, pp. 90-100, 1983.

Corr, P. B., and Witkowski, F. X., "Potential Electrophysiological Mechanisms for Dysrhythmias Associated with Reperfusion of Ischemic Myocardium," Circulation, in press.

Cox, J. R., (ed.), Proceedings of the Workshop on Time-of-Flight Tomography, IEEE Catalog No. 82CH1791-3, Washington University, St. Louis, Missouri, May 17-19, 1982.

Cox, J. R., Blaine, G. J., Hill, R. L., Jost, R. G., and Shum, C. D., "Some Design Considerations for Picture Archiving and Communication Systems," IEEE Computer Magazine, in press.

Dunham, J. G., Hill, R. L., Blaine, G. J., Snyder, D. L., and Jost, R. G., "Compression for Picture Archiving and Communication in Radiology," Proceedings of the Second International Conference and Workshop on Picture Archiving and Communications Systems (PACS II) for Medical Applications, Proceedings of SPIE, vol. 418, pp. 201-208, 1983.

Ficke, D. C., "Description and Performance of Super PETT," invited presentation of Positron Tomography Workshop at the IEEE Nuclear Science Symposium, Washington, D. C., October 20-22, 1982.

Ficke, D. C., Beecher, D. E., Blaine, G. J., Hitchens, R. E., Holmes, T. J., Ter-Pogossian, M. M., and Yamamoto, M., "TOF Acquisition: System Design and Experimental Results," Proceedings of the Workshop on Time-of-Flight Tomography, IEEE Catalog No. 82CH1791-3, Washington University, St. Louis, Missouri, pp. 139-141, May 17-19, 1982.

Fox, K. A. A., Bergmann, S. R., Rand, A. L., Ambos, H. D., and Sobel, B. E., "External Measurement of Myocardial Oxygen Extraction with O-15 Labeled Oxygen," The Journal of Nuclear Medicine, vol. 24, no. 5, p. P20, 1983 (abstract).

Fox, K. A. A., Nomura, H., Sobel, B. E., and Bergmann, S. R., "Constant Myocardial Substrate Utilization Despite Reduction in Flow in Isolated Rabbit Hearts Performing Constant Work," American Journal of Physiology: Heart and Circulatory Physiology, in press.

Fox, K. A. A., Nomura, H., Sobel, B. E., and Bergmann, S. R., "Persistent Substrate Utilization Despite Decreased Flow in Hearts Performing Constant Work," Circulation, vol. 66, p. II-199, 1982 (abstract).

Geltman, E., Bergmann, S. R., and Sobel, B. E., "Cardiac Positron Emission Tomography," in Positron Emission Tomography, M. Reivich, ed., Alan R. Liss, New York, in press.

Geltman, E. M., Smith, J. L., Beecher, D. E., Ludbrook, P. A., Ter-Pogossian, M. M., and Sobel, B. E., "Altered Regional Myocardial Metabolism in Congestive Cardiomyopathy Detected by Positron Tomography," American Journal of Medicine, in press.

Geltman, E. M., and Sobel, B. E., "Cardiac Positron Tomography," Chest, in press.

Gray, A. J., and Blaine, G. J., "Terranet: A Modest Terminal-Processor Interconnect for the Laboratory Environment," Proceedings of the 7th Conference on Local Computer Networks, IEEE Catalog No. 82CH1800-2, Minneapolis, Minnesota, pp. 12-19, October 12-13, 1982.

Gregory, R. O., "Some Limitations of Time-of-Flight Detectors," Proceedings of the Workshop on Time-of-Flight Tomography, IEEE Catalog No. 82CH1791-3, Washington University, St. Louis, Missouri, pp. 83-88, May 17-19, 1982.

Gross, R. W., Corr, P. B., Lee, B. I., Saffitz, J. E., Crafford, Jr., W. A., and Sobel, B. E., "Incorporation of Radiolabeled Lysophosphatidyl Choline into Canine Purkinje Fibers and Ventricular Muscle: Electrophysiological, Biochemical and Autoradiographic Correlations," Circulation Research, vol. 51, p. 27, 1982.

Gurumurthy, K. V., and Arthur, R. M., "A Dispersive Model for the Propagation of Ultrasound in Soft Tissue," Ultrasonic Imaging, vol. 4, pp. 355-377, 1982.

Hagen, R. W., "A Chromatic Visual Field Measurement System," seminar presented for Washington University Biomedical Engineering Program Series, St. Louis, Missouri, October 26, 1982.

Hart, Jr., W. M., "Three Dimensional Topography of the Central Visual Field," Proceedings of the 24th International Congress of Ophthalmology, in press.

Hart, Jr., W. M., and Burde, R. M., "Three Dimensional Topography of the Central Visual Field: Sparing of Foveal Sensitivity in Macular Disease," Ophthalmology, in press.

Hart, Jr., W. M., Burde, R. M., Johnston, G. P., and Drews, R. C., "Static Perimetry in Chloroquine Retinopathy: Perifoveal Patterns of Visual Field Depression," Archives of Ophthalmology, in press.

Hart, Jr., W. M., and Kolker, A. E., "Computer Generated Display for Three-Dimensional Static Perimetry: Correlation of Optic Disc Changes with Glaucomatous Defects," Documente Ophthalmologica, in press.

Hauser, C. R., Hendry, S. H. C., Jones, E. G., and Vaughn, J. E., "Morphological Diversity of Immunocytochemically Identified Neurons in Monkey Sensory-Motor Cortex," Journal of Neurocytology, in press.

Henkelman, R. M., and Wong, J. W., "The Physics of the Inhomogeneity Problem and the Present Status of Clinical Dosimetry," in Computed Tomography in Radiotherapy, C. C. Ling, C. C. Rodgers, and J. Morton, eds., Raven Press, pp. 199-208, 1983.

Hermes, R. E., "Ventricular Arrhythmia Detector Performance Evaluation," Master of Science thesis, Department of Electrical Engineering, Washington University, St. Louis, Missouri, September 1982.

Hermes, R. E., and Cox, J. R., "A Model for Performance Evaluation of Ventricular Arrhythmia Detectors," Proceedings of the IEEE Conference on Computers in Cardiology, IEEE Catalog No. 82CH1814-3, Seattle, Washington, pp. 197-200, October 12-15, 1982.

Herscovitch, P., Markham, J., and Raichle, M. E., "Accuracy of the Kety Autoradiographic Measurement of Cerebral Blood Flow Adapted for Positron Emission Tomography," presented at the 29th Annual Meeting of the Society of Nuclear Medicine, Miami Beach, Florida, June 15-18, 1982.

Herscovitch, P., Markham, J., and Raichle, M. E., "Brain Blood Flow Measured with Intravenous $H_2{}^{15}O$. I. Theory and Error Analysis," Journal of Nuclear Medicine, in press.

Hillman, L. S., "Mineralization and Late Mineral Homeostasis in Infants: Role of Mineral and Vitamin D Sufficiency and Other Factors," in Neonatal Calcium Metabolism, M. Hollid, K. Gray, and C. Anast, eds., Elsevier North Holland Biochemical Press, in press.

Hillman, L. S., and Haddad, J. G., "Hypocalcemia and Other Abnormalities of Mineral Homeostasis During the Neonatal Period," in Butterworths International Medical Reviews, Clinical Endocrinology 2, Calcium Disorders, D. Heath, and S. J. Marx, eds., Butterworth Scientific, Boston, pp. 248-276, 1982.

Hillman, L. S., and Haddad, J. G., "Serial Analysis of Serum Vitamin D-Binding Protein in Preterm Infants from Birth to Postconceptual Maturity," Journal of Clinical Endocrinology and Metabolism, vol. 56, no. 1, pp. 189-191, 1983.

Hillman, L. S., and Hollis, B. W., "Serum Vitamin D (D) in Premature Infants; Evidence for Decreased Conversion to 25-hydroxyvitamin D (25-OHD)," Pediatric Research, vol. 17, p. 290A, 1983 (abstract).

Hillman, L., Salmons, S., and Fiore, B., "Treatment Trials of Higher Dose Vitamin D and 25-hydroxcholecalciferol in Premature Infants: A Preliminary Report," in Vitamin D, Chemical, Biochemical and Clinical Endocrinology of Calcium Metabolism, A. W. Norman, K. Schaefer, D. V. Herrath, and H. Grigoleit, eds., Walter de Gruyter, Berlin, pp. 781-783, 1982.

Hillman, L. S., Salmons, S. J., Haussler, M. R., and Dokoh, S., "Serial 1,25-dihydroxyvitamin D ($1,25(OH)_2D$) Serum Concentrations in Premature Infants on Varying Feeding Regimens," Pediatric Research, vol. 17, p. 290A, 1983 (abstract).

Holmes, T. J., "Predicting Count Loss in Modern Positron-Emission Tomography Systems," IEEE Transactions on Nuclear Science, vol. NS-30, no. 1, pp. 723-727, February 1983.

Holmes, T. J., Blaine, G. J., Hitchens, R. E., and Ficke, D. C., "Implications of Event Rate and Study Parameters on System Architecture," Proceedings of the Workshop on Time-of-Flight Tomography, IEEE Catalog No. 82CH1791-3, Washington University, St. Louis, Missouri, pp. 147-152, May 17-19, 1982.

Holmes, T. J., Hitchens, R. E., Blaine, G. J., Ficke, D. C., and Snyder, D. L., "A Dedicated Hardware Architecture for Data Acquisition and Processing in a Time-of-Flight Emission Tomography System (SUPER-PETT)," IEEE Transactions on Nuclear Science, vol. NS-30, no. 1, pp. 170-174, February 1983.

Holmes, T. J., Snyder, D. L., Ficke, D. C., and Yamamoto, M., "Maximum-Likelihood Estimation Applied to Some Calibration Problems in Time-of-Flight Emission Tomography Systems," Proceedings of the Workshop on Time-of-Flight Tomography, IEEE Catalog No. 82CH1791-3, Washington University, St. Louis, Missouri, pp. 161-166, May 17-19, 1982.

Hughes, B., Bergmann, S. R., and Sobel, B. E., "External Detection of β-Adrenoceptor Occupancy in Isolated Perfused Hearts," Circulation, vol. 66, p. II-206 (abstract).

Jaffe, A. S., Geltman, E. M., Tiefenbrunn, A. J., Ambos, H. D., Strauss, H. D., Sobel, B. E., and Roberts, R., "Reduction of Infarct Size in Patients with Inferior Infarction with Intravenous Glyceryl Trinitrate: A Randomized Prospective Study," British Heart Journal, vol. 49, pp. 452-460, 1983.

Jaffe, A. S., Mazey, R. M., Harter, H., and Roberts, R., "The Enzymatic Diagnosis of Myocardial Infarction in Patients with Renal Failure," Circulation, vol. 66, p. II-183, October 1982 (abstract).

Jaffe, A. S., Schechtman, K., Spadaro, J., Roberts, R., Geltman, E. M., and Sobel, B. A., "Increased Congestive Heart Failure after Infarction of Modest Extent in Diabetics," Circulation, vol. 66, p. II-370, October 1982 (abstract).

Krone, R. J., Friedman, E., Thanavaro, S., Miller, J. P., Kleiger, R. E., and Oliver, G. C., "Longterm Prognosis after First Q-Wave (Transmural) and Non Q-Wave (Nontransmural) Myocardial Infarction: Analysis of 593 Patients," American Journal of Cardiology, in press.

Larson, K. B., "Physical and Mathematical Principles of Tracer Kinetics in Biological Applications," seminar presented to Washington University Three-Two Program students, St. Louis, Missouri, January 13, 1983.

Lerch, R. A., Bergmann, S. R., Ambos, H. D., Welch, M. J., Ter-Pogossian, M. M., and Sobel, B. E., "Effect of Flow-Independent Reduction of Metabolism in Regional Myocardial Clearance of ^{11}C-Palmitate," Circulation, vol. 65, pp. 731-738, 1982.

Lim, W. Y-P., and Cox, J. R., "Clocks and the Performance of Synchronisers," IEE Proceedings, vol. 130, Pt.E, no. 2, pp. 57-64, March 1983.

Ludbrook, P. A., Tiefenbrunn, A. J., Reed, F. R., and Sobel, B. E., "Acute Hemodynamic Responses to Sublingual Nifedipine: Dependence on Left Ventricular Function," Circulation, vol. 65, p. 489, 1982.

Madaras, E. I., Barzilai, B., Perez, J. E., Sobel, B. E., and Miller, J. G., "Changes in Myocardial Backscatter Throughout the Cardiac Cycle," Ultrasonic Imaging, in press.

Madaras, E. I., Barzilai, B., Perez, J. E., Sobel, B. E., and Miller, J. G., "Systematic Variations of Myocardial Ultrasonic Backscatter During the Cardiac Cycle in Dogs," Ultrasonic Imaging, vol. 4, no. 2, p. 185, 1982 (abstract).

Main, D. M., Main, E. K., and Maurer, Jr., M. M., "Cesarian Section Versus Vaginal Delivery for the Less than 1500 Gram Breach Fetus," American Journal of Obstetrics and Gynecology, in press.

McCluskey, E. R., Corr, P. B., Lee, B. I., Saffitz, J. E., and Needleman, P., "The Arachidonic Acid Metabolic Capacity of Canine Myocardium Is Increased During Healing of Acute Myocardial Infarction," Circulation Research, vol. 51, p. 743, 1982.

Mead, C. N., Pull, H. R., Clark, K. W., and Thomas, Jr., L. J., "Expanded Frequency-Domain ECG Waveform Processing: Integration into a New Version of Argus/2H," Proceedings of the IEEE Conference on Computers in Cardiology, IEEE Catalog No. 82CH1814-3, Seattle, Washington, pp. 205-208, October 12-15, 1983.

Miller, T. R., Goldman, K. J., Sampathkumaran, K. S., Biello, D. R., Ludbrook, P. A., and Sobel, B. E., "Analysis of Cardiac Diastolic Function: Application in Coronary Artery Disease," Journal of Nuclear Medicine, vol. 24, p. 2, 1983.

Moses, R. A., "Intraocular Blood Flow from Analysis of Angiograms," Investigative Ophthalmology and Visual Science, vol. 24, no. 3, pp. 354-360, March 1983.

Moses, R. A., and Arnzen, R. J., "Instantaneous Tonometry," Archives of Ophthalmology, vol. 101, p. 249, 1983.

Moss, A. J., Bigger, Jr., J. T., Case, R. B., Gillespie, J., Goldstein, R. E., Greenberg, H. M., Krone, R., Marcus, F. I., Odoroff, C. L., and Oliver, G. C., "Risk Stratification and Survival after Myocardial Infarction," New England Journal of Medicine, in press.

Mottley, J. G., Glueck, R. M., Perez, J. E., Sobel, B. E., and Miller, J. G., "Regional Differences in the Cyclic Variation of Myocardial Backscatter and Modification by Ischemia," Ultrasonic Imaging, vol. 5, p. 183, 1983 (abstract).

Mukharji, J., Rude, R. E., Poole, K., Croft, C., Thomas, Jr., L. J., Strauss, H. W., Roberts, R., Raabe, Jr., D. S., Braunwald, E., Willerson, J. T., and Cooperating Investigators, "Late Sudden Death Following Acute Myocardial Infarction: Importance of Combined Presence of Repetitive Ventricular Ectopy and Left Ventricular Dysfunction," Clinical Research, vol. 30, p. 208A, 1982 (abstract).

Nomura, H., Bergmann, S. R., Fox, K. A. A., McElvany, K. D., Welch, M. J., and Sobel, B. E., "Myocardial Fatty Acid Metabolism Quantified Externally with ^{11}C-Palmitate," Circulation, vol. 66, p. II-147, 1982 (abstract).

Perez, C. A., and Purdy, J. A., "Computed Tomography in Treatment Planning, Technical and Clinical Considerations," in Monograph on Computerized Treatment Planning Systems, F. Bagne, ed., in press.

Perez, J. E., Barzilai, B., Madaras, E. I., Saffitz, J. E., Johnston, P. H., Miller, J. G., and Sobel, B. E., "Calcification and Fibrosis: Determinants of Ultrasonic Backscatter in Cardiomyopathy," Circulation, vol. 66, p. II-29, 1982 (abstract).

Pogwizd, S. M., Sharma, A. D., and Corr, P. B., "The Influences of Labetalol, a Combined α- and β-Adrenergic Blocking Agent on the Dysrhythmias Induced by Coronary Occlusion and Reperfusion," Cardiovascular Research, vol. 16, p. 398, 1982.

Politte, D. G., Holmes, T. J., and Snyder, D. L., "Effects of Quantization of Time-of-Flight (TOF) Measurements on Image Signal-to-Noise Ratio in TOF Emission Tomography," IEEE Transactions on Nuclear Science, vol. NS-30, no. 1, pp. 720-722, February 1983.

Politte, D. G., and Snyder, D. L., "A Simulation Study of Design Choices in the Implementation of Time-of-Flight Reconstruction Algorithms," Proceedings of the Workshop on Time-of-Flight Tomography, IEEE Catalog No. 82CH1791-3, Washington University, St. Louis, Missouri, pp. 131-136, May 17-19, 1982.

Purdy, J. A., "Computer Applications in Radiation Therapy Treatment Planning - A Review," presented at the 10th Japan PC Users Meeting, Osaka, Japan, April 4, 1983.

Purdy, J. A., "Radiation Therapy Treatment Planning System," presented at the Radiological and Medical Physics Society of New York Meeting, New York, New York, April 20, 1983.

Purdy, J. A., and Prasad, S. C., "Current Treatment Planning Techniques - A Review of Methods and Algorithms in Radiation Absorbed Dose Calculation, and the Role of CT," in Computed Tomography in Radiotherapy, C. C. Ling, C. C. Rogers and J. Morton, eds., Raven Press, pp. 187-197, 1983.

Raichle, M. E., Martin, W. R. W., Herscovitch, P., Mintun, M. A., and Markham, J., "Brain Blood Flow Measured with Intravenous $H_2{}^{15}O$. II. Implementation and Validation," Journal of Nuclear Medicine, in press.

Roberts, R., Ambos, H. D., and Sobel, B. E., "Estimation of Infarct Size with MB Rather than Total CK: Avoidance of Distortion from Occult Release of Noncardiac Enzyme," International Journal of Cardiology, vol. 2, pp. 479-489, 1983.

Saffitz, J. E., Corr, P. B., Lee, B. I., Gross, R. W., and Sobel, B. E., "Pathophysiological Concentrations of Lysophosphoglycerides Quantified by Electron Microscopic Autoradiography," Laboratory Investigation, in press.

Sedlis, S. P., Corr, P. B., Sobel, B. E., and Ahumada, G. G., "Lysophosphatidyl Choline Potentiates CA^{2+} Accumulation in Rat Cardiac Myocytes," American Journal of Physiology, vol. 244, no. 1, pp. H32-H38, January 1983.

Shafer, K. E., Santoro, S. A., Sobel, B. E., and Jaffe, A. S., "Monitoring Activity of Fibrinolytic Therapy: A Therapeutic Challenge," American Journal of Medicine, in press.

Sharma, A. D., and Corr, P. B., "Adrenergic Factors in Arrhythmogenisis in Ischemic and Reperfused Myocardium," invited review in European Heart Journal, in press.

Sharma, A. D., Saffitz, J. E., Lee, B. I., Sobel, B. E., and Corr, P. B., "α-Adrenergic Mediated Accumulation of Calcium in Reperfused Myocardium," Journal of Clinical Investigation, in press.

Shum, C-D., "Network Models for PACS," seminar presented to Electronic Radiology Group at the Mallinckrodt Institute of Radiology, St. Louis, Missouri, April 15, 1983.

Smith, J. L., Ambos, H. D., Gold, H. K., Muller, J. E., Poole, W. K., Raabe, D. S., Rude, R. E., Passamani, E., Braunwald, E., Sobel, B. E., Roberts, R., and the MILIS Study Group," Enzymatic Estimation of Infarct Size when Early CK Values Are Not Available," American Journal of Cardiology, vol. 51, pp. 1294-1300, May 1983.

Snyder, D. L., "Preimage Selection in Time-of-Flight Emission Tomography," IEEE Transactions on Nuclear Science, vol. NS-30, no. 1, pp. 701-702, February 1983.

Snyder, D. L., and Chen, C-W., "Optically Tracking a Moving Object in a Randomly Varying Image," Proceedings of the 16th Annual Conference on Information Sciences and Systems, Princeton University, Princeton, New Jersey, p. 539, 1982.

Snyder, D. L., and Georghiades, C., "Modulator Design for Power Efficient Use of a Bandlimited Optical Communication Channel," IEEE Transactions on Communications, vol. COM-31, no. 4, pp. 560-565, April 1983.

Snyder, D. L., and Politte, D. G., "Image Reconstruction from List-Mode Data in an Emission Tomography System Having Time-of-Flight Measurements," IEEE Transactions on Nuclear Science, vol. NS-30, no. 3, pp. 1843-1849, June 1983.

Snyder, D. W., and Sobel, B. E., "Treatment of Ischemic Heart Disease: Clinical Therapy of Ischemic Heart Disease," in Medical Management of Ischemic Heart Disease, M. Rosen and B. Hoffman, eds., Martinus Nijhoff Publishers, The Hague, The Netherlands, in press.

Sobel, B. E., "Cardiological Considerations Demanding Rapid Data Acquisition and Processing," IEEE Proceedings of the Workshop on Time-of-Flight Tomography, IEEE Catalog No. 82CH1791-3, Washington University, St. Louis, Missouri, pp. 11-14, May 17-19, 1982.

Sobel, B. E., "Diagnostic Promise of Positron Tomography," American Heart Journal, vol. 103, p. 673, 1982.

Sobel, B. E., and Bergmann, S. R., "Cardiac Positron Emission Tomography," International Journal of Cardiology, vol. 2, pp. 273-277, 1982.

Sobel, B. E., and Bergmann, S. R., "Coronary Thrombolysis: Some Unresolved Issues," vol. 72, pp. 1-4, 1982 (editorial).

Sobel, B. E., and Geltman, E.M., "Localization and Quantification of Myocardial Ischemia and Infarction with Positron Emission Tomography," in Cardiovascular Medicine, vol. 1, J. H. K. Vogel, ed., Raven Press, New York, pp. 33-54, 1982.

Sobel, B. E., Geltman, E. M., and Bergmann, S. R., "Quantitative Assessment of Infarct Size and Its Influence by Thrombolysis," in Cardiology, E. I. Chazov, V. N. Smirnov, and R. G. Oganov, Plenum Publishing, New York, in press.

Ter-Pogossian, M. M., Bergmann, S. R., and Sobel, B. E., "Influence of Cardiac and Respiratory Motion on Tomographic Reconstructions of the Heart: Implications for Quantitative Nuclear Cardiology," Journal of Computer Assisted Tomography, vol. 6, pp. 1148-1155, 1982.

Ter-Pogossian, M. M., Ficke, D. C., Yamamoto, M., and Hood, Sr., J. T., "Design Characteristics and Preliminary Testing of Super PETT I, A Positron Emission Tomograph Utilizing Photon Time-of-Flight Information (TOF PET)," Proceedings of the Workshop on Time-of-Flight Tomography, IEEE Catalog No. 82CH1791-3, Washington University, St. Louis, Missouri, pp. 37-41, May 17-19, 1982.

Ter-Pogossian, M. M., Ficke, D. C., Yamamoto, M., and Hood, Sr., J. T., "Super PETT I: A Positron Emission Tomograph Utilizing Photon Time-of-Flight Information," IEEE Transactions in Medical Imaging, vol. MI-1, pp. 179-187, 1982.

Thanavaro, S., Kleiger, R. E., Province, M. A., Hubert, J. W., Miller, J. P., Krone, R. J., and Oliver, G. C., "Effect of Infarct Location on the In-Hospital Prognosis of Patients with First Transmural Myocardial Infarction," Circulation, vol. 66, pp. 742-747, 1982.

Thomas, Jr., L. J., "Computers, Cardiologists and Cardiograms," seminar presented to Washington University Three-Two Program students, St. Louis, Missouri, January 10, 1983.

Thomas, Jr., L. J., "Perspectives on Computers in Biomedical Research," invited paper for the AAMSI Congress 83, San Francisco, California, May 1-4, 1983, in press.

Thomas, Jr., L. J., Clark, K. W., and Miller, J. P., "Perspectives on Quality Control for Long-Term ECG Analysis in Multicenter Clinical Trials," presented at the Fourth Annual Meeting of the Society for Clinical Trials, St. Louis, Missouri, May 1983.

Thomas, Jr., L. J., and Miller, J. P., "Long-Term Ambulatory ECG Recording in the Determination of Antidysrhythmic Drug Efficacy," NIH Workshop on Pharmacology of Antiarrhythmic Therapy, Bethesda, Maryland, September 1-2, 1982, in press.

Tilton, R. G., Larson, K. B., Udell, J. R., Sobel, B. E., and Williamson, J. R., "External Detection of Early Microvascular Dysfunction after No-Flow Ischemia Followed by Reperfusion in Isolated Rabbit Hearts," Circulation Research, vol. 52, pp. 210-225, 1983.

Wong, J. W., "Inhomogeneity Corrections for Photon Beams," presented at the Workshop for Radiotherapy Treatment Planning, Cross Cancer Institute, Edmonton, Canada, March 1983.

Wong, J. W., and Henkelman, R. M., "A New Approach to CT Pixel-Based Photon Dose Calculations," Medical Physics, vol. 9, no. 4, p. 626, July/August 1982 (abstract).

Wong, J. W., and Henkelman, R. M., "A New Approach to CT Pixel-Based Photon Dose Calculations in Heterogeneous Media," Medical Physics, vol. 10, no. 2, pp. 199-208, March/April 1983.

Wong, J. W., and Rosenberger, F. U., "Photon Dose Calculations in Radiotherapy Treatment Planning," presented as part of a course titled "Computation in Radiation Therapy," sponsored by the Canadian College of Physicists in Medicine, at the 46th annual meeting of the Canadian Association of Radiologists, Quebec, Canada, June 23, 1983; Proceedings in press.

Wong, J. W., Slessinger, E., Stein, D., Rosenberger, F. U., and Purdy, J. A., "Implementation and Verification of a New CT Based 3-Dimensional Photon Dose Calculation Algorithm," accepted for presentation at the American Association of Physicists in Medicine Annual Meeting, New York, New York, July 31-August 4, 1983.

Yamamoto, M., Hoffman, G. R., Ficke, D. C., and Ter-Pogossian, M. M., "Imaging Algorithm and Image Quality in Time-of-Flight Assisted Positron Computed Tomography: Super PETT I," Proceedings of the Workshop on Time-of-Flight Tomography, IEEE Catalog No. 82CH1791-3, Washington University, St. Louis, Missouri, pp. 125-129, May 17-19, 1982.

X. MONOGRAPHS AND WORKING NOTES

The Biomedical Computer Laboratory's Monograph Series was established to systematize the many reports, reprints, program descriptions and other documents written at BCL or supported in part by the Laboratory's facilities or staff.

A forum, much less formal than our monograph series, has been instituted to serve as a repository for materials such as: research notes, system and component documentation, technical survey notes and prepublication drafts. A Working Note File is maintained for access by anyone associated with the Washington University Computer Labs. Distribution for outside use can be made available with the consent of the contributor.

Monographs

Following is a list of the monographs published by BCL during the past year. Copies of the complete index to the Monograph Series are available on request.

Monograph Number	Author(s)	Title	Date
414	Thomas, Jr., L. J.	Long-Term Ambulatory ECG Recording in the Determination of Antidysrhythmic Drug Efficacy	9/82
415	Hermes, R. E.	Ventricular Arrhythmia Detector Performance Evaluation	9/82
416	Gray, A. J. Blaine, G. J.	TERRANET: A Modest Terminal-Processor Interconnect for the Laboratory Environment	10/82
417	Holmes, T. J.	Predicting Count Loss in Modern Positron-Emission Tomography Systems	10/82
418	Snyder, D. L.	Preimage Selection in Time-of-Flight Emission Tomography	10/82
419	Holmes, T. J. Hitchens, R. E. Blaine, G. J. Ficke, D. C. Snyder, D. L.	A Dedicated Hardware Architecture for Data Acquisition and Processing in a Time-of-Flight Emission Tomography System (Super-PETT)	10/82
420	Peterson, M. L.	A Feasibility Study for an Optical Atmospheric Communication Link	12/82

Monograph Number	Author(s)	Title	Date
421	Snyder, D. L. Politte, D. G.	Image Reconstruction from List-Mode Data in an Emission-Tomography System Having Time-of-Flight Measurements	11/82
422	Gurumurthy, K. V. Arthur, R. M.	A Dispersive Model for the Propagation of Ultrasound in Soft Tissue	12/82
423	Blaine, G. J.	Digital-Image Archiving and Communication Systems	1/83
424	Blaine, G. J.	Networks and Distributed Systems: A Primer	1/83
425	Hermes, R. E. Cox, Jr., J. R.	A Model for Performance Evaluation of Ventricular Arrhythmia Detectors	2/83
426		WITHDRAWN	
427	Politte, D. G. Holmes, T. J. Snyder, D. L.	Effects of Quantization of Time-of-Flight (TOF) Measurements on Image Signal-to-Noise Ratio in TOF Emission Tomography	2/83
428		WITHDRAWN	
429	Holmes, T. J. Snyder, D. L. Ficke, D. C. Yamamoto, M.	Maximum-Likelihood Estimation Applied to Some Calibration Problems in Time-of-Flight Emission Tomography Systems	3/83
430	Politte, D. G. Snyder, D. L.	A Simulation Study of Design Choices in the Implementation of Time-of-Flight Reconstruction Algorithms	3/83
431	Holmes, T. J. Blaine, G. J. Hitchens, R. E. Ficke, D. C.	Implications of Event Rate and Study Parameters on System Architecture	3/83
432	Dunham, J. G.	Optimal Delta Modulation System	6/83
433	Arthur, R. M.	Signal Quality of Resting Electrocardiograms	6/83

Monograph Number	Author(s)	Title	Date
434	Cheng, N. C.	Image-Reconstruction Algorithms for Positron-Emission Tomography Systems	12/82

Working Notes

Following is an index of notes submitted during the current reporting period.

Working Note Number	Author(s)	Title	Date
28	Hermes, R. E.	Estimation of Model Parameters for Detector Performance Evaluation	7/82
29	Holmes, T. J. Hitchens, R. E. Ficke, D. C. Blaine, G. J.	Evaluation of Some Commercially Available High Speed (50 ns) Analog to Digital Converters for a Time-of-Flight Emission Tomography System (Super-PETT)	8/82
30	Stein, D. W.	TERM Terminal Control Program Program Reference Manual	5/82
31	Blaine, G. J. Browder, M. W. Phillips, S. R.	VER Acquisition System Configuration Memory and Aging Project: Interconnect Diagram	9/82
32	Blaine, G. J. Hill, R. L. Cox, Jr., J. R. Jost, R. G.	A PACS Workbench at MIR	12/82
33	Gray, A. J.	TERRANET Tap Unit Post-Assembly Checkout Procedure	1/83
34	Brandenburger, G. Klepper, J.	Supplement to the BIOMATION 8100 Manual	1/83
35	Gray, A. J.	An Informal Power Line Disturbance Survey	1/83
36	Holmes, T. J.	Implications of the Slice Processor Architecture on Image Processing Efficiency and Dollar Cost for Super-PETT I	1/83

Working Note Number	Author(s)	Title	Date
37	Gray, A. J.	TERRANET Reliability Tests: Recent Results	1/83
38	Phillips, S. R. Blaine, G. J.	TERRANET: Four-Port Insert Unit	1/83
39	Gray, A. J.	TERRANET: Tap Unit Software Manual	1/83
40	Gray, A. J.	DNA Gel Reading System Data Acquisition and Band Detection Algorithms	2/83
41	Gray, A. J.	DNA Mapping System Hardware Description	2/83
42	Phillips, S. R. Rainey, M. J.	Printed Circuit Board Cost Quotes for TERRANET	4/83
43	Stein, D. W.	A User's Guide to the RTP System	4/83
44	Stein, D. W.	The Programmer's Reference Manual to the RTP System	5/83
45	Markham, J.	Peak Detector for DNA Gel Reading System	5/83
46	Phillips, S. R.	TERRANET: 60 Channel Configuration	5/83
47	Beecher, D. E.	Three Dimensional Image Construction Utilizing a Voxel Model Approach and A Computational Geometry Approach	5/83
48	Stein, D. W.	QANDA Q and A Package Programmer's Reference Manual and User's Guide	6/83